

**MODELING INDIVIDUALIZED THERMOREGULATORY RESPONSES TO
CLOTHING AND ACTIVITY, IN HOT AND COLD ENVIRONMENTS**

**By
Adam W. Potter**

A Dissertation Submitted

**In partial fulfillment of the Requirements for the Degree of
Doctor of Philosophy in Biomedical Informatics**

**Department of Health Informatics
Rutgers, The State University of New Jersey
School of Health Related Professions,**

May 2019



Final Dissertation Defense Approval Form

Modeling Individualized Thermoregulatory Responses to Clothing and Activity, in Hot
and Cold Environments

BY

Adam W. Potter

Dissertation Committee:

Shankar Srinivasan, PhD

Suril Gohel, PhD

David P. Looney, PhD

Xiaojiang Xu, PhD

William R. Santee, PhD

Approved by the Dissertation Committee:

_____	Date: _____
_____	Date: _____
_____	Date: _____
_____	Date: _____
_____	Date: _____

TABLE OF CONTENTS

<u>Section</u>	<u>Page</u>
Acknowledgments.....	iv
List of Tables	v
List of Figures	vi
Abstract	ix
I. Introduction	1
1.1 Statement of the Problem.....	1
1.2 Background of the Problem	1
1.3 Research Hypotheses	1
1.4 Objectives of the Research.....	2
II. Literature Review	3
2.1 Incidences of Heat and Cold Related Injuries.....	3
2.1.1 Clinical Definitions of Heat Injuries.....	4
2.1.2 Military Incidences of Heat Related Injuries	5
2.1.3 Clinical Definitions of Cold Injuries.....	7
2.1.4 Military Incidences of Cold Related Injuries	11
2.2 Thermophysiology Basics.....	14
2.3 Importance of Clothing	18
2.3.1 Biophysics of Clothing	19
III. Methods	29
3.1 Overall Study Design	29
3.2 Human Research Study Design	31
3.2.1 Assessment 1 – Heat Stress Analysis.....	31
3.2.2 Assessment 2 – Cold Stress Analysis	32
3.3 Non-Human Research Design.....	34
3.4 Modeling Risk and Predicting Heat and Cold Related Injuries	35
3.4.1 Rational Models	36
3.4.2 Empirical Models.....	39
3.4.3 Statistical Methods and Software.....	45
3.5 Methods for Model Verification	45
IV. Results.....	47
4.1 Assessment 1 – Heat Stress Analysis.....	47
4.2 Assessment 2 – Cold Stress Analysis	58
V. Discussion	71
5.1 Limitations	71
5.2 Other Modeling Methods to Consider	73
5.2 Future Direction	77
VI. Conclusions.....	80
References.....	81
Appendix.....	104

Acknowledgments

I would like to thank some of my influential colleagues: Mr. William Tharion, Ms. Laurie Blanchard, Mr. Alexander Welles, and Dr. Larry Berglund, for their guidance and discussions related to this work. Thanks to Dr. Kenneth Larsen, Dr. Karl Friedl, and Dr. Reed Hoyt for mentorship and scientific guidance along the way. A very special thank you to Mr. Julio Gonzalez for constantly providing me with thermal manikin data and enjoyable scientific and personal discussions.

Thank you to my advisor and committee chair Professor Shankar Srinivasan for mentorship and for shepherding me through the [random] forest of biomedical informatics. I would also like to send a special thanks to my committee members, mentors, and colleagues: Professor Suril Gohel, Dr. Xiaojiang Xu, Dr. William Ross Santee, and Dr. David Looney. Their help has been instrumental to ensuring I actually finish this work and move on to the next set of scientific ventures.

Thank you to “the reviewers”. While my ego initially predisposes me to disagree with most of your comments; I have come to appreciate the significant contribution that you bring to ensuring quality of published works.

Readers.... Hope you like it. Comments or critiques are welcome but citations are preferred ☺

A special thank you to my siblings Stephanie, Rebecca, Erik (“FG”), my parents Paul and Mary, and my extended siblings Jason, Ryan, Geoff, and Faith. Without the presence of these people my scientific and general competitiveness could have been stunted. We will always be in a competition... whether you like it or not.

I would especially like to thank my lovely wife Ginnie and my children, Kate, Ryan and Lily. I love you each very much. Thank you for tolerating my often rambling rants about heat exchange and thermoregulation. My passion is my work and I am a nerd by choice. However, it would be all-for-naught if you were not in my life to share my nerdiness with.

List of Tables

<u>Table</u>	<u>Page</u>
1 Incidences of Heat Injuries for U.S. Armed Services, 2006-2016	6
2 Levels of Hypothermia and Physiological Responses	10
3 1997-2017 Summarized Incidences of Cold Related Injuries for Active U.S. Military	12
4 American Society for Testing and Materials standard chamber and manikin conditions for testing thermal (R_t) and evaporative (R_{et}) resistance	21
5 Summary of Study Data	30
6 Assessment 1 – Heat Stress. Human Data Descriptive Statistics	32
7 Assessment 2 – Cold Stress. Human Data Descriptive Statistics	34
8 Summary of Non-human (clothing) data	35
9 Required inputs to HSDA model	40
10 HSDA Fundamental Equations	40
11 Inputs for metabolic cost estimations – Assessment 1	48
12 Estimated metabolic costs for each activity – Assessment 1	48
13 Accuracy of HSDA model when predicting T_c ($^{\circ}\text{C}$) in individuals wearing different chemical protective clothing ensembles during exercise in hot and humid conditions.	53
14 Measured biophysical properties and predicted DLE for select cold weather clothing	59
15 Cold exposure skin temperature predictions to observations grouped regions	67
16 Cold exposure IREQ and DLE predictions to Gonzalez et al., [80] data	70
17 Cold exposure reported resting endurance time (minutes) to DLE predictions to Gonzalez et al., [80] data	70

List of Figures

<u>Figure</u>		<u>Page</u>
1	Hospitalized incidences of heat- and cold-related injuries US Military, 2006-2016	4
2	US Military Incidences of Heat-Related Injuries, 2006-2016	7
3	US Military Incidences of Heat Stroke, 2006-2016	7
4	Onset conditions for Cold Injuries [26]	11
5	Incidences of Cold Injuries, Active U.S. Armed Forces, 1997-2017	13
6	Incidences, by type, of Cold Injuries, Active U.S. Armed Forces, 1997-2017	13
7	Rate of Incidences, per 100,000 person years, of Cold Injuries, Active U.S. Armed Forces, 1997-2017	14
8	Vasoconstriction and vasodilation in response to environmental conditions	17
9	Environmental Impact on the Human and Effects of Protective Clothing	19
10	Wind chill temperature chart [65] modified to include levels of risk [20]	24
11	Spectrophotometric measures of a material	25
12	Predicted core body temperature response during moderate walking – a comparison of two different head-worn covers [73]	28
13	Surface area of the manikin	28
14	Levels of clothing system testing [69]	29
15	SCENARIO Model fundamental rational basis [64]	37
16	Comparison of one- and six-cylinder thermoregulatory models	38
17	Dynamic model of human thermoregulation Xu and Werner [90]	38
18	Schematic of the heat strain decision aid (HSDA) [60]	42
19	Notional use of Bland-Altman for comparing two methods [105]	46
20	Human Research Study Design – Assessment 1	47
21	Measured rectal core body temperature (°C) – Assessment 1	49
22	Aggregate of measured core temperature across trials	49
23	Overall comparison of model predictions and observed data	50

<u>Figure</u>		<u>Page</u>
24	Comparison of observed and modeled for ensemble A	50
25	Comparison of observed and modeled for ensemble B	51
26	Comparison of observed and modeled for ensemble C	51
27	Accuracy of predicted core temperature to observed SD	54
28	Side-by-side comparison of the individual predictions and observed measures of core body temperature from the laboratory study	55
29	Individual prediction errors by elapsed time points (minutes)	56
30	Mean error by elapsed time points (minutes)	56
31	Observed to modeled core body temperatures for both laboratory and field studies	57
32	Modeled DLE _{range} (minutes) using the IREQ method for each clothing ensemble for both rest and light work (1MET, 58 Wm ² ; 2MET, 116 Wm ²) in -15°C and -25°C	58
33	Survival at rest as a function of air temperature (°C) and clothing insulation (clo)	60
34	Surface plot of survival at rest as a function of air temperature (°C) and clothing insulation (clo)	61
35	Expanded survival plot to include lower and higher clothing insulation (clo) values	61
36	Comparison of IREQ calculated DLE and empirical survival surface plot	62
37	Observed to modeled skin temperature responses; CoWEDA and Castellani et al., [82]	63
38	Observed to modeled finger temperatures; CoWEDA and Gonzalez et al., [80] during rest at 0, -20, and -30°C	64
39	Observed to modeled finger temperatures; CoWEDA and Gonzalez et al., [80] during exercise [\sim 2.4MET] at 0, -20, and -30°C	64
40	Observed to modeled mean skin temperatures; CoWEDA and Gonzalez et al., [80] during rest at 0, -20, and -30°C	65
41	Observed to modeled mean skin temperatures; CoWEDA and Gonzalez et al., [80] during exercise [\sim 2.4MET] at 0, -20, and -30°C	65
42	Observed to modeled mean skin temperatures; CoWEDA and Hickey et al., [81] for 100 minute exposure to extreme cold conditions -40°C	66
43	Observed to modeled temperatures; CoWEDA and published data [80-82]	67

<u>Figure</u>		<u>Page</u>
44	Observed to modeled finger temperatures; CoWEDA and published data [80-82]	68
45	Observed to modeled mean skin temperatures; CoWEDA and published data [80, 82]	69
46	Graphical example of random decision forests method [136]	75
47	Notional example of neural network method for injury prediction	77

Abstract

The US military operate in complex and harsh environments with regular risks of succumbing to heat- or cold-related injuries that could have both negative mission and individual health consequences. Objective and Methods: This effort collects human rest and exercise-based research data to compare and validate methods and mixed modeling approaches to provide a clear outline of predictive methods for determining physiological responses to hot and cold exposure (e.g., rise or fall in skin and core body temperatures) based on individual, environment, clothing, and activity. Data: This study collects human and non-human (clothing biophysics) data. Human research data used is from individuals during rest and exercise exposed to hot and cold environments ($n = 51$); while clothing data is a full range of clothing tested on sweating thermal manikins for measures of thermal and evaporative resistance ($n = 93$). From this combined data, the goal is test equations or methods for predicting general risk of heat- and cold- related injuries based on individual inputs. Two assessments are conducted, one to assess heat stress predictions (rise of core body temperature) and a second for assessing cold stress predictions (skin temperature fall). Conclusions: Analyses in the heat stress assessment showed empirical methods are capable of predicting within acceptable accuracy rise in core body temperature from group mean data; while individual-based predictions have been shown to be accurate to within an acceptable bias of $\pm 0.27^{\circ}\text{C}$ for both in hot and humid environments laboratory (-0.10 ± 0.36) and field conditions (0.23 ± 0.32). Both rational and empirical methods were shown to acceptably predict skin temperatures to within the observed standard deviation (23.14 ± 9.35) (bias, $-0.77 \pm 3.69^{\circ}\text{C}$; MAE, $2.22 \pm 3.05^{\circ}\text{C}$; and RMSE, $1.49 \pm 3.05^{\circ}\text{C}$).

I. Introduction

1.1 Statement of the Problem

US Armed Service members operate in a wide array of areas, under many different environmental conditions, and conduct varied and dynamic activities. Given these complex settings, the individuals within the Armed Forces constantly face the threat of succumbing to heat or cold related injuries [1-3].

1.2 Background of the Problem

Mitigating hot and cold injuries is a complex and has been shown to have significant links to a number of individualized factors, to include race, gender, job specialty, and geographical origin [1-2]. There are many other individualized elements (e.g., fitness, body composition, and genetics) that are intuitively linked to these health outcomes; however, there is a lack of data to scale that sufficiently addresses these issues.

1.3 Hypotheses

H₁: Thermoregulatory responses (e.g., skin and core temperature rise/fall) can be mathematically described and accurately predicted

H₂: Existing population-based models can acceptably predict group mean responses and can accurately predict individualized rise in core body temperature to within $\pm 0.27^{\circ}\text{C}$ of observed data with the inclusion of individual characteristics

H₃: Existing rational models can be modified to accurately predict skin temperature to within observed SD of collected data.* (*SD of observed skin temperatures during cold exposure is typically high)

1.4 Objectives

The purposes of this effort are to: 1) conduct broad literature review and report an aggregation of incidences of hot and cold related injuries among active duty US Army Soldiers, 2) evaluate existing methods for modeling human thermoregulatory responses to hot and cold related exposure, 3) collect human research data to validate and evaluate existing models / methods, and 4) apply machine learning techniques to collated datasets to develop or outline predictive methods to forecast thermoregulatory responses (e.g., rise and fall in skin and core body temperatures) based on individual, environment, clothing, and activity.

Envisioned Functional Deliverables:

1. A set of equations or methods for predicting situational risk of heat- and cold-related injuries based on predicted increases to core body temperature; including individualized inputs, environmental inputs, and contextual inputs (e.g., clothing, activity)

II. Literature Review

2.1 Incidences of Heat and Cold Related Injuries

With climate changes alone, environmental extremes continue to be observed in both hotter and colder conditions [4] the impact on human health is significant and likely to be an enduring concern. The Centers for Disease Control and Prevention (CDC) has published reports on the incidences of both cold- and heat-related deaths for the population within the United States. An average of 688 heat-related deaths occurred in the U.S. between 1999 and 2003. States with the highest rates (per 100,000) of hyperthermia-related fatalities during this same period were Arizona (1.7), Nevada (0.8), and Missouri (0.6) [5]. A nearly identical annual average of 689 cold-related deaths occurred between 1979 and 2002. This national rate 0.2 per 100,000 was reported to be higher in states that experienced rapid temperature changes such as North and South Carolina (0.4 and 0.4) and in areas of higher elevation (e.g., Arizona (0.3) [6].

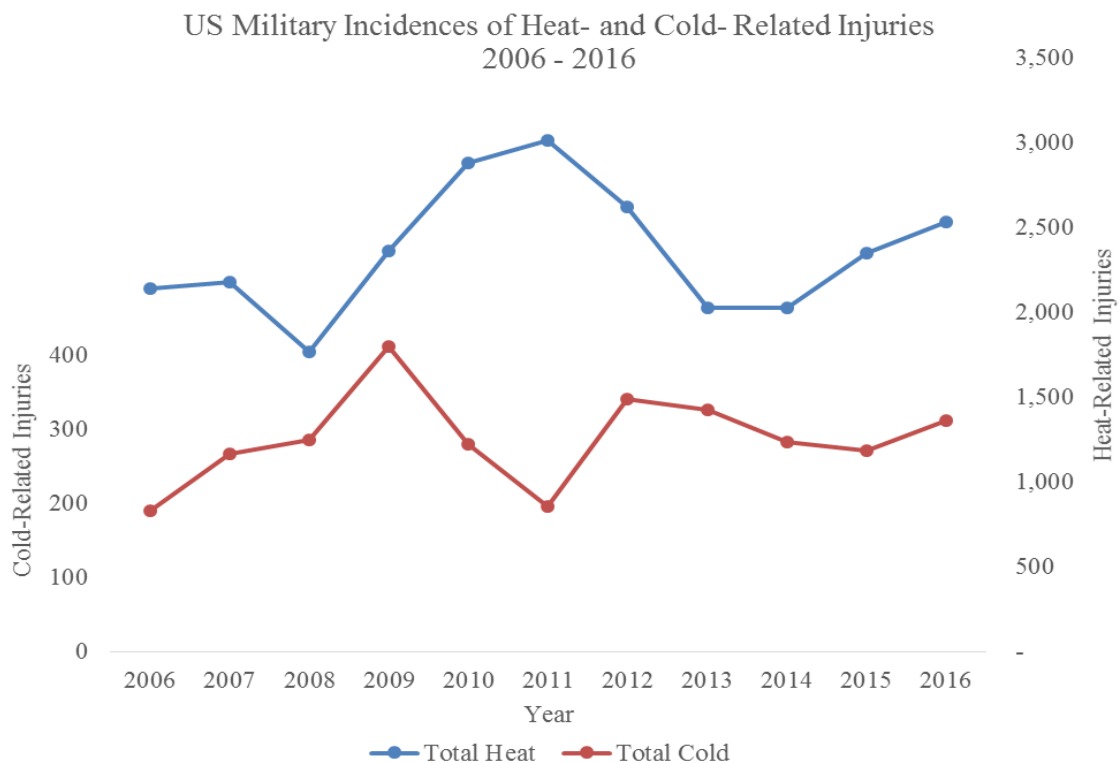
In a recent report from Berko et al., [7], an analysis of weather related deaths in the U.S. between 2006 and 2010 showed the incidences of weather related deaths to be approximately 2,000 annually (10,649 total for the period). Interestingly, cold related deaths (e.g., hypothermia) were twice as prevalent (63%; n = 6,660) than that of heat related deaths (e.g., heat stroke) (31%; n = 3,332); while other weather events (floods, storms, lightning) accounted for the last six percent (n = 662).

Exposure to natural weather events, such as extreme heat or cold, is a national and international concern. However, this is even more of an acute issue for the U.S. military, as they routinely travel and conduct a range of physical activities around the world within the full spectrum of extreme environmental conditions. Furthermore, the complexity of

military operations and activities within this range of environments is more dynamic than that of civilian exposure events.

For the US military the incidences of heat- and cold-related injuries is a continued problem (Figure 1) that is often planned for with the assumption that they will happen rather than the assumption that they are all preventable.

Figure 1. Hospitalized incidences of heat- and cold-related injuries US Military, 2006-2016



2.1.1 Clinical Definitions of Heat Injuries

From a clinical perspective, heat related injuries are typically binned into four categories: heat stress, heat exhaustion, hyperthermia, and heat stroke. Heat stress is

generally categorized as physiological strain and a perceived discomfort typically associated to physical activity during exposure to hot environmental conditions [8].

Clinical terminologies define heat injuries as events at varied levels of discomfort and physiological and neurological impairment along with specific levels of core body temperature. Heat exhaustion is clinically defined as an illness, of mild to moderate severity, where core body temperature is abnormal, low or high (over 37°C (98.6°F) but below 40°C (104°F)). Heat exhaustion typically presents as fatigue symptoms such as dizziness, fainting, discomfort, etc. [8]. Hyperthermia is seen when heat dissipating mechanisms are impaired with a rise in core body temperature above the hypothalamic set point, typically recognized as over approximately 40°C (104°F) [8-10]. Heat stroke is considered a severe illness event caused by exposure to heat and/or during physical activity; where core body temperature has exceeded 40°C (104°F) and noticeable impact on the central nervous system (e.g., delirious, convulsions) [8-10].

2.1.2 Military Incidences of Heat Related Injuries

The U.S. Army faces significant issues associated with heat illness and heat injuries during training. During 2016, the Armed Forces Health Surveillance Center (AFHSC) estimated a total rate of 1.65 heat injuries per 1,000 individuals per year (total n = 2,536); heat strokes specifically being 0.31 per 1,000 per year (n = 401) [11].

Over a 12 year period, from 2005 to 2016, using published reports from the Medical Surveillance Monthly Report (MSMR) Table 2 was created outlining incidences of heat-related injuries for active duty members within the entire Armed Forces (U.S. Army, Marine Corps, Navy, and Air Force) [11-19]. From 2005 to 2016, the total reported

incidences of heat-related injuries was generally lumped into two categories, heat stroke and all others. These instances are shown as the number of cases (n) and rate (per 1,000 person-years); where heat stroke totaled 3,761 (2.7 p-yrs), other instances totaled 22,145 (15.9 p-yrs), and collectively 25,906 (18.6 p-yrs). The average annual incidences and rates were: heat stroke 342 (0.2 p-yrs), other 2,013 (1.4 p-yrs), and total 2,355 (1.7 p-yrs) (Table 1, Figs 2-3)

Table 1. Incidences of Heat Injuries for U.S. Armed Services, 2006-2016

Year	Heat Stroke		Other		Total	
	Cases (n)	Rate (p-yrs)	Cases (n)	Rate (p-yrs)	Cases (n)	Rate (p-yrs)
2016	401	0.31	2135	1.65	2536	1.96
2015	417	0.32	1933	1.49	2350	1.81
2014	344	0.25	1683	1.22	2027	1.47
2013	324	0.23	1701	1.21	2025	1.44
2012	365	0.25	2257	1.57	2622	1.82
2011	362	0.25	2652	1.82	3014	2.07
2010	311	0.21	2572	1.77	2883	1.98
2009	323	0.22	2038	1.41	2361	1.63
2008	299	0.21	1467	1.04	1766	1.25
2007	329	0.24	1853	1.38	2182	1.62
2006	286	0.21	1854	1.36	2140	1.57
Total	3,761	2.7	22,145	15.9	25,906	18.6
Average	342	0.2	2,013	1.4	2,355	1.7
Standard Deviation	41.04	0.04	368.44	0.24	381.67	0.26

**Figure 2. US Military Incidences of Heat-Related Injuries
2006 - 2016**

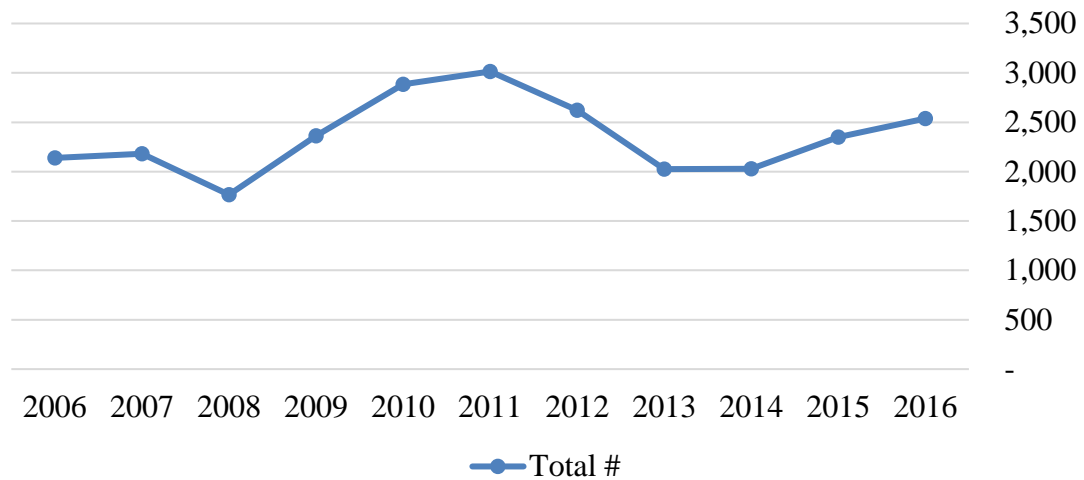
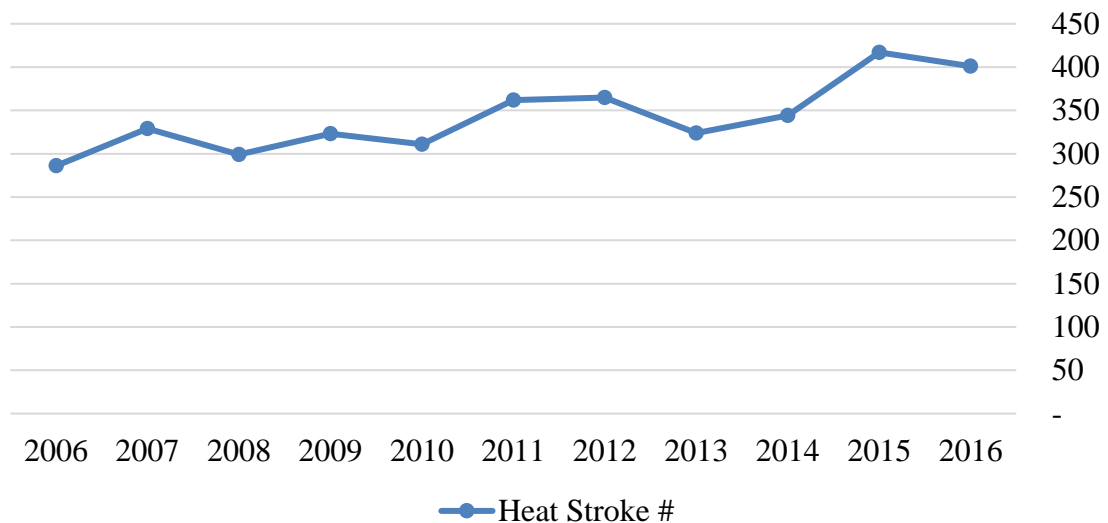


**Figure 3. US Military Incidences of Heat Stroke
2006 - 2016**



2.1.3 Clinical Definitions of Cold Injuries

Characterizing cold related injuries is fairly complex, as the responses to cold have higher individual variability when compared to that of heat related injuries. From a clinical perspective, cold related injuries can be broadly binned into three categories: frostbite,

nonfreezing cold injuries, and hypothermia. In addition, each of these has varying levels of severity and subcategories associated to them.

Frostbite is below the point at which skin tissue begins to freeze. While 0°C (32°F) is traditionally considered the freezing point of water, the freezing point of skin is understood to be marginally less due to electrolytes [20]. Observed freezing points range from as low as -4.8°C to as high as -0.6°C [20-21].

Nonfreezing cold injuries include an array of injury events where tissue freezing has not occurred but damage occurs. The level of severity of nonfreezing injuries is determined by the temperature, duration, and wetness of the exposure to the tissue. Four of the more common specific types of nonfreezing injuries include immersion (trench) foot, chilblain, cold urticaria, and cold-induced bronchoconstriction [22].

Immersion foot is a nonfreezing injury where the foot becomes swollen, the skin is red initially but as severity increases the skin becomes lower in oxygen saturation and becomes cyanotic (purple, bluish discoloration) [20, 22]. Immersion foot is most often reported after tissue have been exposed for extended periods of time to non-freezing temperatures, between 0-15°C (32-60°F) [22]. The 'immersion' term refers to when the foot is actually immersed but more typically when the foot becomes immersed and wet within boots [20, 22].

Chilblains is considered a fairly common nonfreezing injury that appears as more superficial than immersion foot and occurs due to shorter term exposure (i.e., 1-5 hours) of temperatures below 16°C (60°F) [20]. Cold urticaria is expressed as a quick onset of redness, swelling and itchiness of the skin in response to short-term exposure (i.e., minutes) to cold environments [22]. Cold-induced bronchoconstriction is a physiological response

where an individual's airways are narrowed during exercise in cold environments [20,22-24].

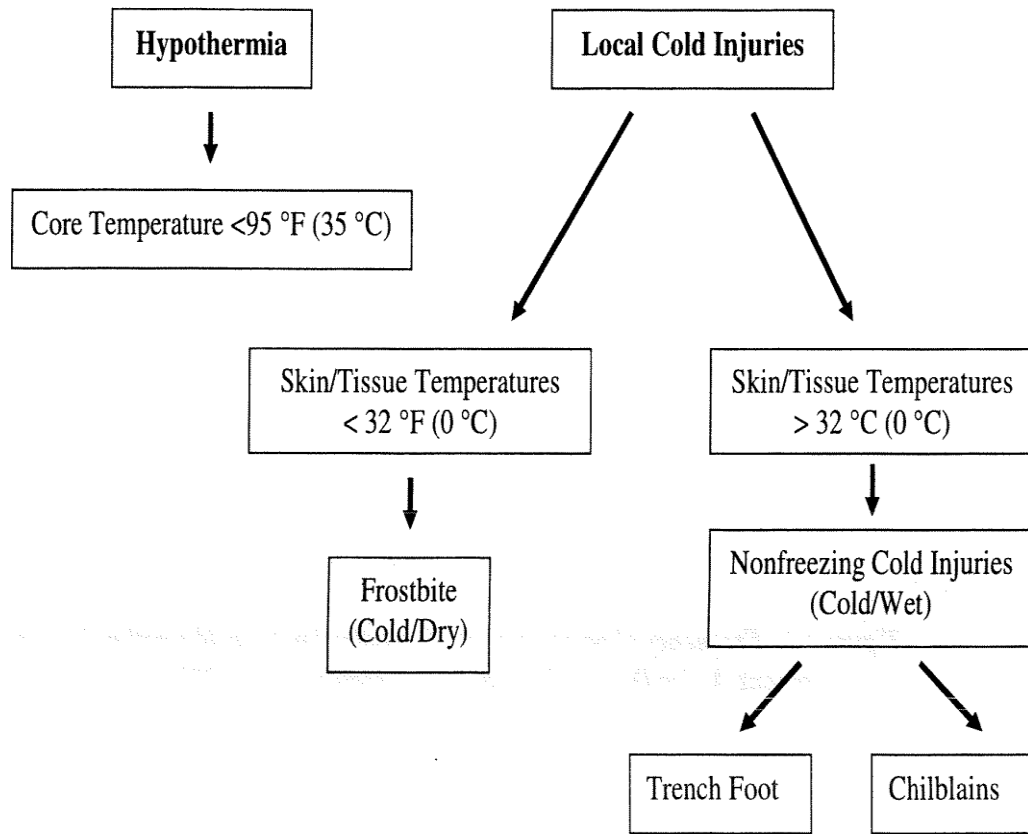
Hypothermia as a broad category of cold injury is clinically described to be the point at which core body temperature has dropped below 35°C (95°F) [25]. However, hypothermia is more specifically defined with four levels of severity; where normothermia (normal temperature level) is approximately 37°C (98.6°F), mild hypothermia is between 35.0 – 36.0°C (95.0 – 96.8°F), moderate hypothermia being 32.0 – 35.0°C (89.6 – 95.0°F), and severe hypothermia being 28.0 – 32.0°C (82.4 – 89.6°F) [20,25]. Table 2 outlines specific core temperature reference points associated with physiological changes / responses using work by Castellani et al., [20] and Pozos and Danzl [25].

The environmental conditions for onset of specific types of cold injuries is simplified in a chart shown in Figure 4 below [26]

Table 2. Levels of Hypothermia and Physiological Responses

Stage	Core Temperature		Physiological Responses
	° F	° C	
Normothermia	98.6	37.0	Normal
Mild Hypothermia	95.0	35.0	Maximal shivering; increased blood pressure
	93.2	34.0	Amnesia; dysarthria; cognitive impairment
	91.4	33.0	Ataxia; apathy
Moderate Hypothermia	89.6	32.0	Stupor
	87.8	31.0	Shivering ceases; pupils dilate
	85.0	30.0	Cardiac arrhythmias; decreased cardiac output
	85.2	29.0	Unconsciousness
Severe Hypothermia	82.4	28.0	Ventricular fibrillation likely; hypoventilation
	80.6	27.0	Loss of reflexes and voluntary motion
	78.8	26.0	Acid-base disturbances; no response to pain
	77.0	25.0	Reduced cerebral blood flow
	75.2	24.0	Hypotension; bradycardia; pulmonary edema
	73.4	23.0	No corneal reflexes; areflexia
	66.2	19.0	Electroencephalographic silence
	64.4	18.0	Asystole
	59.2	15.2	Lowest recorded infant survival
	56.7	13.7	Lowest recorded adult survival

Figure 4. Onset conditions for Cold Injuries [26]



2.1.4 Military Incidences of Cold Related Injuries

Table 3 was created outlines the cold injury incidences for active duty members of the U.S. military using a collection of published reports from the Medical Surveillance Monthly Report (MSMR) over a 20 year period [27-44]. From 1997 to 2017, the total reported incidences of clinically reported cold injuries for the active duty U.S. military is broken out into four main areas: frostbite, immersion foot and hand, hypothermia, and unspecified. The instances are shown as number of cases (n) and rate (per 100,000 person-years (p-yrs)); where frostbite (n=3,323; 33.3 p-yrs), immersion foot (n=839; 8.4 p-yrs), hypothermia (n=648; 6.4 p-yrs), and unspecified (n=1,873; 18.9 p-yrs), totaling 6,683; 67.5 p-yrs (Table 3, Figs 5-7).

TABLE 3. 1997-2017 Summarized Incidences of Cold Related Injuries for Active U.S. Military

Timeframe	Frostbite		Immersion Foot		Hypothermia		Unspecified		Total	
	Cases (n)	Rate (p-yrs)	Cases (n)	Rate (p-yrs)	Cases (n)	Rate (p-yrs)	Cases (n)	Rate (p-yrs)	Cases (n)	Rate (p-yrs)
2016–2017	112	24.3	27	5.9	34	7.4	17	3.7	190	41.2
2015–2016	104	21.6	68	14.2	37	7.7	58	12.1	267	55.6
2014–2015	136	27.4	19	3.8	55	11.1	75	15.1	285	57.4
2013–2014	209	40.1	50	9.6	55	10.6	97	18.6	411	78.9
2012–2013	149	27.7	46	8.6	29	5.4	56	10.4	280	52
2011–2012	99	17.7	14	2.5	27	4.8	55	9.8	195	34.9
2010–2011	176	31.2	32	5.7	43	7.6	89	15.8	340	60.2
2009–2010	150	27.2	44	8	37	6.7	95	17.2	326	59.1
2008–2009	139	25.7	38	7	27	5	78	14.4	282	52.1
2007–2008	132	25.4	34	6.5	31	6	74	14.2	271	52.2
2006–2007	154	30.7	37	7.4	28	5.6	92	18.3	311	61.9
2005–2006	109	22.5	39	8	15	3.1	72	14.8	235	48.4
2004–2005	168	34.3	43	8.8	20	4.1	84	17.2	315	64.3
2003–2004	174	35.3	49	9.9	27	5.5	74	15	324	65.8
2002–2003	183	37.7	62	12.8	35	7.2	101	20.8	381	78.6
2001–2002	182	38.2	32	6.7	23	4.8	67	14.1	304	63.9
2000–2001	189	39.8	53	11.2	38	8	102	21.5	382	80.5
1999–2000	178	37.8	58	12.3	26	5.5	320	68	582	119.6
1998–1999	428	90.5	58	12.3	34	7.2	166	35.1	686	151.9
1997–1998	152	31.6	36	7.5	27	5.6	101	21	316	71.4
Total (1997–2017)	3,323	666.7	839	168.7	648	128.9	1,873	377.1	6,683	1,349.9
Average	166	33.3	42	8.4	32	6.4	94	18.9	334	67.5
Standard Deviation	68.84	14.95	14.01	3.04	10.14	1.99	60.43	13.07	117.99	26.69

Figure 5. Incidences of Cold Injuries, Active U.S. Armed Forces, 1997-2017

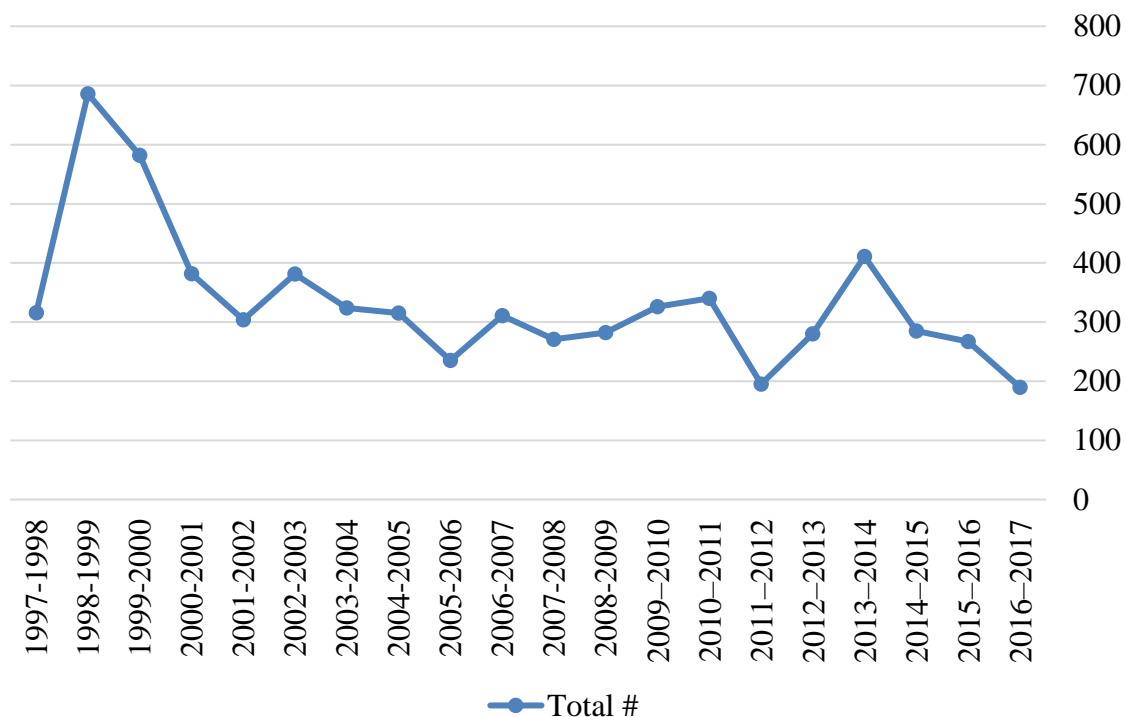


Figure 6. Incidences, by type, of Cold Injuries, Active U.S. Armed Forces, 1997-2017

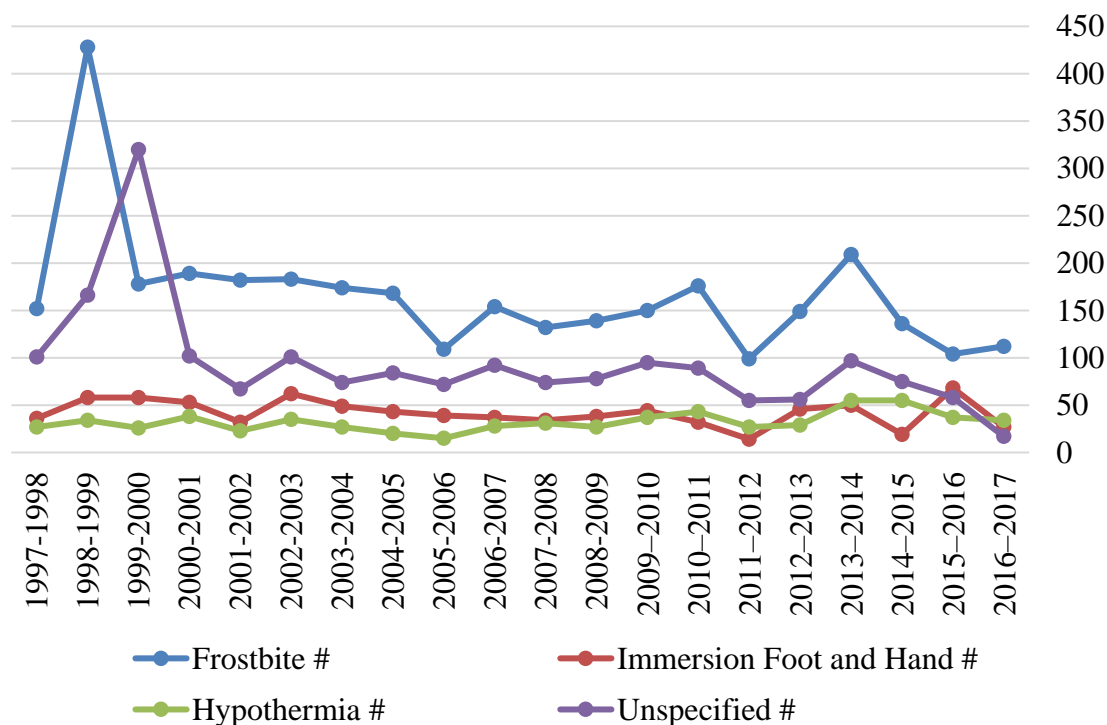
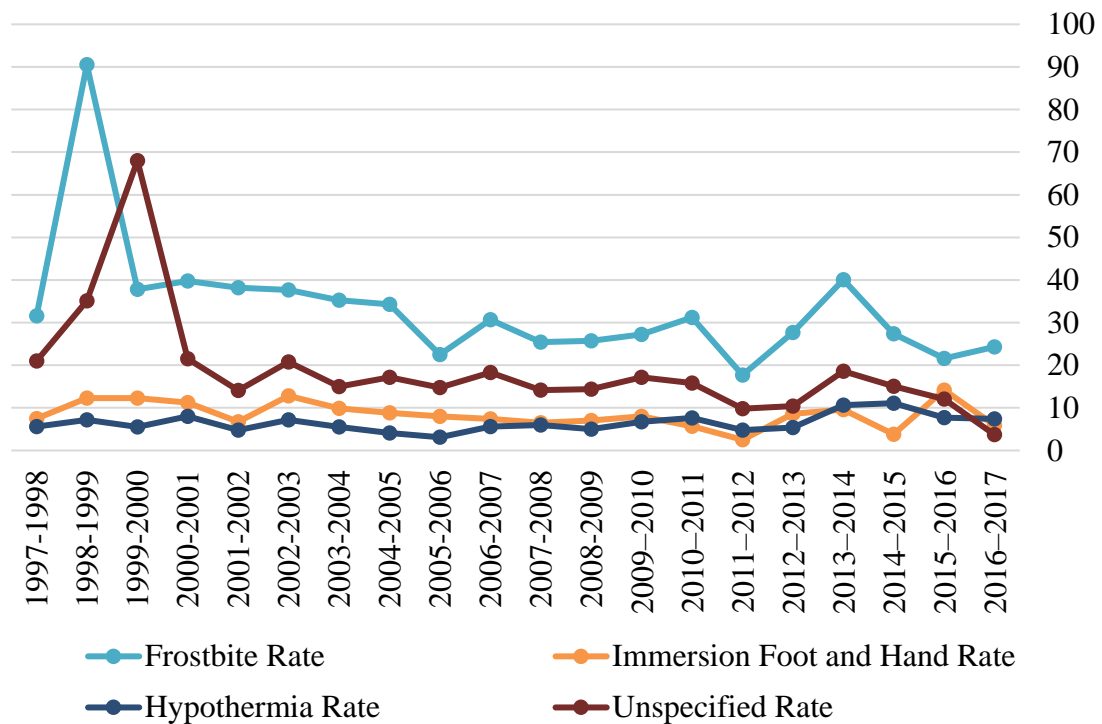


Figure 7. Rate of Incidences, per 100,000 person years, of Cold Injuries, Active U.S. Armed Forces, 1997-2017



2.2 Thermophysiology Basics

The human body is capable of maintaining thermal balance while operating within a wide range of temperatures. The human system generally maintains an internal core temperature (T_c) of approximately 37°C . Due to natural circadian rhythm, T_c fluctuates $\sim 0.5^{\circ}\text{C}$ daily. However, T_c can fluctuate based on physical activity or environmental conditions, and may range from $36.0 - 40.0^{\circ}\text{C}$. The microenvironment created between human skin and clothing typically must remain within $28-30^{\circ}\text{C}$ to maintain thermal homeostasis at rest [45]. This microenvironment changes significantly with physical activity due to metabolic heat production and air movement.

Fitness is a factor in coping with compensable heat stress, where thermoregulatory demands can be met by the body and the environment. Uncompensable heat stress occurs when thermoregulatory demands cannot be met by the body and the environment and poses a higher injury risk. Studies have shown that during activities or environments where uncompensable heat stress is imposed there is a 50% likelihood of injury at or around 39.5°C [46]. Most modeled endurance limits are set at 39°C for this reason. It is also important to mention that because of the complexity and inherent risks associated to operating at these higher thermal limits there is little research data collected with core body temperatures beyond these.

Humans have an internal control system, primarily the preoptic area of the anterior_hypothalamus, responsible for maintaining healthy body temperature. The hypothalamus uses feedback from two main sources, the skin and the blood. When temperature changes (hot or cold) are identified by either of these two sources, impulses are sent to the hypothalamus which in turn directs physiological changes to compensate for these temperatures. To protect from cold or heat injury, the human body attempts to either generate or dissipate heat to stay warm or cool off. Heat production is a natural process for humans and is a function of metabolism, oxidation of foods, and muscular activity. Heat transfer between the human and environment occurs via four pathways: conduction, convection, radiation, and evaporation. This heat exchange process is typically referred to as heat or thermal energy balance, and can be described as in the below equation:

$$S = M \pm W \pm R \pm C \pm K - E \text{ [W/m}^2\text{]} \quad (\text{Eq 1})$$

where S is heat storage; M is metabolic rate; W is work rate; R is radiation; C is convection; K is conduction; and E is evaporation. Radiation is heat that is transferred via electromagnetic waves (e.g., solar radiation). Conduction is heat transfer due to the body's direct contact with a solid object (e.g., touching a cold surface). Convection is heat transfer between the body and a fluid such as air or water. Evaporation is heat loss to the environment due to the phase change from liquid to vapor, typically associated with evaporation from sweat or respiratory water loss. Since evaporative heat is only lost to the environment, the sign is negative in Eq 1.

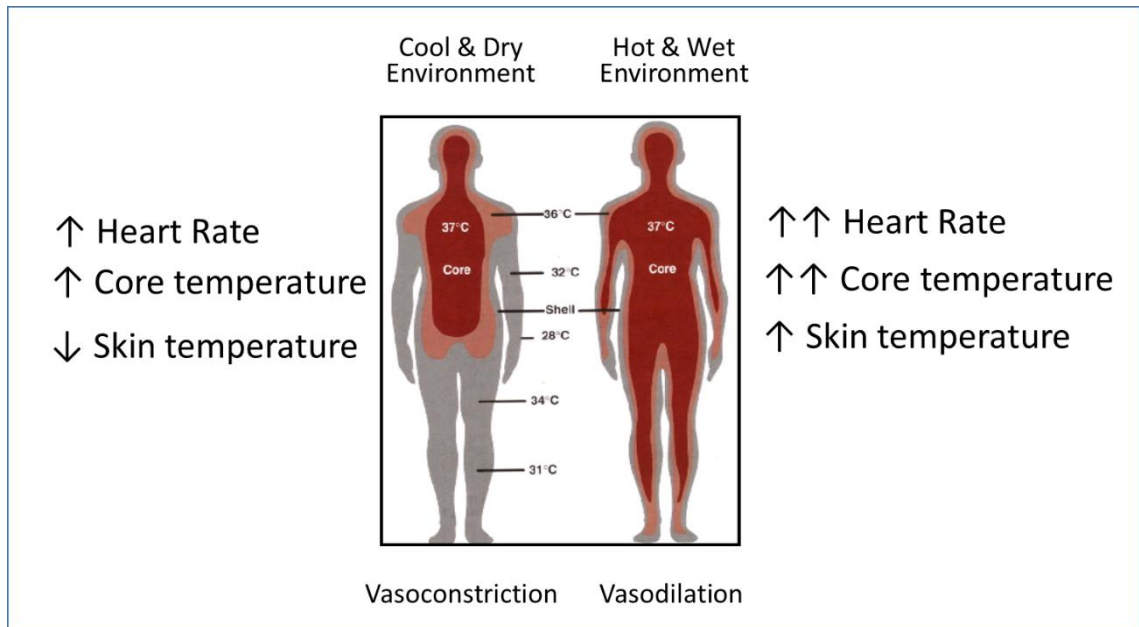
Looking at injuries for the two typical extremes of heat- (hyperthermia) and cold-related injuries (hypothermia), we can see that the general instances of these two events occur when the ability to maintain thermal balance is shifted in one direction. The body becomes hyperthermic when it is unable to dissipate enough heat to compensate for the heat gain from the environmental exposure and activity and thus is above goes above a safe core body temperature; while it becomes hypothermic when it is unable to produce or maintain enough heat to compensate with the environment and thus drops below the safe core body temperature [47].

Two key physiological responses include vasoconstriction and vasodilation [48-49]. Vasoconstriction is the constriction of blood vessels and occurs in response to cold environments to reduce the amount of blood flow to the extremities. Vasoconstriction protects the internal organs from cold exposure increases cold injury risk in the extremities due to lower blood flow and in-turn lower temperatures. Vasodilation is the essentially the opposite of vasoconstriction; where blood vessels are widened to allow increased blood flow across the body and out to the extremities to enable increased heat

dissipation [48-49]. During these responses, there are other associated physiological responses that help compensate for these demands (e.g., increased heart rate for increased blood flow, increased core temperature due to increased heart rate and blood flow).

Figure 8 shows these responses graphically.

Figure 8. Vasoconstriction and vasodilation in response to environmental conditions



When the human body begins to cool, blood flow is often reduced to the extremities (i.e., the hands and feet) decreasing the amount of warm blood flowing to these areas. For this reason, the extremities are more affected by cold exposure than other parts of the body. Also compounding this is the fact that the hands and feet have little local metabolic heat production capabilities. This lack of metabolic heat production is due to their inherently small muscle mass and large surface area to mass ratio that increases heat transfer from the body to the environment.

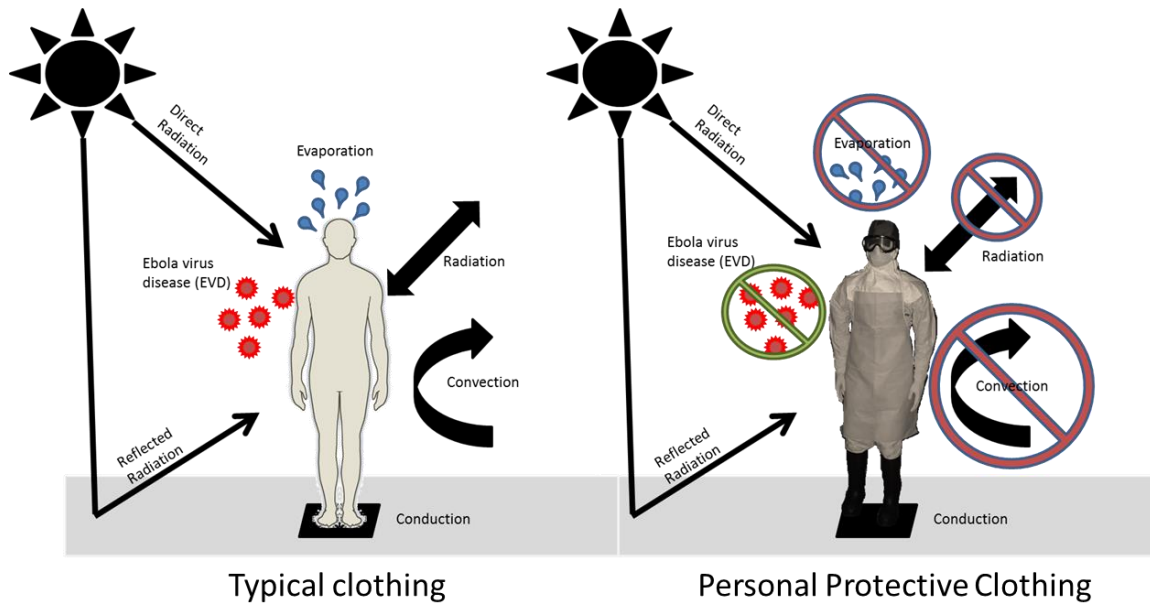
2.3 Importance of Clothing

For humans, clothing has long provided protection from environmental elements (heat, cold, etc.) or physical or biological hazards (e.g., rocks, thorns). Through changes in the human lifestyle and progression of civilizations, the aspects of protection have been less emphasized except for within harsher environments and activities. These include protection from the climatic elements (e.g., heat, cold, sun, rain, snow) but also include activities where hazards are expected such as during contact sporting events (football, hockey, etc.) or during military, law enforcement, or first responder operations (e.g., body armor, flame resistant clothing).

Performance needs vary widely among users and use cases. Due to this specificity, clothing systems need to be optimized to meet defined demands. Clothing can be optimized to account for several variables but is not likely, given current technologies, to be optimized for full spectrum of environmental hazards. For example, a single clothing ensemble cannot protect an individual from the extremes of the temperature spectrum of earth, being approximately -89°C at its coldest and 58°C at its warmest. However, optimal clothing for each end of this spectrum can be achieved; specifically from a thermal protection perspective, humans can survive in these environmental extremes given proper clothing [45]. Similarly, protections based on use cases should be designed with consideration for the specific end use. For example, protective equipment for American football players (i.e., pads and helmet) is vastly different than protective equipment worn by soldiers (i.e., body armor, ballistic helmet). Often added protection increases the thermal burden to wearers, and thus increases risk of heat injuries.

It is critical to understand the tradespace in order to predict and prepare for the impact clothing has on protecting or impairing human health. That is to say, understanding the human (physiology, anthropology, etc.), anticipated human activities (i.e., work rate and metabolic heat production), work environments (temperature, humidity, etc.), and the biophysical properties of clothing worn (heat transfer performance) in each scenario. An extreme example of this importance can be seen from healthcare responders working in West Africa during the Ebola response; where protective clothing is very effective at restricting viruses from infecting workers but at the same time reduces the individual's ability to dissipate heat to the environment [50; Fig 9).

Figure 9. Environmental Impact on the Human and Effects of Protective Clothing



2.3.1 Biophysics of Clothing

Clothing protects the wearer from environmental threats and imposes a level of thermal burden. Both the biophysical resistances (thermal and evaporative) and spectrophotometric (reflectance, absorptivity, and transmittance) properties of clothing

can have a significant influence on the impact of the environment on the wearer. To model these impacts on human thermal sensation (e.g., thermal comfort) and thermoregulatory responses (e.g., heat strain, cold protection), measurements of the biophysical properties and the spectrophotometric measures need to be used in mathematical models to simulate responses based on environmental conditions and activities. Critical measurements that are needed for modeling the impact of clothes on thermophysiological responses include thermal and evaporative resistances, wind effects, and spectrophotometric values.

Thermal and Evaporative Resistance

Sweating thermal manikins have long been used to provide biophysical measures of clothing and equipment worn by the human [51]. These measures can be used to estimate the level of imposed thermal stress (hot environment) or thermal protection (cold environment) provided by the ensemble. While direct biophysical comparisons can be helpful, i.e., comparing one ensemble's value to another [52], a more informative approach is to combine these measured values with thermoregulatory modeling. Models enable the prediction of thermoregulatory responses based on different individuals, as well as varied environments, clothing, or activity levels.

The current standard for testing using sweating thermal manikins calls for two fundamental measures: thermal resistance (R_t) [53] and evaporative resistance (R_{et}) [54]. These two measures represent the dry heat exchange (R_t : convection, conduction, and radiation) and wet heat exchange (R_{et} : evaporation). After converting both R_t and R_{et} into

units of clo and i_m [55, 56], a ratio can be used to describe an ensemble's evaporative potential (i_m/clo) [57].

Each ensemble should be tested using chamber conditions from the American Society for Testing and Materials (ASTM) standards for assessing R_t (ASTM F1291-10) and R_{et} (ASTM F2370-10) [53, 54] (Table 4).

Table 4. American Society for Testing and Materials standard chamber and manikin conditions for testing thermal (R_t) and evaporative (R_{et}) resistance

Variable (unit)	Skin / surface temperature (T_s , °C)	Ambient temperature (T_a , °C)	Relative humidity (RH, %)	Wind velocity (V , ms ⁻¹)	Saturation (%)
R_t (m ² K/W)	35	20	50	0.4	0
R_{et} (m ² Pa/W)	35	35	40	0.4	100

Thermal resistance (R_t) is the dry heat transfer from the surface of the manikin through the clothing and into the environment, mainly from convection, described as:

$$R_t = \frac{(T_s - T_a)}{Q/A} [\text{m}^2 \text{K/W}] \quad (\text{Eq 3})$$

where T_s is surface temperature and T_a is the air temperature, both in °C or °K. Q is power input (W) to maintain the surface (skin) temperature (T_s) of the manikin at a given set point; A is the surface area of the measurement in m². These measures of R_t can then be converted to units of clo:

$$1 \text{ clo} = 6.45(I_T) \quad (\text{Eq 4})$$

where I_T is the total insulation including boundary air layers. Evaporative resistance (R_{et}) is heat loss from the body in isothermal conditions ($T_s \approx T_a$), described as:

$$R_{et} = \frac{(P_{sat} - P_a)}{Q/A} [\text{m}^2 \text{Pa/W}] \quad (\text{Eq 5})$$

where P_{sat} is vapor pressure in Pascal at the surface of the manikin (assumed to be fully saturated), and P_a is vapor pressure, in Pascal, of the chamber environment. Measures of R_{et} can then be converted to a vapor permeability index (i_m), a non-dimensional measure of water vapor resistance of materials defined as:

$$i_m = \frac{60.6515 \frac{\text{Pa}}{^\circ\text{C}} R_{\text{ct}}}{R_{\text{et}}} \quad (\text{Eq 6})$$

Wind Effects on Thermal and Evaporative Resistance

In order to use the biophysical measures i.e., measures of R_t (clo) and R_{et} (i_m) for thermoregulatory modeling there is typically a need to first estimate the effects of wind velocity on the ensemble's biophysical characteristics (i.e., how changes in wind affect clo and i_m values). These effects are typically referred to as wind velocity coefficients or gamma values (γ) [58]. Historically, obtaining these coefficients consisted of collecting measurements of both R_t and R_{et} at multiple wind velocities, above the ASTM standard of 0.4 m/s. However, recent work suggests estimating these coefficient values can be estimated from single wind velocity tests [58-59].

Clothing properties and wind coefficients are critical inputs to predictive mathematical models such as the Heat Strain Decision Aid (HSDA) [60-62], or SCENARIO [63-64]. Additionally, a number of models use biophysical elements to describe wind-related effects using values such as as they use these values to describe wind-related effects, such as intrinsic insulation (I_{cl}) and intrinsic permeability index (i_{cl}) for either the whole body or segments of the body, as seen with:

$$I_{cl} = I_t - \left(\frac{I_a}{f_{cl}} \right) \quad (\text{Eq 7})$$

where I_a is insulation measured on a nude thermal manikin, I_t is total insulation, and (f_{cl}) is clothing area factor, calculated by:

$$f_{cl} = \frac{A}{A_{cl}} \quad (\text{Eq 8})$$

where A (m^2) is surface area of the nude manikin, and A_{cl} (m^2) is surface area the clothed manikin.

While true measures of A_{cl} require a three-dimensional scan; methods for estimating A_{cl} have been derived by McCullough et al., [65-66]. Simplified or estimated A_{cl} and f_{cl} is often used where a value of 1 is assumed for warm-weather or indoor clothing. For cold-weather clothing a value would be calculated from:

$$f_{cl} = 1.0 + .3 \cdot I_{cl} \quad (\text{Eq 9})$$

While these estimation methods have been studied and produce acceptable variance between estimated and direct measured results [67], there are questions whether estimates remain acceptable for clothing insulation outside typical cold weather clothing insulation ranges, e.g., 0.2-1.7 clo [68]. These models, by design, predict human thermoregulatory responses to various environmental conditions and therefore require quantitative insights into the change in clothing properties with changes in wind velocity. Furthermore, elements of wind can significantly influence physiological responses and injury outcomes in cold environments due to wind chill effects [20, 69-70]. There has

been work to determine a chart with points of predicted injury (e.g., frostbite) that will likely occur due to temperature and levels of wind speed exposure [69; Figure 10].

Figure 10. Wind chill temperature chart [69] modified to include levels of risk [20]

Air Temperature (°C)												
Wind Speed (km/h)	5	0	-5	-10	-15	-20	-25	-30	-35	-40	-45	-50
5	4	-2	-7	-13	-19	-24	-30	-36	-41	-47	-53	-58
10	3	-3	-9	-15	-21	-27	-33	-39	-45	-51	-57	-63
15	2	-4	-11	-17	-23	-29	-35	-41	-48	-54	-60	-66
20	1	-5	-12	-18	-24	-30	-37	-43	-49	-56	-62	-68
25	1	-6	-12	-19	-25	-32	-38	-44	-51	-57	-64	-70
30	0	-6	-13	-20	-26	-33	-39	-46	-52	-59	-65	-72
35	0	-7	-14	-20	-27	-33	-40	-47	-53	-60	-66	-73
40	-1	-7	-14	-21	-27	-34	-41	-48	-54	-61	-68	-74
45	-1	-8	-15	-21	-28	-35	-42	-48	-55	-62	-69	-75
50	-1	-8	-15	-22	-29	-35	-42	-49	-56	-63	-69	-76
55	-2	-8	-15	-22	-29	-36	-43	-50	-57	-63	-70	-77
60	-2	-9	-16	-23	-30	-36	-43	-50	-57	-64	-71	-78
65	-2	-9	-16	-23	-30	-37	-44	-51	-58	-65	-72	-79
70	-2	-9	-16	-23	-30	-37	-44	-51	-58	-65	-72	-80
75	-3	-10	-17	-24	-31	-38	-45	-52	-59	-66	-73	-80
80	-3	-10	-17	-24	-31	-38	-45	-52	-60	-67	-74	-81

FROSTBITE GUIDE	
Low risk of frostbite for most people	
Increasing risk of frostbite for most people in 10 to 30 minutes of exposure	
High risk for most people in 5 to 10 minutes of exposure	
High risk for most people in 2 to 5 minutes of exposure	
High risk for most people in 2 minutes of exposure or less	

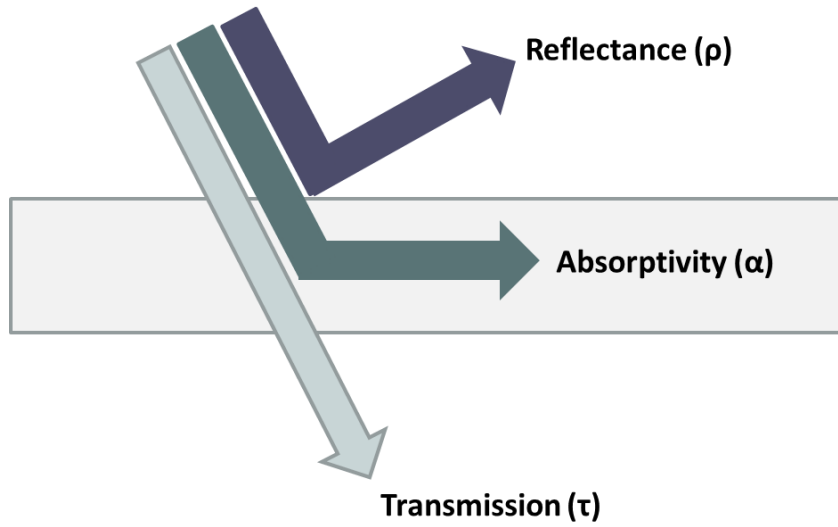
Spectrophotometry

Thermal effects from solar load (i.e., net radiant load) are dependent on the intensity of that load (i.e., radiant flux), clothing properties (i.e., emissivity, absorptivity, transmissivity) and the total area exposed to that given load [71]. The radiant balance can be used to describe the net solar effect; where the net solar balance (G_{λ}) is a function of reflection ($G_{\lambda}\rho$), absorption ($G_{\lambda}\alpha$), and transmission ($G_{\lambda}\tau$):

$$G_{\lambda} = G_{\lambda}\rho + G_{\lambda}\alpha + G_{\lambda}\tau \quad (\text{Eq 10})$$

Reflection ($G_{\lambda}\rho$) is radiation redirected back into the environment, absorption ($G_{\lambda}\alpha$) is absorbed into the material or surface, and transmission ($G_{\lambda}\tau$) is passed through the material (Figure 11).

Figure 11. Spectrophotometric measures of a material



Key equations for these spectrophotometric measurements include:

$$G_{\lambda}\rho = \frac{I_{\lambda}(\text{reflected})}{I_{\lambda}(\text{incident})} \quad (\text{Eq 11})$$

$$G_{\lambda}\alpha = \frac{I_{\lambda}(\text{absorbed})}{I_{\lambda}(\text{incident})} \quad (\text{Eq 12})$$

$$G_{\lambda}\tau = \frac{I_{\lambda}(\text{transmitted})}{I_{\lambda}(\text{incident})} \quad (\text{Eq 13})$$

where I_{λ} is the monochromatic intensity of radiation given as a unit of time.

Whole-human and components

An additional element for consideration is the difference between use and measurement of whole-human ensembles versus component pieces (e.g., gloves, boots). The same principles of testing can be applied to whole ensembles or individual components. However, it is important to understand that the collection of items cannot be simply summed to make the value of a total ensemble or added layers [72]. This is mainly due to the difference in air space within layers or across surfaces. The biophysical properties of clothing include the air gap (R_{gap}), clothing textile (R_{cl}), and boundary layer (R_{bl}); where the total resistance is: $Resistance = R_{gap} + R_{cl} + R_{bl}$. The air gap factor is influential as a role in determining the overall value; therefore the amount of space between the head and material can change the overall thermal properties.

All this said, component items can be tested individually using the above principles outlined in equations 3 and 5. However, if these tests were to be used with the intent of being included into modeling of a full ensemble we must account for sections of the full manikin using the below set of equations.

$$Q_i = \frac{A_i \cdot (T - T_a)}{R_i} \quad (\text{Eq. 14})$$

$$Q_{total} = \sum_i^n Q_i = \frac{A_{total} \cdot (T - T_a)}{R_{total}} \quad (\text{Eq. 15})$$

$$\frac{A_{total}}{R_{total}} = \sum_i^n \frac{A_i}{R_i} \quad (\text{Eq. 16})$$

$$R_{total} = \frac{A_{total}}{\sum_i^n \frac{A_i}{R_i}} \quad (\text{Eq. 17})$$

where Q is heat loss (W); A is the surface area of the section (m^2); R is thermal resistance ($\text{m}^2\text{C}/\text{W}$); T is surface temperature of the manikin ($^{\circ}\text{C}$); i is the section number; and n is the total number of sections.

This approach may be useful when specifically modeling the effect one item has on a human's response. For example, if the materials are changed for a set of gloves or head worn item, a mathematical replacing of data could be done to a whole ensemble to provide an estimate of the change in total biophysical properties of an ensemble as a result of that item. However, it is often difficult to see meaningful differences in the total values, as component items generally cover relatively small surface areas in comparison to the overall human. An example of this can be found in the application of this approach by Potter et al., [73], where values of two different head worn covers were tested and 'swapped' into a full ensemble and then modeled. While if there are differences in the component item properties they will be reflected in the modeled outcomes; these differences may be in effect negligible (Figure 12). As the head and neck account for ~ 8% (0.14 m^2) of a total surface area of a full human or test manikin (1.81 m^2), the total uncovered face and neck account for the majority of this space leaving only 1-2 % surface area coverage from a military cover. Weighting these values has a proportionate effect. Figure 13 shows a surface area breakdown of a 20 zone manikin (Newton model, Thermetrics, Seattle, WA; www.Thermetrics.com).

Figure 12. Predicted core body temperature response during moderate walking – a comparison of two different head-worn covers [73]

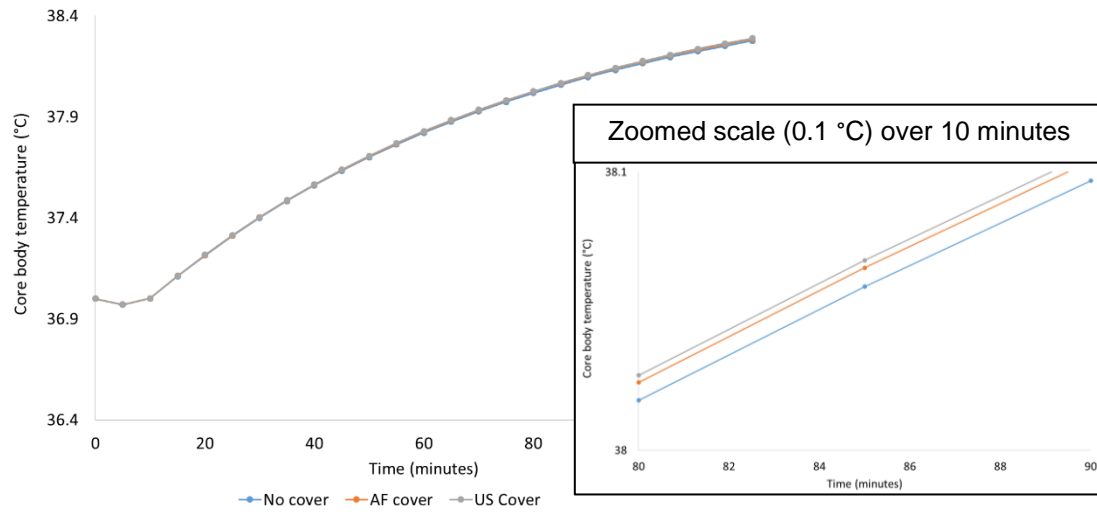
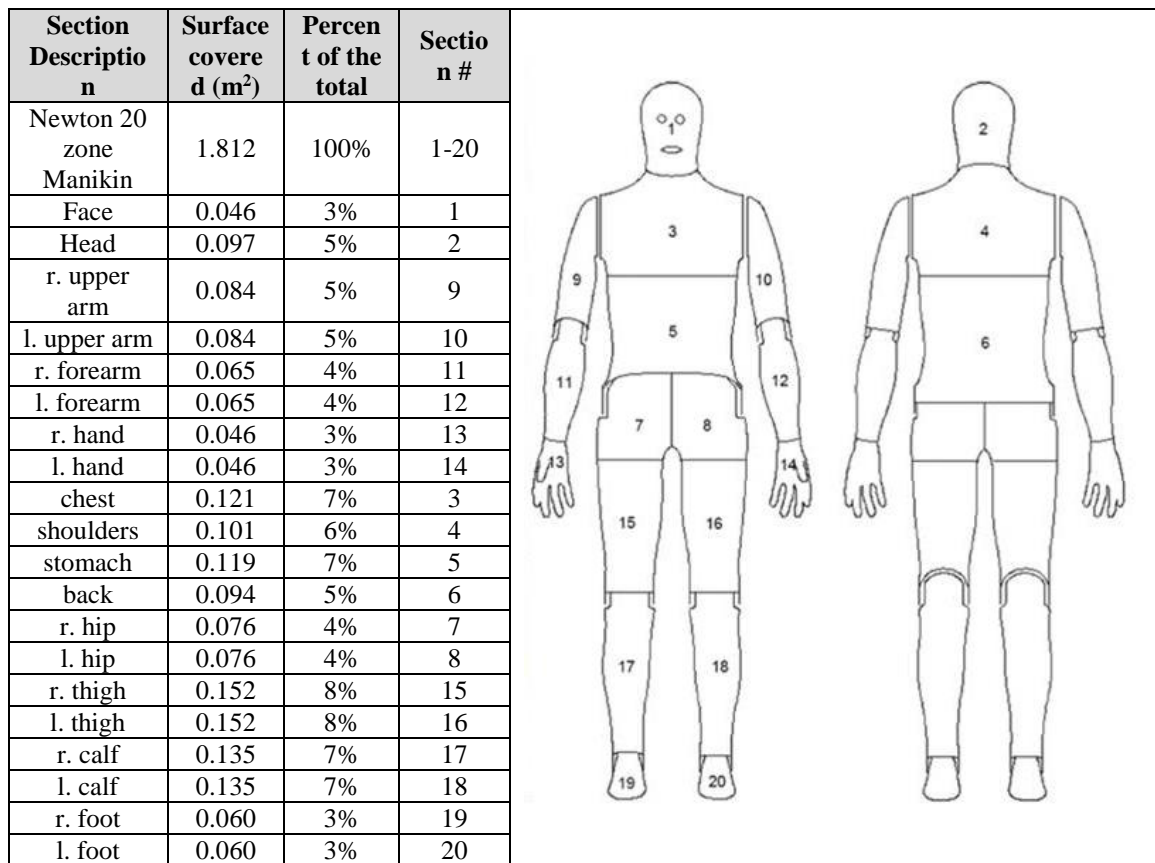


Figure 13. Surface area of the manikin

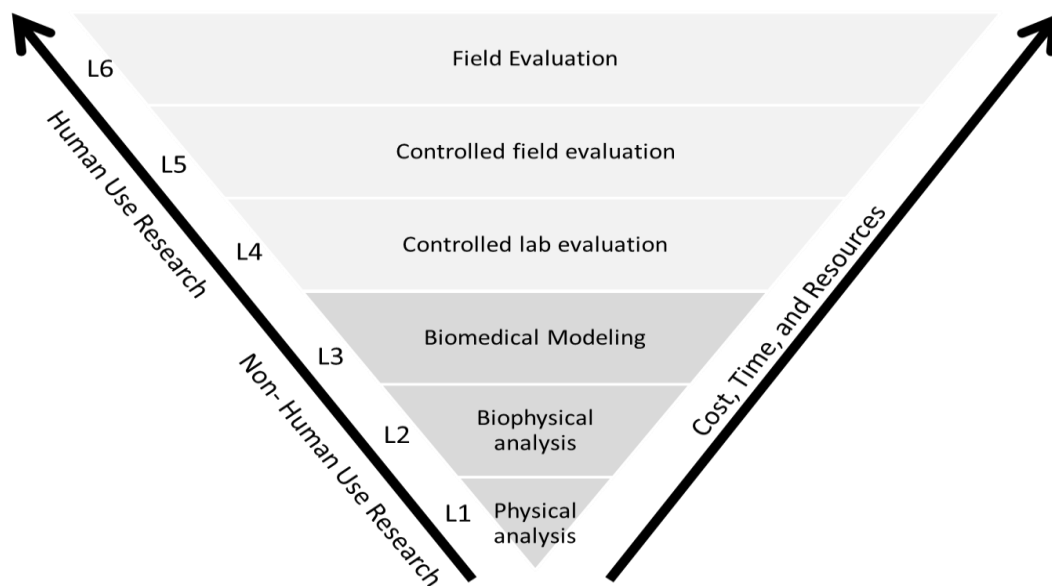


III. Methods

3.1 Overall Study Design

This study uses a model-test-model paradigm [74] and advocates for stepwise order of testing to ensure efficient use of resources and effective use of human research. Figure 14 outlines the ideal stages of testing related to studying the properties of clothing as they relate to their influence on humans. The basics include testing of the physical clothing and properties and then progressing to more elaborate and typically resource costly human studies.

Figure 14. Levels of clothing system testing [69]



The general steps of the model-test-model design for this study are:

- Conduct broad literature review and evaluation, as well as re- and reverse-engineering of existing published modeling methods (*Model*)

- Collate, collect, and evaluate human research data to investigate the individualized relationship to clothing, thermoregulation, and environment (*Test*)
- Develop rational, empirical, and machine learning methods for predicting thermoregulatory responses and/or injury risks based on individual, clothing, activity, and environment (*Model*)

Data collected for this work are summarized in Table 5. For this study a combination of human data and non-human (clothing) data will be used to conduct two broad assessments; one assessment will specifically look at the predictability of heat stress response (i.e., core body temperature changes) and the second will look at cold stress responses (i.e., skin temperature changes).

Table 5. Summary of Study Data

Type →	Human	Non-human (clothing)
Data Sample Size	N = 51	N = 93
Population	Adult Males / Females	Thermal Sweating Manikin
Ages	Ages 18-48	N/A
Setting	Laboratory and Field	Controlled climate chamber - Laboratory
Measures, Variables, etc.	ECG/HR, T _c , T _{sk} , VO ₂ , accelerometry Chamber / Environmental conditions (Ta, RH, wind velocity, T _{mr})	Thermal Resistance (R_t) Evaporative Resistance (R_{et}) Vapor permeability (i_m) Evaporative potential (i_m/clo) Chamber conditions (Ta, RH, wind velocity, T _{mr})

3.2 Human Research Study Design

This study is divided into two distinct test assessments: Assessment 1 relates to heat stress responses to hot environmental conditions and Assessment 2 relates to cold stress response to cold environmental conditions. Previously collected and proactively collected experimental data from human physiological studies will be used to refine and develop models to predict thermal injuries (via changes in skin and core body temperature). Targeted study data and descriptions are included in the sections below. Modeling approaches seek to develop rational and empirically-based equations and methods that will be combined for hybrid or multi-model designed solutions.

Algorithms and more complex mathematical models offer useful ways to organize scientific knowledge and to predict human performance. However, as part of a model-test-model process [74], it is important for continued research specific to populations and scenarios to ensure optimal estimations. For cost effectiveness, a continued approach to simulations and modeling methods should be sought rather than moving directly into human research and user field evaluations.

3.2.1 Assessment 1 – Heat Stress

For Assessment 1, the accuracy of the HSDA [60] was assessed for predicting T_c changes during a laboratory and a field experiment. This modeling method for both the laboratory and field experiments assessed healthy individuals wearing chemical protective clothing ensembles during activities. The laboratory study volunteers (n=8) conducted intermittent treadmill marching in a hot and humid environmental chamber; while the field experiment monitoring individuals (n=20) during a prolonged road march in hot and humid outdoor conditions. The volunteer descriptive data are included in Table 6.

The volunteers for the field study wore different chemical protective clothing ensembles during four field tests scheduled every other day. During each test, volunteers marched for 120 min at a set pace of $1.10 \text{ m}\cdot\text{s}^{-1}$ on a 0% grade paved road. The combined weight of clothing and external loading was $15.6 \pm 1.1 \text{ kg}$. Core body temperature was measured minute-by-minute using a rectal thermometer (Respironics Mini Mitter, Inc., Bend, OR).

For the laboratory testing, volunteers wore a different chemical clothing ensembles for the three tests in a controlled environmental chamber. During each trial, volunteers walked for 60 min on a treadmill at $0.84 \text{ m}\cdot\text{s}^{-1}$ on a 0% grade, rested for 10 min, and then walked for 30 min at $1.68 \text{ m}\cdot\text{s}^{-1}$ on a 3% grade. Core body temperature was measured minute-by-minute using a rectal thermometer (Edale Instruments Ltd, U.K.) intent of this data has been previously published [75-76].

Table 6. Assessment 1 – Heat Stress. Human Data Descriptive Statistics

Conditions	Sample	Age (years)	Height (cm)	Weight (kg)	Body surface area (m^2)
Laboratory – $T_a 29.3 \pm 0.3^\circ\text{C}$; RH $56 \pm 7\%$; wind speed $0.4 \pm 0.1 \text{ m}\cdot\text{s}^{-1}$	N = 8 (males)	24 ± 6	178 ± 5	76.6 ± 8.4	1.94 ± 0.1
Field – $T_a 26.0 \pm 0.5^\circ\text{C}$; RH $55 \pm 3\%$; wind speed $4.3 \pm 0.7 \text{ m}\cdot\text{s}^{-1}$	N = 20 (1 female)	26 ± 5	175 ± 8	80.2 ± 12.1	2.0 ± 0.2

Assessment 2 – Cold Stress

For assessment 2, four different studies were combined for a total of 23 healthy human research volunteer individual datasets. All data used for this work have been collected from published datasets [77-82] and is summarized in Table 7.

Volunteers for the laboratory study by Santee et al., [77-79] were assessed during treadmill walking (120 minutes) and sitting (125 minutes) in cold climate chamber (-6.7 and 0°C). During testing temperatures measures were obtained for core body and fingers, along with continuous heart rate (HR) [77-79]. Volunteers from the laboratory study by Gonzalez et al., [80] sat at rest and conducted treadmill walking in three cold chamber conditions (0, -20, and -30°C) for a maximum of 120 minutes per test. Continuous temperature measures of core body, middle finger, and mean weighted skin were collected, along with periodic measures of heart rate and VO_2 [80]. Volunteer information from Hickey et al., [81] is not reported. During this study, subjects were monitored in extreme cold climate chamber conditions (-40°C) for trials in 120 minute and 240 minute exposures, where they sat and conducted treadmill walking. Measures of core body and skin temperature were collected during study activities [81]. Volunteers from the laboratory study by Castellani et al., [82] were monitored while sitting in cold climate conditions (0.48°C). During trials skin temperature and heat flux was measured at 13 points of the body [82].

Table 7. Assessment 2 – Cold Stress. Human Data Descriptive Statistics

Conditions	Sample	Age (years)	Height (cm)	Weight (kg)	Body surface area (m ²)
Laboratory – T_a 0 and -6.7°C; wind speed 1.1 m·s ⁻¹)	N = 5	22 ± 3	172 ± 5	71.6 ± 7	1.85 ± 0.1
Laboratory – T_a 0, -20, -30°C; RH 20%; wind speed 1.34 m·s ⁻¹	N = 6	24 ± 5	175 ± 4	68.8 ± 11.1	1.83 ± 0.2
Laboratory – T_a -40°C	N = 4	UNK	UNK	UNK	UNK
Laboratory – T_a 0.47°C ± 0.5°C; RH 51 ± 3%; wind speed 1.34 m·s ⁻¹	N = 8 (2 females)	26 ± 9	170 ± 6	77.6 ± 16.2	1.89 ± 0.2

3.3. Non-Human Research Design

Standard testing were conducted to assess the biophysical properties for 93 different types of clothing ensembles using a thermal sweating manikin (Newton model, Thermetrics, Seattle, WA; www.Thermetrics.com). The thermal and evaporative resistances (R_t and R_{et}) were assessed according to American Society for Testing and Materials (ASTM) standard (ASTM F1291-16 & ASTM F2370-16) [53-54]. Tested ensembles included various levels of clothing to include: simple exercise clothing (n=5), general clothing (e.g., long sleeve shirt and pants) (n=8), military combat clothing (e.g., general clothing with body armor and equipment) (n=22), chemical protective clothing (e.g., hazmat suits) (n=26), explosive ordnance disposal suits (n=4), and various cold weather clothing ensembles (n=28). A summary of this clothing is shown in Table 8 and biophysical values are outlined in the results section of this report. Full descriptions and

pictures of many of these ensembles can be found in various papers and government technical reports [50, 52, 71, 83-87].

Table 8. Summary of Non-human (clothing) data

Group#	Sample	Type of Clothing (Simple)	Clothing Details	Variables	Comments
1	N=5	Fitness clothing	T-Shirts, Shorts, Sneakers, underwear	Thermal Resistance ($R_{t,clo}$) Evaporative Resistance (R_{et}) Vapor permeability (i_m) Evaporative potential ($i_{m/clo}$) Multiple wind speed conditions Spectrophotometric values	Spectrophotometry used for comparison of color in materials to compare solar impact of black versus grey
2	N=8	Regular clothing	Long-sleeve shirt, undershirt, underwear, pants, boots	Thermal Resistance ($R_{t,clo}$) Evaporative Resistance (R_{et}) Vapor permeability (i_m) Evaporative potential ($i_{m/clo}$) Multiple wind speed conditions	Multiple configurations and material designs
3	N=22	Combat clothing with body armor	Long-sleeve shirt, undershirt, underwear, pants, helmet, body armor vest (with and without ceramic plate inserts), boots	Thermal Resistance ($R_{t,clo}$) Evaporative Resistance (R_{et}) Vapor permeability (i_m) Evaporative potential ($i_{m/clo}$) Multiple wind speed conditions	Multiple configurations and material designs
4	N=26	Chemical protective clothing	Chemical, biological, radiological, nuclear (CBRN) clothing. Respirators, face/gas masks, full clothing ensemble, underwear, boots and over boots	Thermal Resistance ($R_{t,clo}$) Evaporative Resistance (R_{et}) Vapor permeability (i_m) Evaporative potential ($i_{m/clo}$) Multiple wind speed conditions	Multiple configurations and material designs
5	N=4	Explosive ordnance disposal suits	Explosive ordnance disposal (EOD) suits, added CBRN protective layers, with and without underclothing	Thermal Resistance ($R_{t,clo}$) Evaporative Resistance (R_{et})* Vapor permeability (i_m)* Evaporative potential ($i_{m/clo}$)* Multiple wind speed conditions	Suits consisted of varied design configurations of full body armor protective suits. *Suits measured as effectively vapor impermeable
6	N=28	Cold weather clothing	Long-sleeve shirt, undershirt, underwear, pants, over suit, parka, jacket liner, winter coat, long-sleeve and pant underwear layer, knit hat, baklava face cover	Thermal Resistance ($R_{t,clo}$) Evaporative Resistance (R_{et}) Vapor permeability (i_m) Evaporative potential ($i_{m/clo}$) Multiple wind speed conditions	Multiple configurations and material designs

3.4 Modeling Risk and Predicting Heat and Cold Related Injuries

Human thermal response (e.g., metabolic heat production, core body temperature (T_c), endurance time) resulting from activity, environment, and clothing can be predicted through mathematical modeling. Mathematical models are typically binned into one of three categories, rational, empirical, and hybrid. Rational (mechanistic) models mathematically represent phenomena based on understanding of physics and physiology (biology, chemistry, physics). In contrast, empirical (functional) models mathematical reflect the observed relationship among experimental data. While both methods, rational

and empirical, are scientifically valid approaches, perhaps the most effective approach is the hybrid or mixed model method that uses a combination of the two.

3.4.1 Rational Models

Rational modeling incorporates equations that describe heat balance and thermoregulatory processes [88]. Two fundamental equations are used to describe internal heat balance and for heat exchange between skin and environment. One equation outlines the temperature gradient change from core to skin and can be seen as:

$$\rho c \cdot \frac{\partial T}{\partial t} = q_m + \lambda \cdot \nabla^2 T + \omega_{bl} \cdot \rho_{bl} c_{bl} \cdot (T_{bl} - T) \quad [W \cdot m^{-3}] \quad (\text{Eq 18})$$

where ρ is tissue mass ($kg \cdot m^{-3}$), c is the specific heat of the tissue ($kJ \cdot kg^{-1} \cdot ^\circ C^{-1}$), T is the tissue temperature ($^\circ C$), t is time (sec), q_m is metabolic heat production rate ($W \cdot m^{-3}$), λ is the tissue heat conductivity ($W \cdot m^{-1} \cdot ^\circ C^{-1}$), ∇^2 is a Laplace transform for heat conduction based on the tissue temperature gradient, ω_{bl} is blood flow rate ($m^3 \cdot s^{-1} \cdot m^{-3}$ tissue), ρ_{bl} is blood flow mass ($kg \cdot m^{-3}$), c_{bl} is the blood specific heat ($kJ \cdot kg^{-1} \cdot ^\circ C^{-1}$), and T_{bl} is the blood temperature ($^\circ C$).

The second equation needed for rationally modeling heat exchange from the skin surface to the environment is:

$$-\lambda \cdot \frac{\partial T}{\partial n} = R + C + K + E \quad [W \cdot m^{-2}] \quad (\text{Eq 19})$$

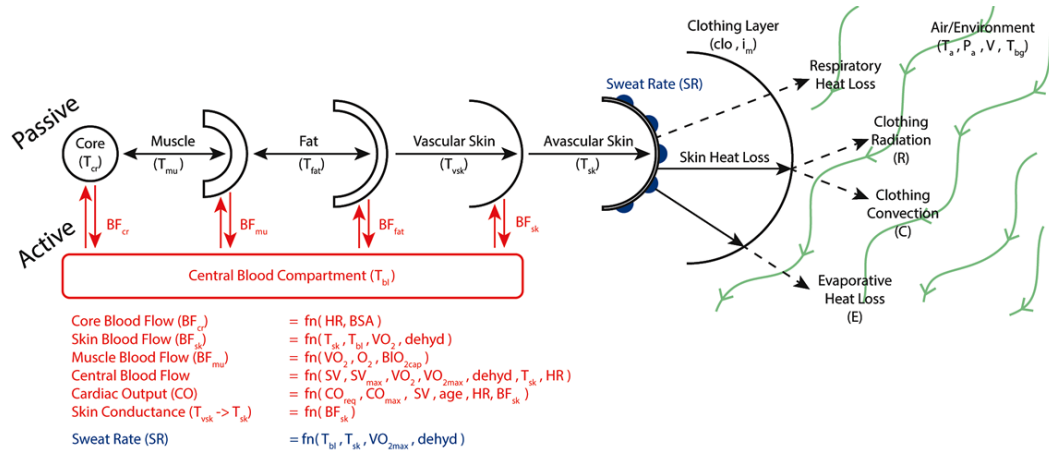
where λ is the tissue heat conductivity ($W \cdot m^{-1} \cdot ^\circ C^{-1}$), T is tissue temperature ($^\circ C$), n is the tissue coordinate normal to the skin surface; while the balance is the array of avenues of heat exchange ($W \cdot m^{-2}$): R is radiative, C is convective, K is conductive, and E is evaporative.

Rational models of thermoregulatory processes usually include equations for the controlling signals of the thermoregulation system and equations for thermoregulatory

actions such as sweating, vasodilation, vasoconstriction, and shivering. Examples of rational models are the 2-node model [89], the SCENARIO one cylinder model [63-64] and the Six Cylinder Thermoregulatory Model (SCTM) [90].

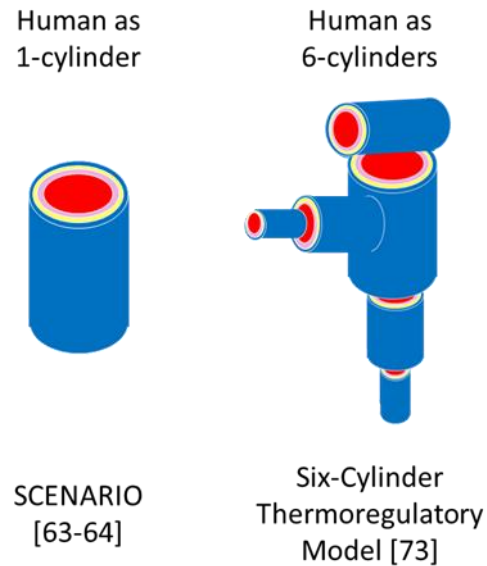
Understanding the interplay between each of the different layers of the human (grossly consisting of core, muscle, fat, and skin) along with clothing and air layers within clothing is only the first step to modeling the human's response in a given environment. Figure 15 shows the rational basis behind the SCENARIO model where the human is mathematically represented as one cylinder, based on the relationship of the layers of the human, their respective physiological responses, and clothing [64].

Figure 15. SCENARIO Model fundamental rational basis [64]



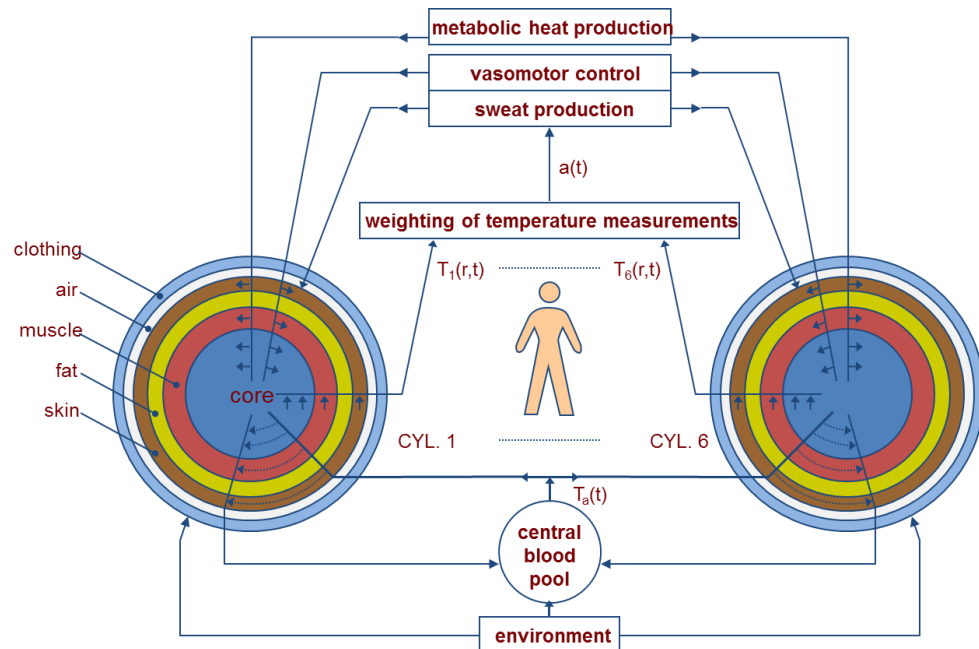
Contrary to the one cylinder approach of the SCENARIO model [64], the model from Xu and Werner [90] pays particular attention to cold exposure thermoregulatory responses, sectioning the human model into six sections (head, torso, arms, hands, legs, and feet) to represent the complex responses of the human extremities within cold environments (Figure 16).

Figure 16. Comparison of one- and six-cylinder thermoregulatory models



A simplification of these key factors is shown in Figure 17, in a recreated figure from Xu and Werner [90]; where heat transfer within these layers is considered, along with environmental conditions and thermoregulatory responses (metabolism, vasomotor control, sweat production, and blood pooling).

Figure 17. Dynamic model of human thermoregulation Xu and Werner [90]



3.4.2 Empirical Models

Empirical models are mathematical representations of data, often using statistical methods such as regression or correlational analysis. The Heat Strain Decision Aid (HSDA) is an empirical model derived from an extensive database of human studies that incorporates the biophysics of heat exchange developed by the U.S. Army Research Institute of Environmental Medicine (USARIEM) [60-62]. HSDA predicts core temperature, maximum work times, sustainable work-rest cycles, water requirements, and the estimated likelihood of heat casualties. This model has been used to support the development of guidance and doctrine for military [91] and fluid intake guidance for the public [92]. The basis of HSDA includes both principles of heat exchange along with empirical predictions of physiological responses. Collectively 16 inputs from four elements (individual characteristics, physical activity, clothing biophysics, and environmental conditions) are used to mathematically predict rise in core body temperature over time [60]. Table 9 and 10 below outline the published equations that make up the required inputs (Table 9) and the fundamental equations of this heat strain specific model (Table 10); while the modeling methods are drawn in the schematic shown in Figure 18 [60].

Table 9. Required inputs to HSDA model

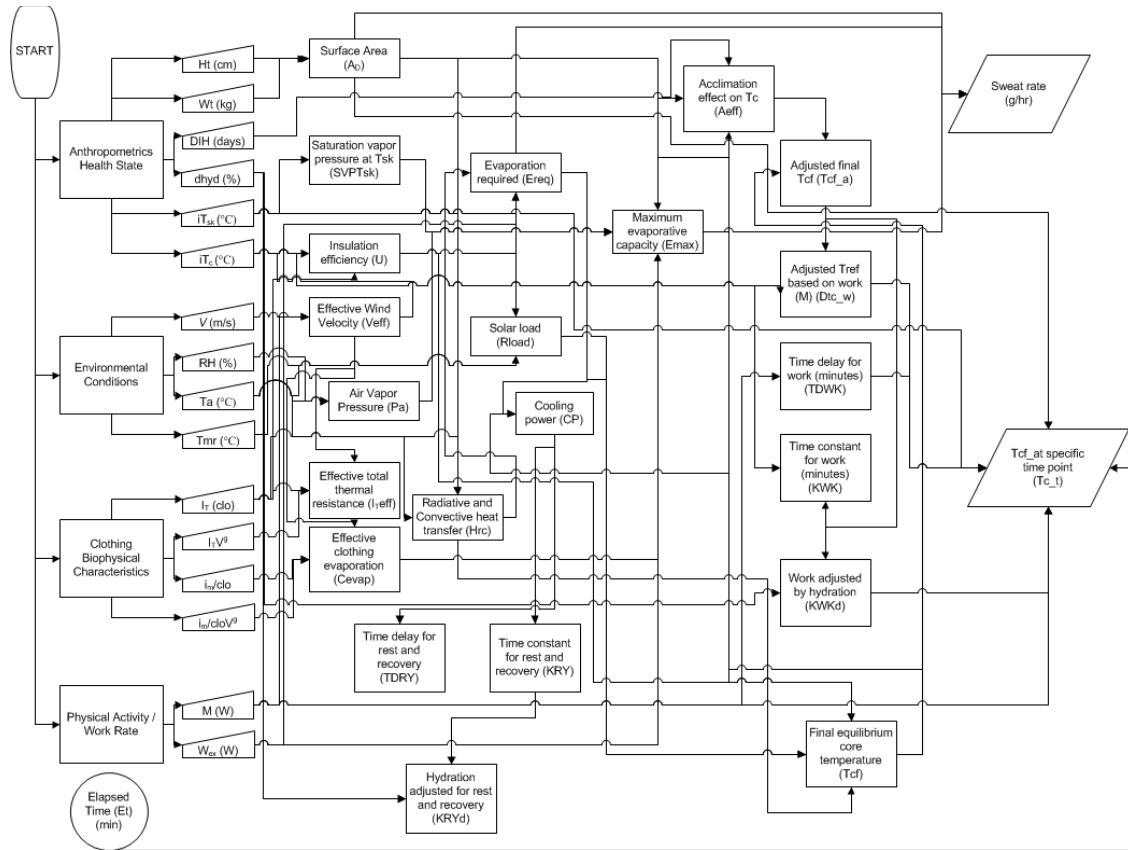
Element	Symbol	Description	units
Anthropometrics / Health State	Ht	Height	cm
	Wt	Weight	kg
	DIH	Days in heat; days of heat acclimation	days
	$dhyd$	Dehydration status	%
	iT_{sk}	Initial skin temperature	°C
	iT_c	Initial core body temperature	°C
Environmental Conditions	V	Wind velocity	m/s
	RH	Relative humidity	%
	T_a	Ambient temperature	°C
	T_{mr}	Mean radiant temperature	°C
Clothing Biophysical Characteristics	I_T	Total thermal resistance	clo
	I_TV^g	Thermal resistance wind velocity coefficient / gamma	N.D.
	i_m/clo	Evaporative potential	N.D.
	$i_m/cloV^g$	Evaporative potential wind velocity coefficient / gamma	N.D.
Physical Activity / Work Rate	\dot{M}	Metabolic heat production / metabolic rate	W
	W_{ex}	External work rate	W

Table 10. HSDA Fundamental Equations

Measure / Component	Equation	units	Eq # this paper
Body Surface Area (A_D)	$A_D = 0.007184 \cdot Ht^{0.725} \cdot Wt^{0.425}$	m ²	20
Effective wind velocity (V_{eff})	$V_{eff} = V + 0.004 \cdot (M - 105)$ $V_{eff} = 0.11 + V + \beta \cdot V_{walk} \ (\beta = 0.67 \text{ for walking})$	m/s	21
Air Vapor Pressure (P_a)	$P_a = 10^{(8.1076 - \frac{1750.286}{T_a + 235})} \cdot (\frac{RH}{100})$	Torr	22
Effective total thermal resistance (I_{Teff})	$I_{Teff} = I_T \cdot V_{eff}^{I_TV^g}$	Clo	23
Effective clothing evaporation (C_{evap})	$C_{evap} = \frac{i_m}{clo} \cdot V_{eff}^{i_m/cloV^g}$	i _m /clo	24
Radiative and Convective heat transfer (H_{rc})	$H_{rc} = 6.45 \cdot A_D \cdot \frac{T_a - T_{sk}}{I_{Teff}}$	W	25
Insulation efficiency (U)	$U = \left(\frac{0.41}{I_T}\right) \cdot V_{eff}^{(-0.43 + cloV^g)}$	N.D.	26
Solar load (R_{load})	$R_{load} = (-0.071 \cdot (T_{mr} - T_a)^2 + 10.432 \cdot (T_{mr} - T_a))$ $\cdot (A_D/1.8)$	W	27

Evaporation required (E_{req})	$E_{req} = H_{rc} + M - W_{ex} + U \cdot R_{load}$	W	28
Saturated Vapor Pressure at skin ($SVPT_{sk}$)	$SVPT_{sk} = 10^{(8.1076 - \frac{(1750.286)}{T_{sk} + 235})}$	Torr	29
Maximum evaporative capacity (E_{max})	$E_{max} = 14.21 \cdot A_D \cdot C_{evap} \cdot (SVPT_{sk} - P_a)$	W	30
Maximum evaporative capacity at altitude (E_{maxA})	$P_{atm} = (1 - 2.5577 \cdot 10^{-5} \cdot Z)^{5.2559}$ $I_{TA} = I_T \cdot (P_{atm} \cdot V_{eff})^{I_T V^g}$ $E_{maxA} = P_{atm}^{-0.45} \cdot LR \cdot 6.45 \cdot A_D \cdot C_{evap} \cdot (SVPT_{sk} - P_a)$	W	31
Final equilibrium core temperature (T_{cf})	$T_{cf} = (36.75 + 0.004 \cdot M + 0.0025 \cdot U \cdot R_{load} + 0.0011 \cdot H_{rc} + 0.8 \cdot \exp(0.0047 \cdot (E_{req} - E_{max})))$	°C	32
Heat acclimation effect on T_c (A_{eff})	$A_{eff} = (0.5 + 1.2 \cdot (1 - \exp(\frac{37.15 - T_{cf}}{2}))) \cdot (1 - \exp(-0.005 \cdot E_{max})) \cdot (\exp(-0.3 \cdot DIH))$	N.D.	33
Adjusted T_{cf} from acclimatization ($T_{cf,a}$)	$T_{cf,a} = T_{cf} + A_{eff}$	°C	34
Adjusted T_c based on work ($D_{tc,W}$)	$D_{tc,W} = T_{cf,a} - T_{c,i}$	°C	35
Sweat rate (Swt)	$Swt = 27.9 \cdot A_D \cdot \left(\frac{E_{req}}{A_D}\right) \cdot \left(\frac{E_{max}}{A_D}\right)^{(-0.455)}$	g/hr	36
Improved piecewise (PW) Swt	$PW = 147 + (1.527 \cdot E_{req}) - (0.87 \cdot E_{max})$	g/hr	37
Time delay for work (TDWK)	$TDWK = \frac{3480}{M}$	°C/min	38
Time constant for work (KWK)	$KWK = \frac{[1 + 3 \cdot \exp(0.3 \cdot (T_{c,i} - T_{cfa}))]}{225}$	N.D.	39
Work adjusted by hydration (KWKd)	$KWKd = KWK \cdot (1 + 0.1 \cdot dhyd)$	N.D.	40
Cooling power (CP)	$CP = 0.015 \cdot (E_{max} - E_{req})$	W	41
Time delay for rest and recovery (TDRY)	$If CP < 0, then TDRY = 15$ $Else (TDRY = 15 \cdot \exp(-0.5 \cdot CP))$	Min	42
Time constant for rest and recovery (KRY)	$KRY = \frac{1 - \exp(-1.5 \cdot abs(CP))}{40}$	N.D.	43
Hydration adjusted for rest and recovery (KRYd)	$KRYd = KRY \cdot (\exp(-0.07 \cdot dhyd))$	N.D.	44
Core temperature by time point ($T_{c,t}$)	$If (M \leq (58.2 \cdot A_D)), then = 0,$ $Else T_{c,i} + D_{tc} \cdot (1 - \exp(-KWKd \cdot If((E_t - TDWK) < 0, 0.5 \cdot (E_t - TDWK) \cdot (\frac{E_t}{TDWK}), E_t - TDWK))))$	°C	45

Figure 18. Schematic of the heat strain decision aid (HSDA) [60]



Mixed models

The majority of usable models (to include those mentioned above), are actually in essence hybrid models. That is to say, they use both rational principles (e.g., heat balance) as well as some empirically derived elements in order to make their predictions work. Along with this concept there are several models that exist and are widely used because of their practical method for implementation or availability of code or pseudo code. Two of these widely used methods include the Predicted Heat Strain (PHS) model [93-95] and the Insulation Required Model (IREQ) [96-97]. Both of these modeling methods rely on the basic principles of maintaining a heat balance within a given environment based on the activity, clothing, and physiologic state of the individual. Due

to the availability of the code, principles, and practical nature both of these methods have been incorporated into International Organization Standardization (ISO) standards (ISO 7933 and 11079) [95, 98].

While the main principle remains, there are several ways of interpreting the thermal balance (Eq 1), to include expansions of terms, such as the parsing of heat loss from respiration into an evaporative (E_{res}) and convective (C_{res}) elements. This is the case for the IREQ method as it describes the basis of the heat balance as:

$$M - W = E_{res} + C_{res} + E + K + R + C + S \quad (\text{Eq 46})$$

where M is metabolic heat produced, W is effective mechanical work and collectively $M - W$ represents the heat produced within the human; while the opposite side of this balance, E_{res} and C_{res} represent the respiratory heat exchange (evaporative and convective), and E , K , R , and C represent the conventional heat exchange methods (evaporative, conductive, radiative, and convective) and S is heat storage.

These elements can also be combined for practical applications, as demonstrated by Santee [77] where dry and wet heat losses are inclusive terms that combine M , R , C , and K into a dry heat loss term, H , and all avenues of E are combined to represent a single wet heat loss term, E . This simplified thermal balance or metabolic equilibrium state (M_e) seen as:

$$M_e = H + E \text{ [W} \cdot \text{m}^{-2}] \quad (\text{Eq 47})$$

The IREQ equation outlines the rational balance of these methods to include a thermal insulation via clothing elements needed to maintain this balance. The simplest form of the *IREQ* equation is shown as the difference between mean skin temperature (\bar{t}_{sk}), clothing surface temperature (t_{cl}), divided by the heat balance, seen as:

$$IREQ = \frac{\bar{t}_{sk} - t_{cl}}{R + C} \quad (\text{Eq 48})$$

more formally as:

$$IREQ = \frac{\bar{t}_{sk} - t_{cl}}{M - W - E_{res} - C_{res} - E} \quad (\text{Eq 49})$$

where t_{sk} is mean skin temperature, t_{cl} clothing surface temperature, and $M - W - E_{res} - C_{res} - E = R + C$

Predictions can be made using this method to describe the insulation required minimum and neutral ($IREQ_{min}$ and $IREQ_{neutral}$) to calculate the minimal and ideal insulation needed to maintain thermal balance (minimum) and to maintain an equilibrium balance (neutral) [98]. These values are also used to calculate a duration limited exposure (DLE) for maximal safe exposure time. This DLE is the balance of the limits of body heat content (Q_{lim}) divided by S :

$$DLE = \frac{Q_{lim}}{S} \quad (\text{Eq 50})$$

There are several simplified models that have been used to model cold protection ($IREQ$) or thermal limits based on the human heat balance equation (PHS) that have been turned into standards as well as usable several iterations of computer applications [99-100]. Recently there have been efforts by the US Army to develop usable decision aids to guide clothing selection and predict whole body and extremity responses to cold exposure [101]. The cold weather ensemble decision aid (CoWEDA), is a usable computer program that is founded on a rationally based six cylinder thermoregulatory model (SCTM) [90].

3.4.3 Statistical Methods and Software

Statistical analysis conducted using a combination of Microsoft Excel 2013, SAS 9.4 (SAS Institute Inc., Cary, NC, USA), SPSS 24 (IBM Corporation), and MATLAB (Version 9.5.0; MathWorks, Inc., Natick, MA, USA).

3.5 Methods for Model Verification

To demonstrate the relevant and appropriate uses of each modeling method, data will be modeled for given scenarios and compared to the actual responses obtained from human data; data will be obtained from laboratory studies, or field studies, from published data, or from real-world data.

There are many methods to assess the accuracy of estimation modeling methods. The specific methods planned include using an acceptable bias, root mean square error (RMSE), and mean absolute error (MAE), for comparing predictions to measured data. The equations for RMSE and MAE:

$$RMSE = \sqrt{\frac{1}{n} \sum_{i=1}^n d_i^2} \quad (\text{Eq 51})$$

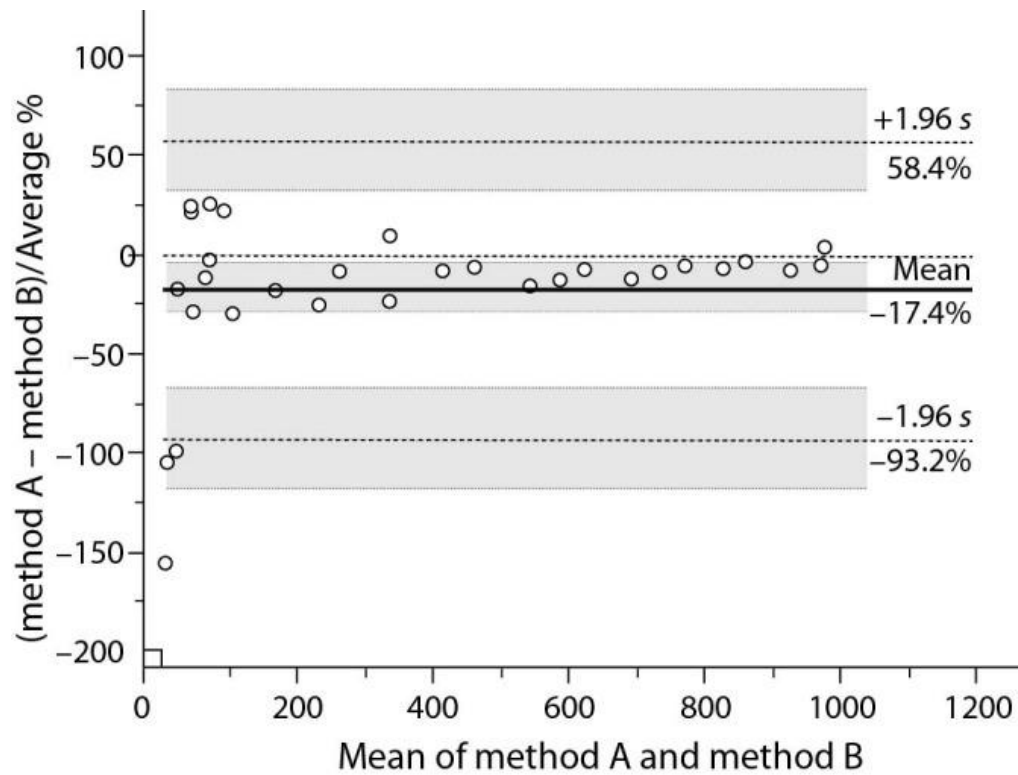
$$MAE = \frac{1}{n} \sum_{i=1}^n |f_i - y_i| = \frac{1}{n} \sum_{i=1}^n |e_i| \quad (\text{Eq 52})$$

where d_i is the difference between observed and predicted i_m/clo for each ensemble, and n is the number of data points. The MAE being the average of the absolute errors within the predictions, in the equation: where f_i is the predicted value, y_i is the actual value, and e_i is the absolute error.

The Bland-Altman method [102-103] can be used to compare methods and outline the limits of agreement (LoA) along with an associated measure of bias and

random error (i.e., precision) [104]. The Bland-Altman method is a way of simply plotting and comparing bias between mean differences and agreement intervals. An example use is shown in Figure 19 below [105].

Figure 19. Notional use of Bland-Altman for comparing two methods [105]



IV. Results

4.1. Assessment 1 Heat Stress Analysis [chemical protective clothing]

For assessment 1, the predictive accuracy was measured using three pieces of data, these included measurement of clothing biophysical properties, collation of human research data, and measurement of environmental conditions and modeling for the predicted core body temperature. For this assessment two datasets were used and evaluated for both population based predictions (sample mean values) as well as individual predictability. All of the tested clothing properties are listed in Appendix Table A1. Ensembles used for this assessment are additionally reported in [106-107]

The laboratory data study design is summarized in Figure 20. This data was used to first make predictions of metabolic heat produced and then to make predictions of core body temperature rise based on the mean of subject values. Metabolic costs were estimated [108-109] based on average values for each subject, shown in Table 11 and calculated in Table 12. For the second analyses focused on individuals, individual predictions of metabolic cost were calculated.

Figure 20. Human Research Study Design – Assessment 1

Exercise Stage 1 (60 min) Treadmill Speed: 3 km/h Grade: 0%	Rest (10 min)	Exercise Stage 2 (30 min) Treadmill Speed: 6 km/h Grade: 3%
Laboratory Environment Air temperature: 29.3°C relative humidity: 56% Radiant temperature: indoor Wind-speed: still air		

Table 11. Inputs for metabolic cost estimations – Assessment 1

Element	Input Value
Weight	By subject (76.6 ± 8.4 kg)
Load	By clothing (10.5, 11, and 11 kg)
Speed	0, 3, and 6 km/h
Grade	0 and 3%
Terrain	Treadmill (value 1.0)

Table 12. Estimated metabolic costs for each activity – Assessment 1

Clothing	Exercise Stage 1	Rest	Exercise Stage 2
A	210 ± 21 W	114 ± 13 W	488 ± 48 W
B	211 ± 21 W	114 ± 13 W	491 ± 48 W
C	212 ± 21 W	114 ± 13 W	493 ± 48 W
Model Inputs	211 W	114 W	490 W

Group Mean Analyses

The collection of measured core body temperatures are shown in Figure 21. As can be seen in Figure 21, one set of data (Subject 1 A) was an obvious error in recorded data and was removed from the average values generated. The averages of these measured core temperatures are shown in Figure 22 for the three separate clothing trials.

Figure 21. Measured rectal core body temperature (°C) – Assessment 1

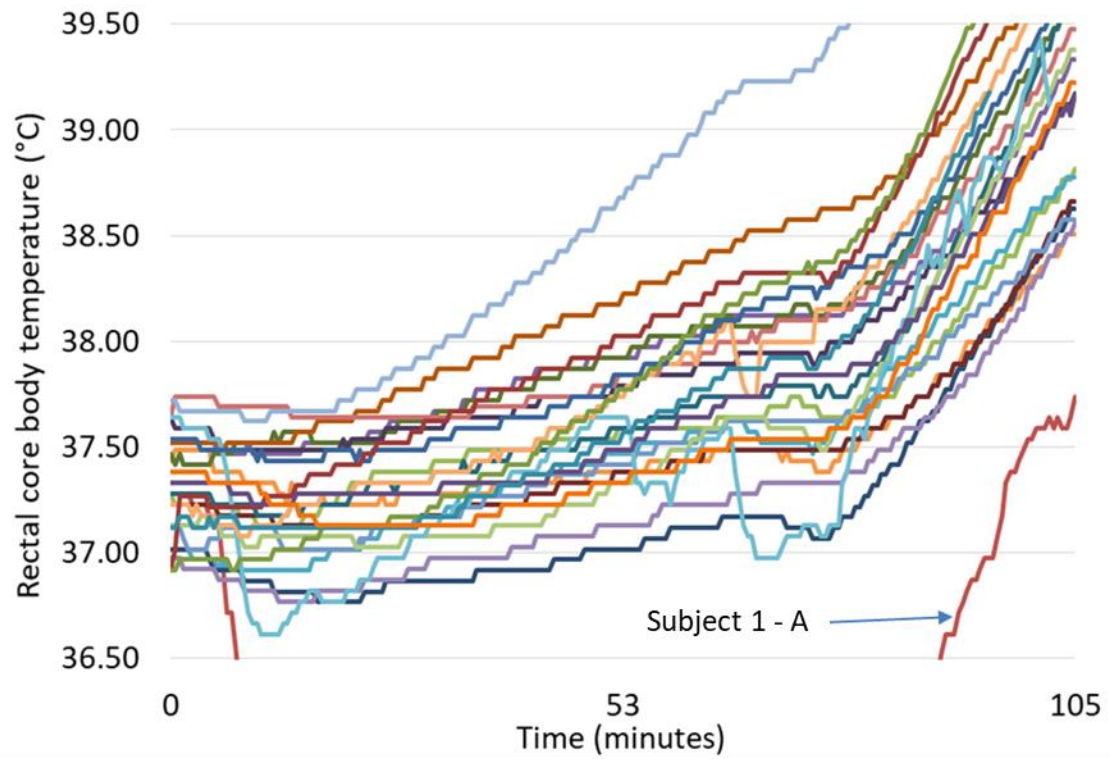
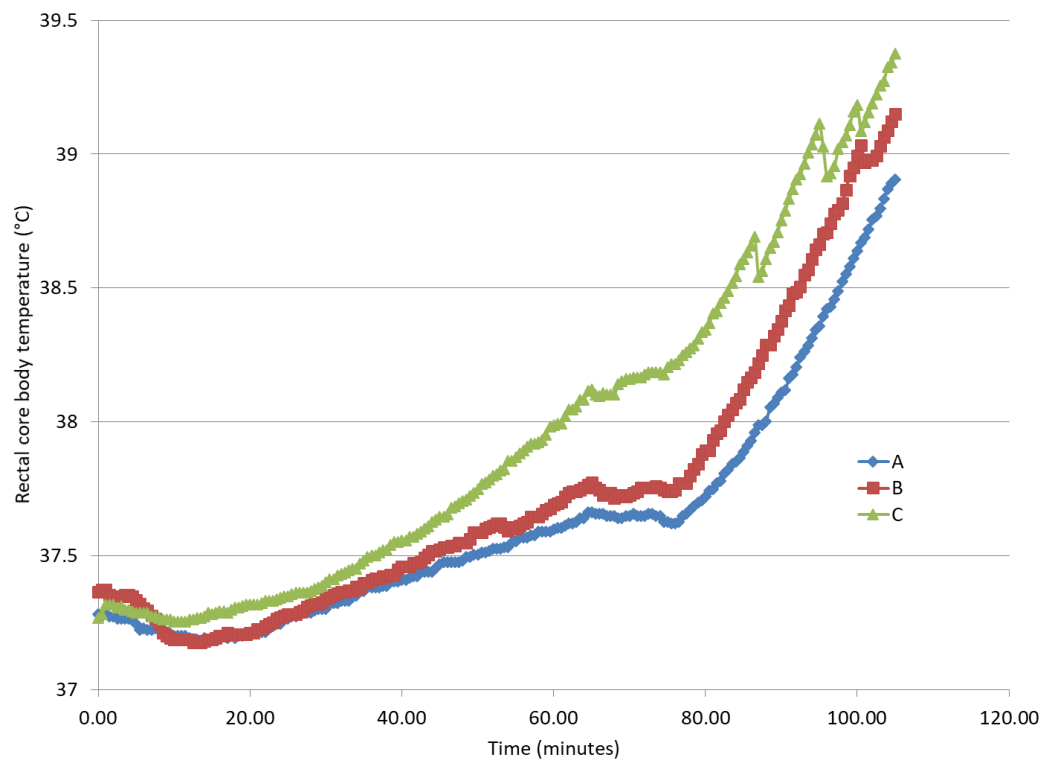


Figure 22. Aggregate of measured core temperature across trials



Modeled comparisons to the overall observed data are shown in Figure 23; while specific trial predictions to observations are shown in Figures 24-26.

Figure 23. Overall comparison of model predictions and observed data

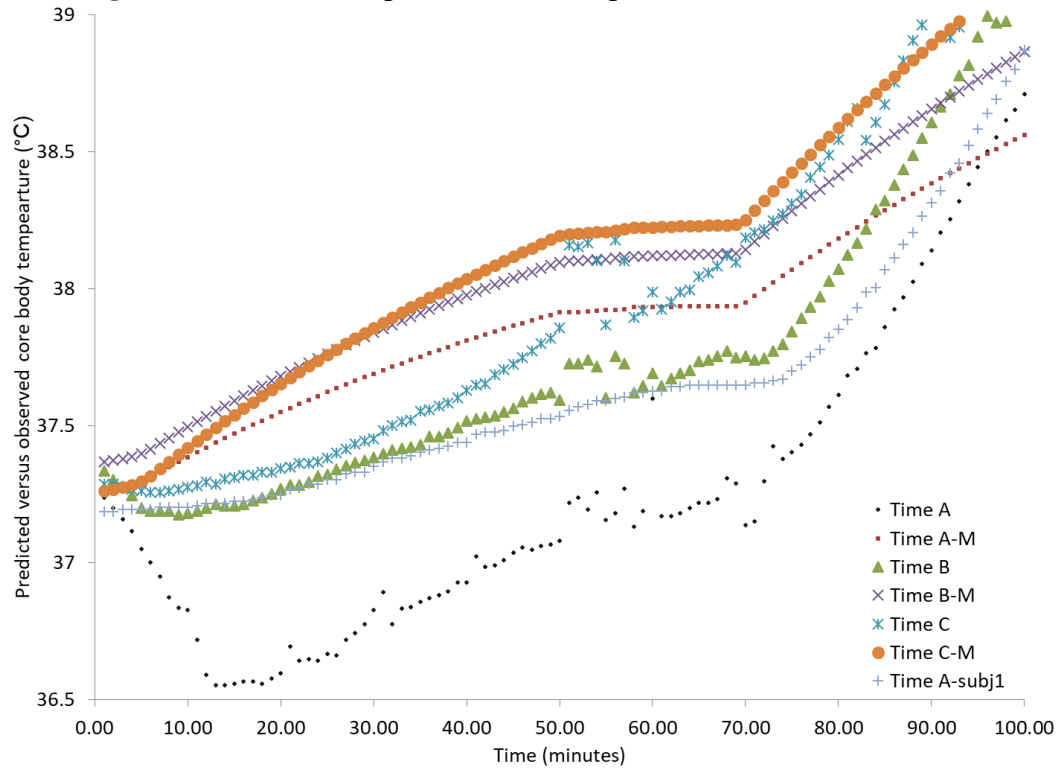
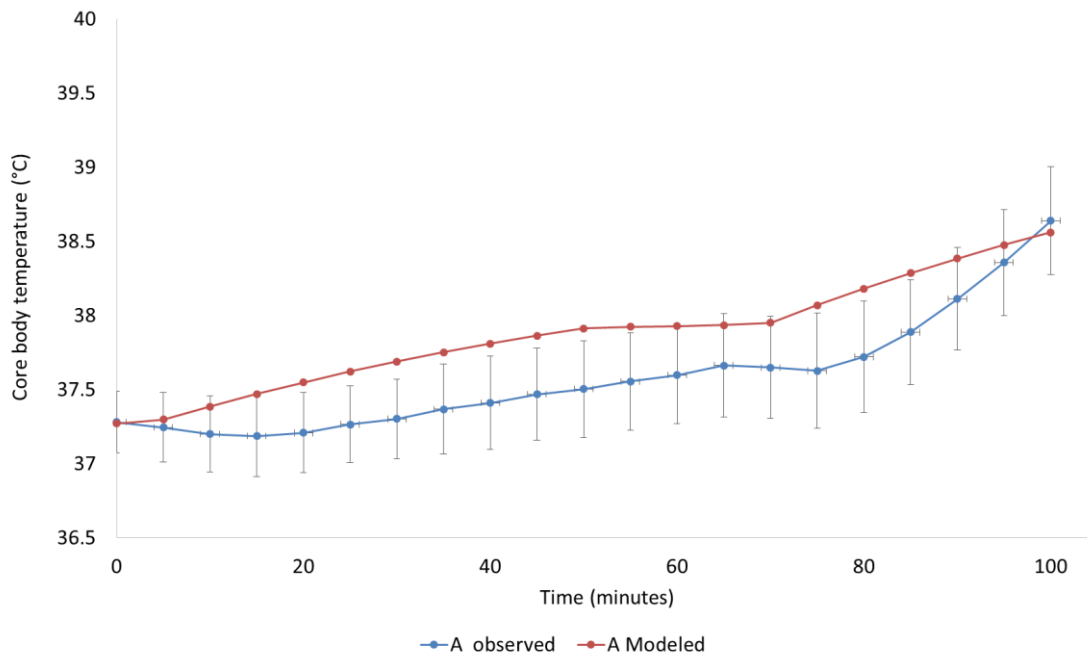
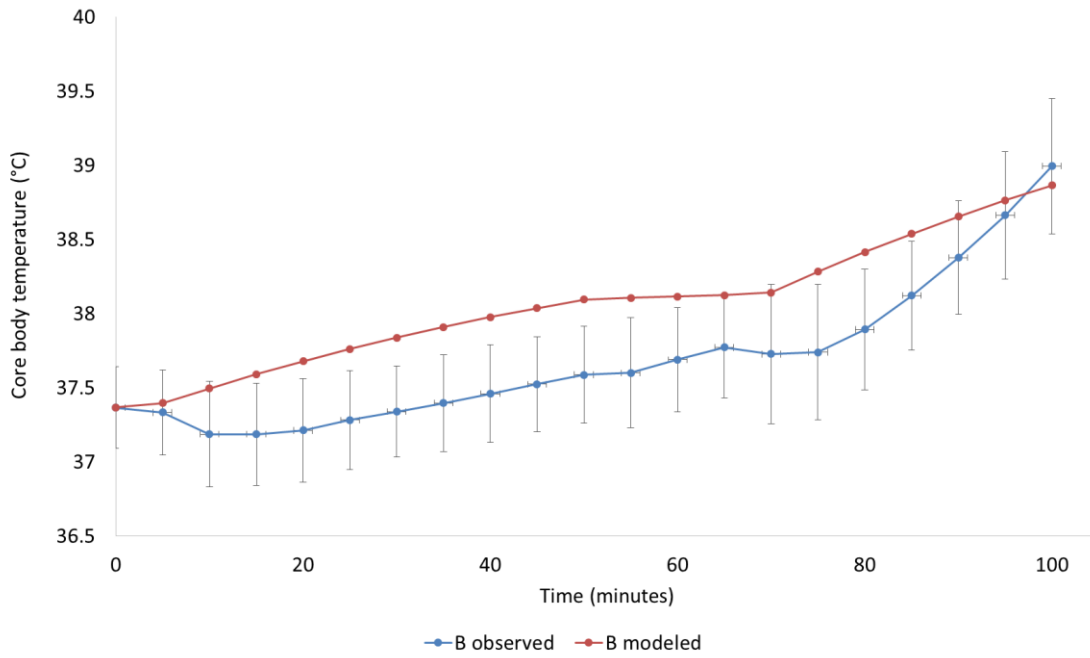


Figure 24. Comparison of observed and modeled for ensemble A



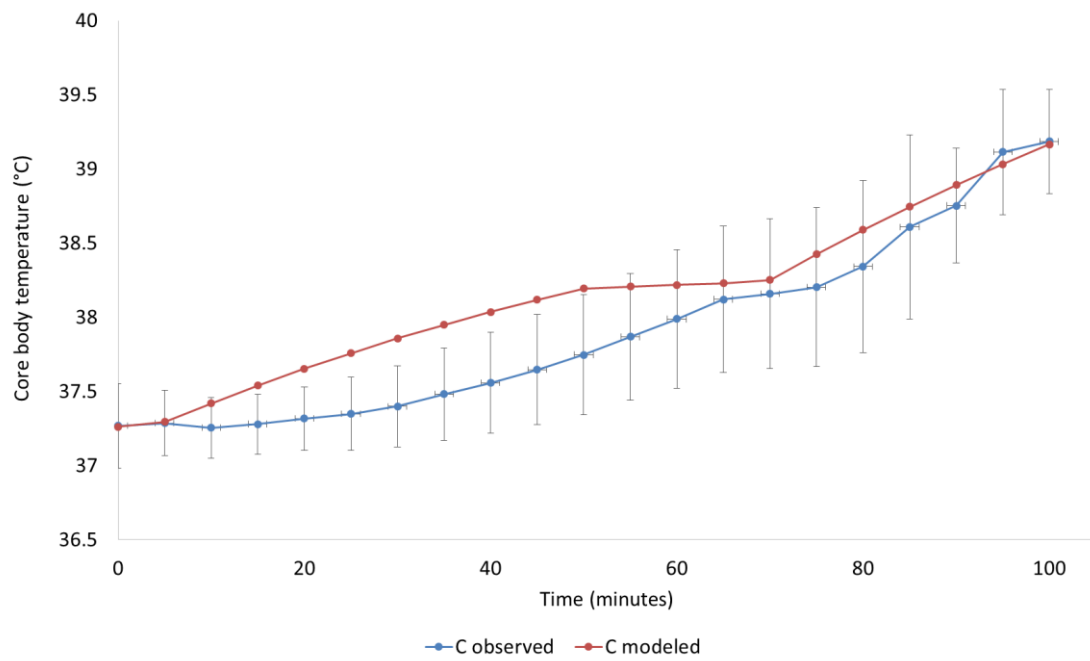
*error bars show observed standard deviation

Figure 25. Comparison of observed and modeled for ensemble B



*error bars show observed standard deviation

Figure 26. Comparison of observed and modeled for ensemble C



*error bars show observed standard deviation

The calculated RMSE was relatively low for each ensemble; 0.70°C for A, 0.37°C for B, and 0.25°C for C. The above figures (24-26) show that the model predictions were all within approximate 1.25 standard deviations of the observed data, indicating an acceptable level of reliability. Cadarette et al., [110], used a threshold of two times the standard deviation to provide an indication that the predictions fall within 95% of an average population's response.

Individual Predictions

A second analysis was conducted for assessment 1 that focused on individual predictions of core body temperature using individual subject inputs and calculations [107]. These inputs specifically include: height, weight, initial physiological states (i.e., hydration status, core and skin temperatures) as well as calculated metabolic rates [108-109]. This analysis used the two datasets outlined in Table 6, to show a laboratory and field based assessment. To provide context for an acceptable level of individual accuracy, this analysis set out to use a few statistical criteria, including comparison of predicted to the observed SD, assessment of MAE, RMSE, and well as a pre-established limit of bias $\pm 0.27^{\circ}\text{C}$. This bias has been previously used to compare direct measurement accuracy of body temperatures devices [111].

Table 13 provides calculated results of the modeled bias, MAE, RMSE, as well as the observed SD for both the laboratory and field studies assessed. As can be seen in Table 13, the predictions of core body temperature during both the laboratory (Bias $-0.10 \pm 0.36^{\circ}\text{C}$; MAE $0.28 \pm 0.24^{\circ}\text{C}$; RMSE $0.37 \pm 0.24^{\circ}\text{C}$) and field trials (Bias $0.23 \pm 0.32^{\circ}\text{C}$; MAE $0.30 \pm 0.25^{\circ}\text{C}$; RMSE $0.40 \pm 0.25^{\circ}\text{C}$) for each chemical protective

clothing ensemble were within acceptable limits for bias, MAE, and RMSE.

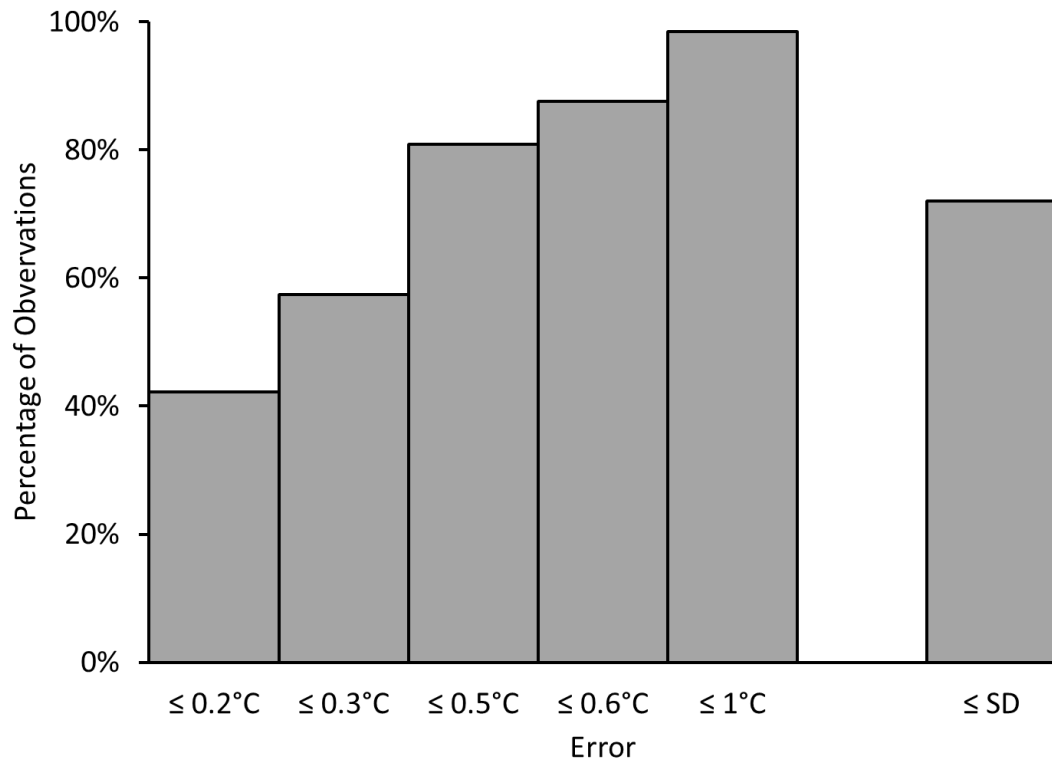
Additionally, the total collated average from both studies had a relatively low positive weighted bias ($0.16 \pm 0.36^{\circ}\text{C}$) well within the pre-established criterion.

Table 13. Accuracy of HSDA model when predicting T_c ($^{\circ}\text{C}$) in individuals wearing different chemical protective clothing ensembles during exercise in hot and humid conditions.

Environment	Clothing	Observed T_c	Bias	MAE	RMSE
Laboratory	L1	37.64 ± 0.55	-0.15 ± 0.26	0.23 ± 0.20	0.30 ± 0.13
	L2	37.75 ± 0.64	-0.14 ± 0.34	0.29 ± 0.24	0.38 ± 0.20
	L3	37.88 ± 0.70	0.03 ± 0.42	0.31 ± 0.28	0.42 ± 0.33
	Total	37.76 ± 0.64	-0.10 ± 0.36	0.28 ± 0.24	0.37 ± 0.24
Field	F1	37.69 ± 0.35	0.22 ± 0.30	0.29 ± 0.24	0.37 ± 0.21
	F2	37.67 ± 0.36	0.21 ± 0.32	0.30 ± 0.24	0.39 ± 0.21
	F3	37.55 ± 0.35	0.36 ± 0.30	0.37 ± 0.28	0.47 ± 0.27
	F4	37.79 ± 0.43	0.13 ± 0.32	0.27 ± 0.23	0.35 ± 0.20
	Total	37.68 ± 0.38	0.23 ± 0.32	0.30 ± 0.25	0.40 ± 0.25
Collective Total	L1-L3 F1-F4	37.69 ± 0.45	0.16 ± 0.36	0.30 ± 0.25	0.39 ± 0.23

An assessment of the overall accuracy of the predictions in comparison to the SD of the observed measures showed 72% of all predictions were within one standard deviation of the observed data including 92% of predictions for the laboratory experiment ($\text{SD} \pm 0.64^{\circ}\text{C}$) and 67% for the field experiment ($\text{SD} \pm 0.38^{\circ}\text{C}$). Figure 27 highlights the percentage of the modeled data that fell within ranges of the observations. As can be seen in this figure, individual-based predictions showed modest errors outside the SD range with 98% of predictions falling $< 1^{\circ}\text{C}$ of the observed data.

Figure 27. Accuracy of predicted core temperature to observed SD



A visual inspection in Figure 28 shows a side-by-side comparison of the individual predictions and the observed measures of core body temperature from the laboratory study. We can see that the general trend remains the same; while we can also see more clearly the outlying data.

Figure 28. Side-by-side comparison of the individual predictions and observed measures of core body temperature from the laboratory study

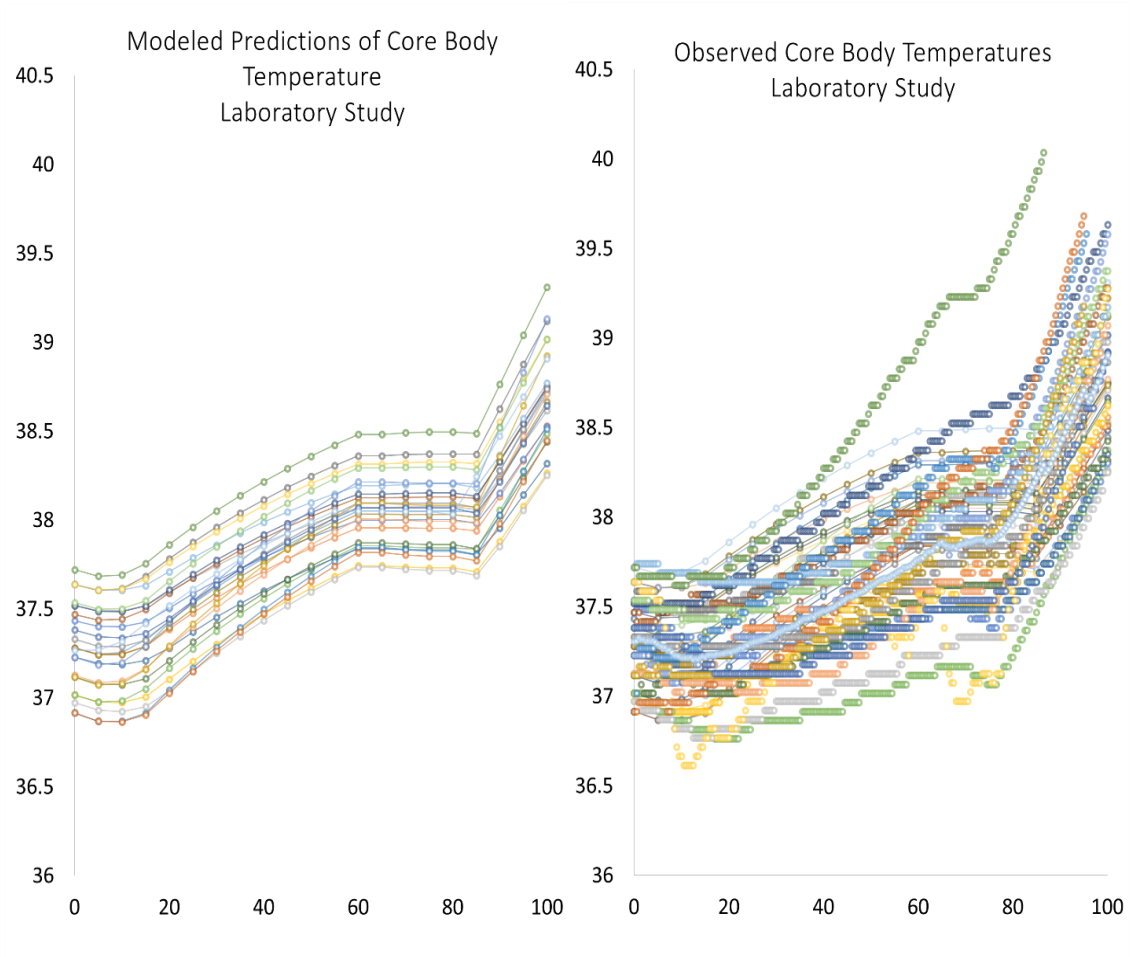


Figure 29 shows individual points and Figure 30 shows the mean and standard deviation prediction errors by observed T_c by elapsed time point. Figure 31 shows the comparison of observed measured to modeled predictions by core temperature.

Figure 29. Individual prediction errors by elapsed time points (minutes)

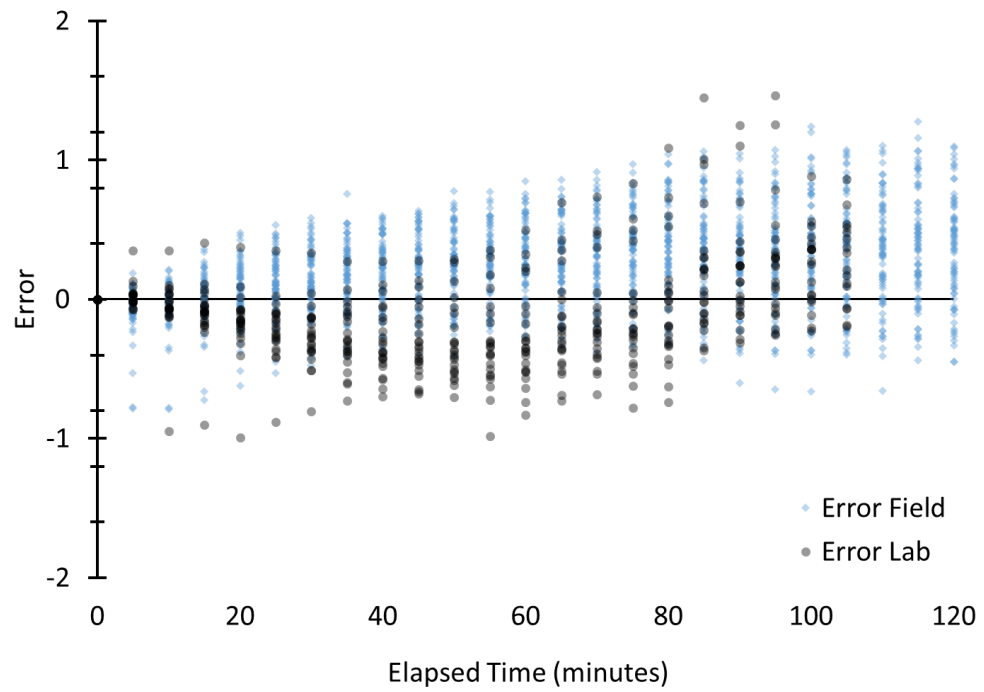


Figure 30. Mean error by elapsed time points (minutes)

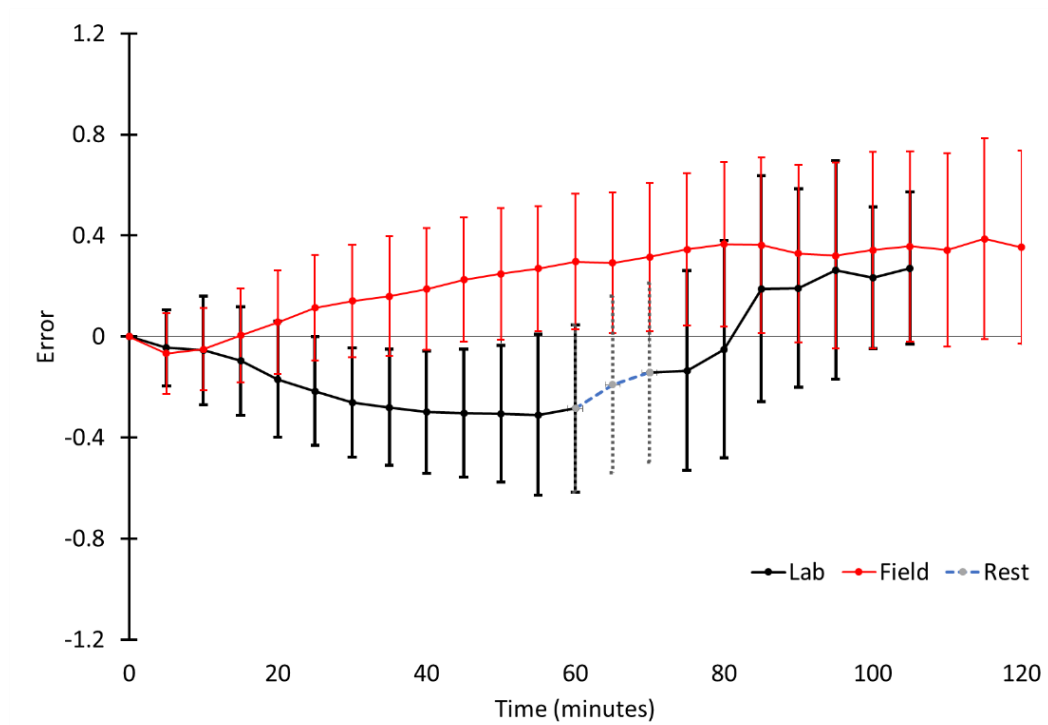
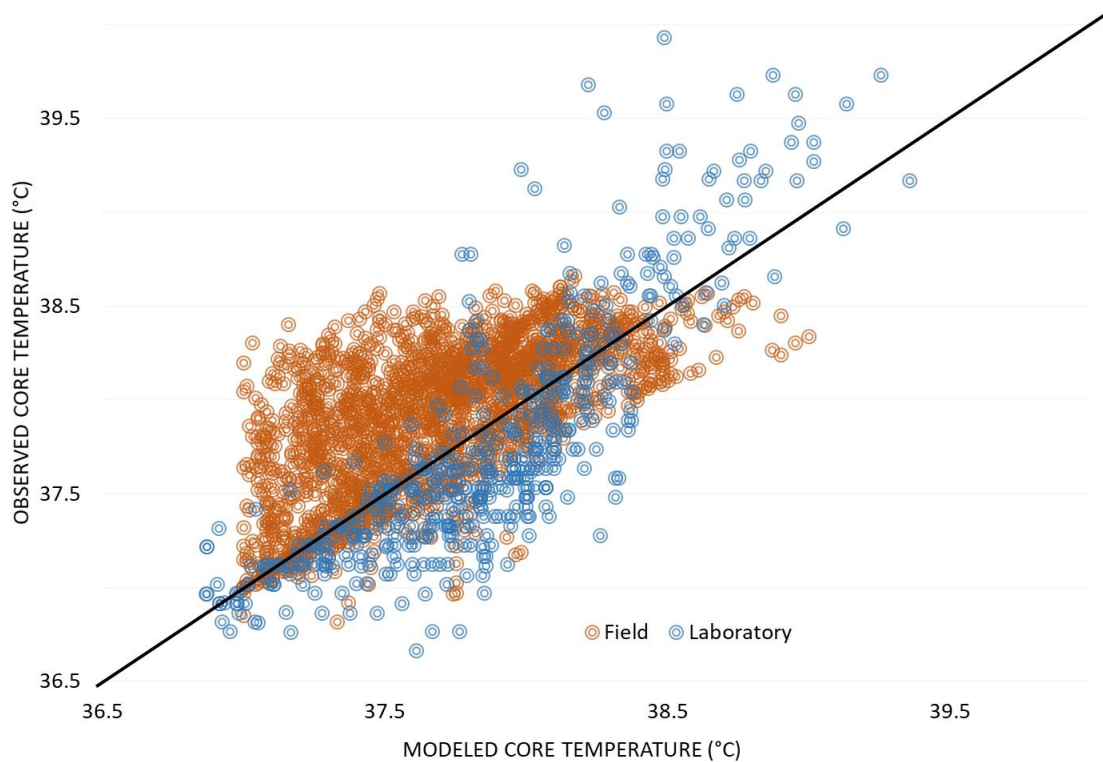


Figure 31. Observed to modeled core body temperatures for both laboratory and field studies



From this analysis we outlined a case where the HSDA method provides an acceptable level of accuracy for predicting core body temperature for individuals wearing chemical protective clothing during exercise in hot and humid environmental conditions. The overall predictive accuracy within an acceptable bias criteria used in direct measure methods ($\pm 0.27^{\circ}\text{C}$) establishes a case for the use of this method in these conditions as a means of accurately predicting heat stress risk specific to body temperature rise.

4.2. Assessment 2 Cold Stress Analysis [cold conditions wearing cold weather clothing]

Biophysical assessments of all of the various clothing ensembles are described in the Appendix Table A1. For this assessment, these are also described specifically and given unique identifiers. Ensembles assessed included cold weather clothing for the US Army (US#), Canadian Defence (CA#), Norwegian military (N#), and US Marine Corps (MC#). Each of these clothing ensembles were assessed using the *IREQ* method to calculate a *DLE* range (minutes) (range values are calculated as the average between *IREQ_{min}* and *IREQ_{neutral}*); assessments were conducted for resting (1 MET; 58 Wm²) and 2 MET (116 Wm²) (Figure 32; Table 14).

Figure 32. Modeled DLE range (minutes) using the *IREQ* method for each clothing ensemble for both rest and light work (1MET, 58 Wm²; 2MET, 116 Wm²) in -15°C and -25°C

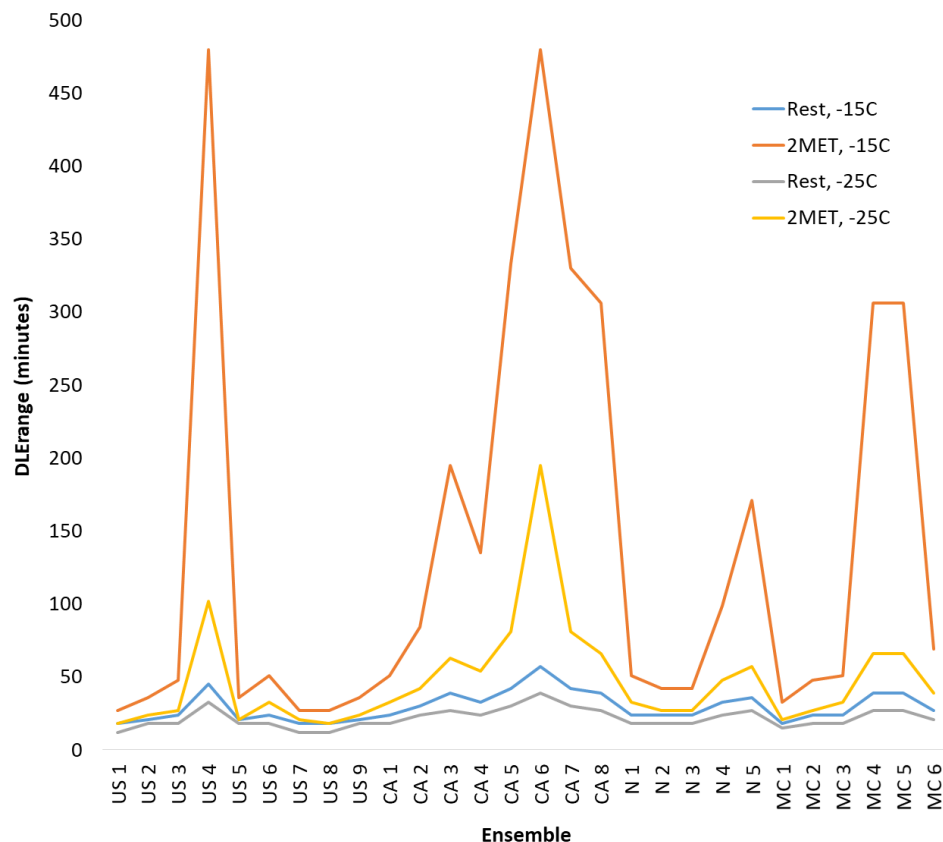


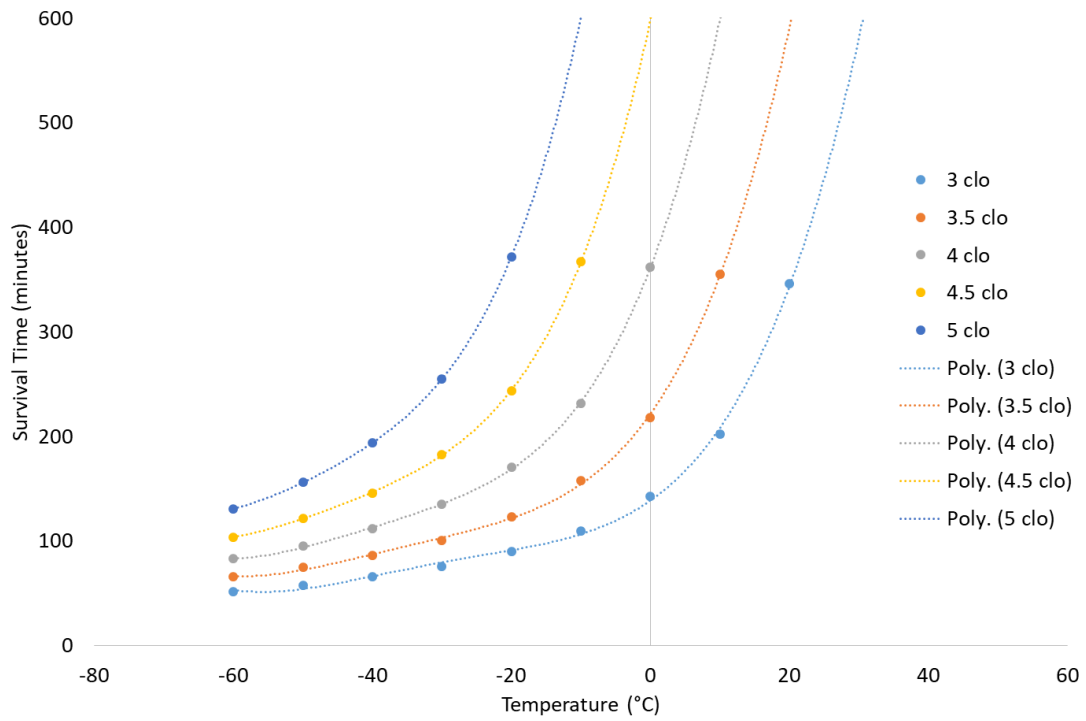
Table 14. Measured biophysical properties and predicted DLE for select cold weather clothing

Ensemble	Thermal Insulation (clo)	DLErange (mins) -15°C, Rest	DLErange (mins) -15°C, 2MET	DLErange (mins) -25°C, Rest	DLErange (mins) -25°C, 2MET
US 1	1.296	18	27	12	18
US 2	1.548	21	36	18	24
US 3	1.729	24	48	18	27
US 4	2.806	45	480	33	102
US 5	1.490	21	36	18	21
US 6	1.825	24	51	18	33
US 7	1.342	18	27	12	21
US 8	1.316	18	27	12	18
US 9	1.554	21	36	18	24
CA 1	1.812	24	51	18	33
CA 2	2.103	30	84	24	42
CA 3	2.445	39	195	27	63
CA 4	2.328	33	135	24	54
CA 5	2.657	42	333	30	81
CA 6	3.109	57	480	39	195
CA 7	2.638	42	330	30	81
CA 8	2.509	39	306	27	66
N 1	1.812	24	51	18	33
N 2	1.638	24	42	18	27
N 3	1.671	24	42	18	27
N 4	2.199	33	99	24	48
N 5	2.406	36	171	27	57
MC 1	1.484	18	33	15	21
MC 2	1.742	24	48	18	27
MC 3	1.806	24	51	18	33
MC 4	2.516	39	306	27	66
MC 5	2.516	39	306	27	66
MC 6	2.000	27	69	21	39

From data collected and reported by Santee [77] fourth order polynomial fits were made to the data (Figure 33), as well as a surface plot of survival time, in minutes, was created as a function of T_a (°C) and clothing insulation (clo) at rest (1MET) (Figure 34).

From this empirically derived plot, we can expand out predicted survival at rest for decreasing levels of clo (Figure 34). Additionally, Figure 35 shows the fit for using the *IREQ* predictions for a standard individual (body surface area 1.8m²) in different cold temperatures at rest (1MET) compared to the surface plot derived from Santee [77].

Figure 33. Survival at rest as a function of air temperature (°C) and clothing insulation (clo)



$$3 \text{ clo poly4th: } y = 3\text{E-}05x^4 + 0.0041x^3 + 0.1839x^2 + 4.6765x + 138.87 \quad (\text{Eq 53})$$

$$3.5 \text{ clo poly4th: } y = 4\text{E-}05x^4 + 0.0059x^3 + 0.3212x^2 + 9.3872x + 221.7 \quad (\text{Eq 54})$$

$$4 \text{ clo poly4th: } y = 5\text{E-}05x^4 + 0.0086x^3 + 0.5409x^2 + 17.424x + 361.66 \quad (\text{Eq 55})$$

$$4.5 \text{ clo poly4th: } y = 6\text{E-}05x^4 + 0.0119x^3 + 0.8553x^2 + 30.517x + 597.83 \quad (\text{Eq 56})$$

$$5 \text{ clo poly4th: } y = 1\text{E-}04x^4 + 0.0189x^3 + 1.4554x^2 + 54.758x + 1021 \quad (\text{Eq 57})$$

Figure 34. Surface plot of survival at rest as a function of air temperature (°C) and clothing insulation (clo)

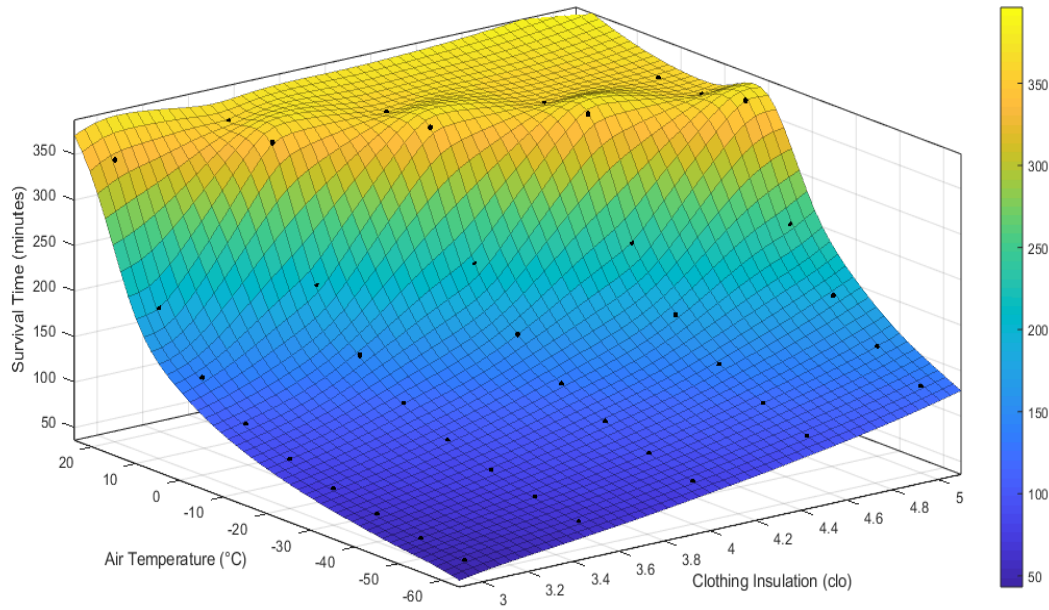
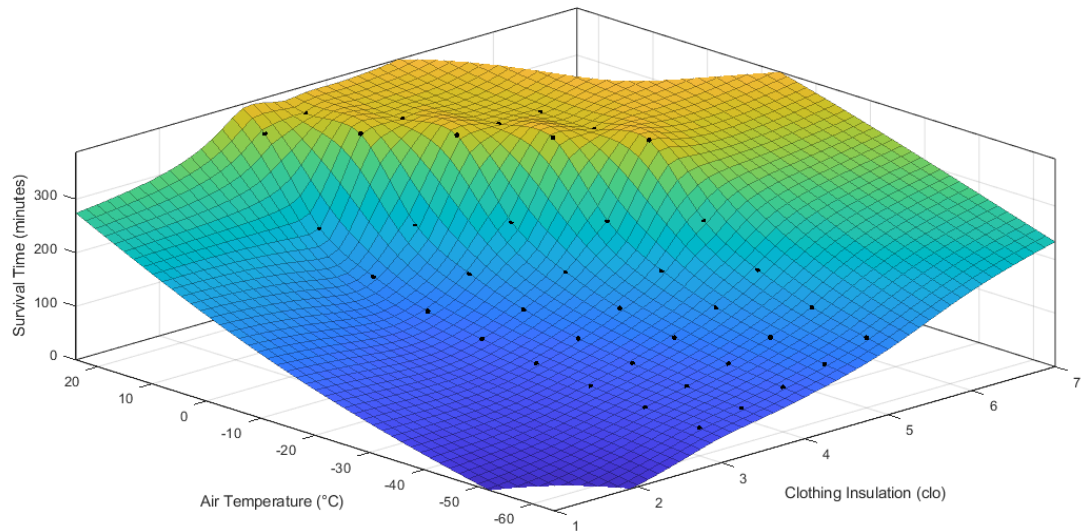
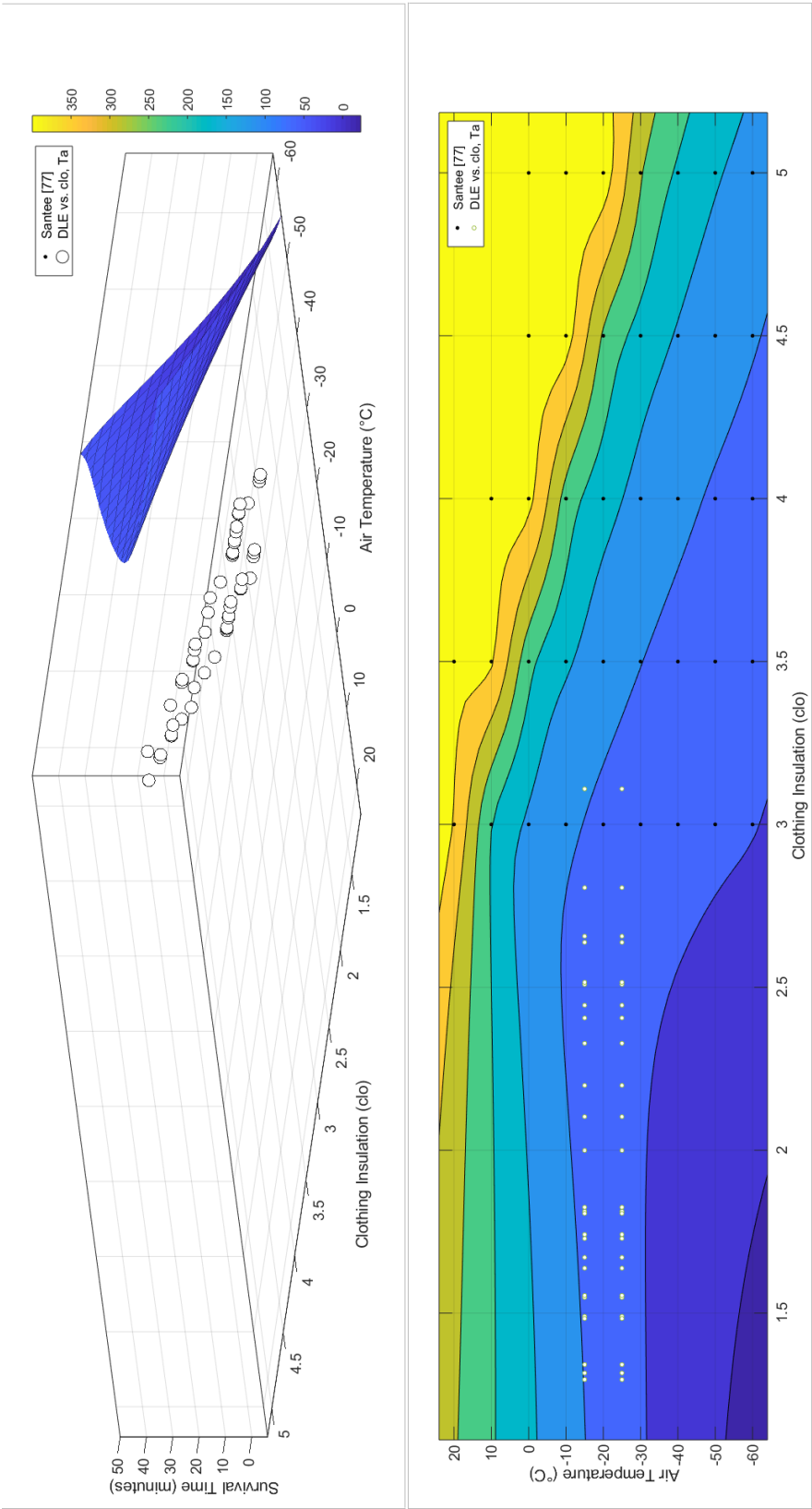


Figure 35. Expanded survival plot to include lower and higher clothing insulation (clo) values



Comparisons of the IREQ calculated data (Table 14) and the empirically-derived surface plot are shown in Figure 36. From this we see a conservative underestimate (acceptable / anticipated) from the IREQ predictions.

Figure 36. Comparison of *IREQ* calculated *DLE* and empirical survival surface plot



Comparisons of published data with predictions made using CoWEDA [101], enabled by the SCTM [90], are shown in Figures 37-39. Figure 37 shows the observed skin temperatures by location after a 90 minute resting exposure in $T_a 0.47^\circ\text{C} \pm 0.5^\circ\text{C}$; RH $51 \pm 3\%$; wind speed $1.34 \text{ m}\cdot\text{s}^{-1}$; this is a comparison of the published data from Castellani et al., [82] to predictions from CoWEDA. Data from Gonzalez et al., [80] were modeled to produce Figures 38-41. Figures 38 and 39 outline the comparison between observed and predicted finger temperatures for three different gloves (A, B, and C) during rest (1MET) (Figure 38) and exercise ($\sim 2.4\text{MET}$) (Figure 39) in cold chamber conditions (0, -20, and -30°C). Figures 40 and 41 outline the comparison between observed and predicted mean skin temperatures for three different glove conditions (A, B, and C) during rest (1MET) (Figure 40) and exercise ($\sim 2.4\text{MET}$) (Figure 41) in cold chamber conditions (0, -20, and -30°C). Data from Hickey et al., [81] was used to compare observed and predicted finger, toe, and back skin temperatures in extreme cold conditions (-40°C) (Figure 42).

Figure 37. Observed to modeled skin temperature responses; CoWEDA and Castellani et al., [82]

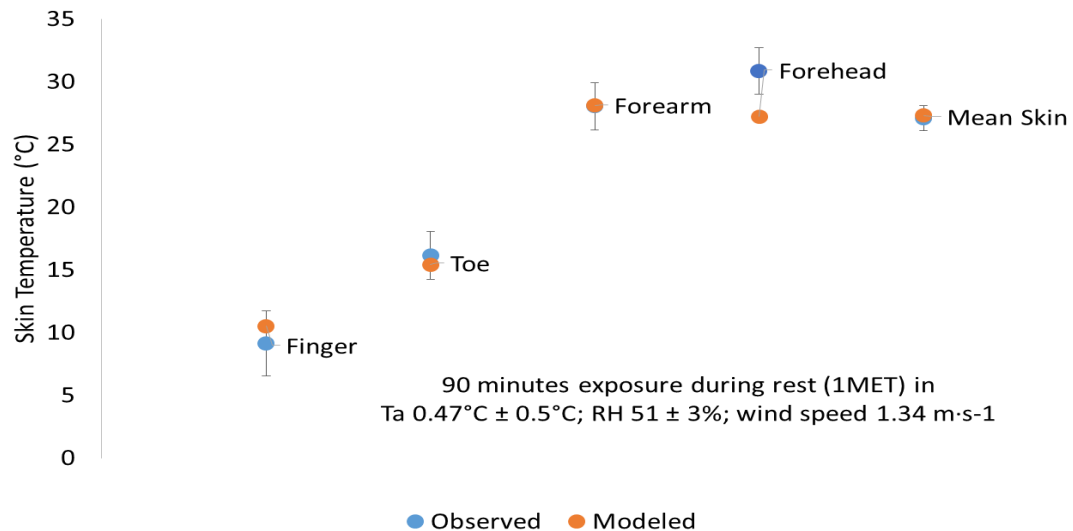
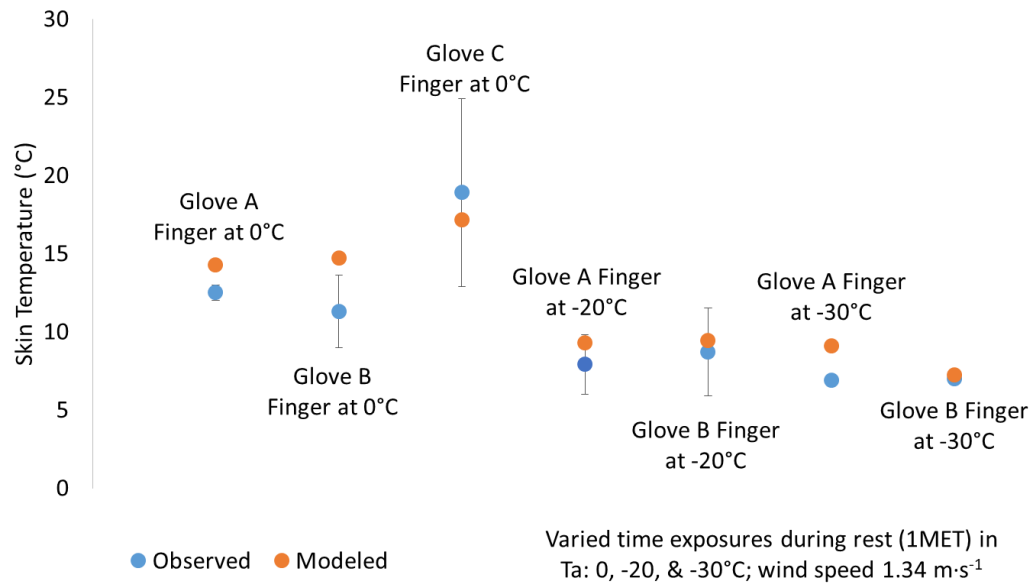
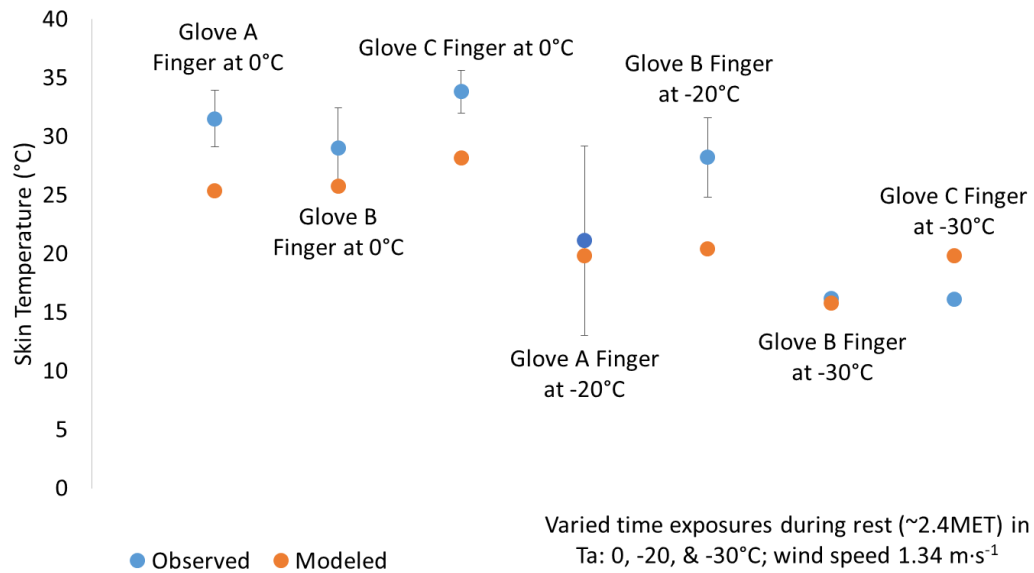


Figure 38. Observed to modeled finger temperatures; CoWEDA and Gonzalez et al., [80] during rest at 0, -20, and -30°C



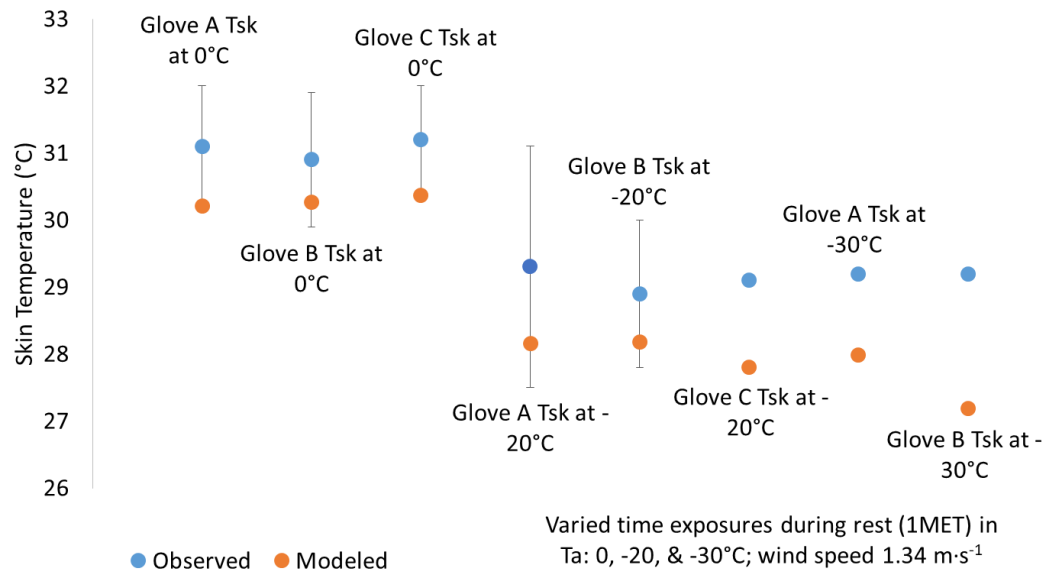
Note: Glove C was not worn in -30°C

Figure 39. Observed to modeled finger temperatures; CoWEDA and Gonzalez et al., [80] during exercise [\sim 2.4MET] at 0, -20, and -30°C



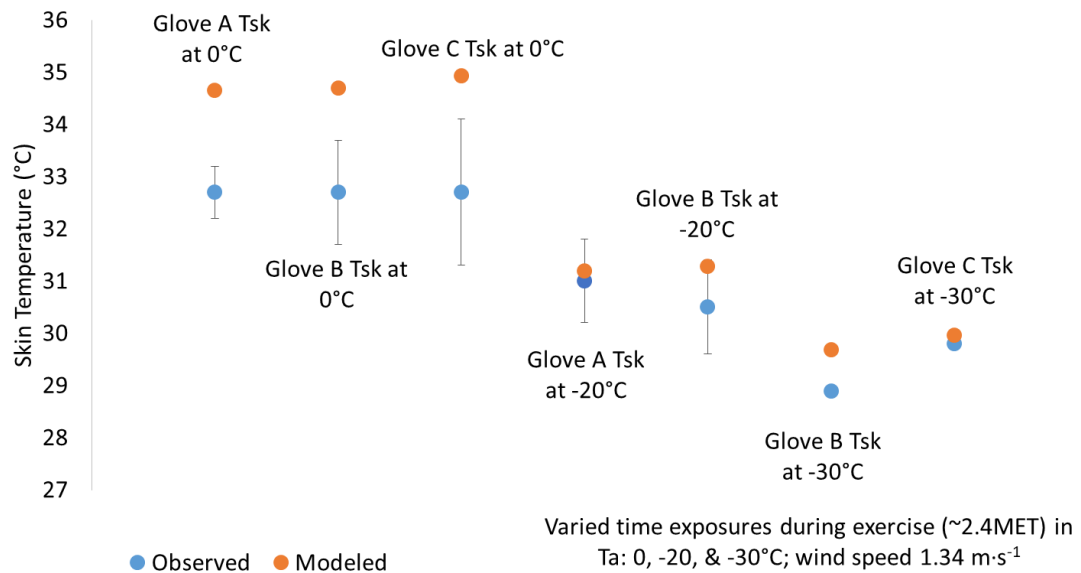
Note: Glove A was not worn in -30°C

Figure 40. Observed to modeled mean skin temperatures; CoWEDA and Gonzalez et al., [80] during rest at 0, -20, and -30°C



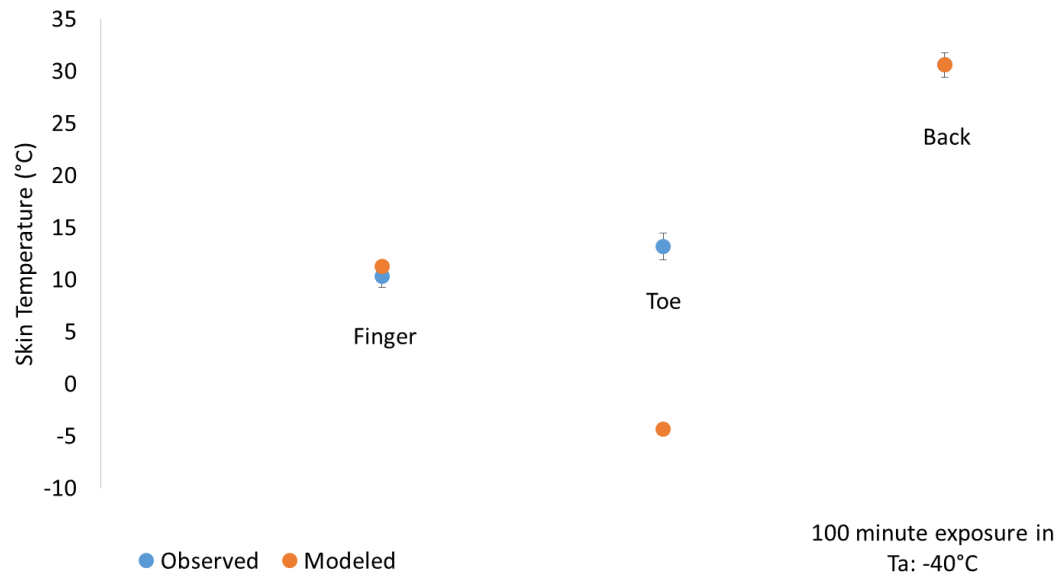
Note: Glove C was not worn in -30°C

Figure 41. Observed to modeled mean skin temperatures; CoWEDA and Gonzalez et al., [80] during exercise [\sim 2.4MET] at 0, -20, and -30°C



Note: Glove A was not worn in -30°C

Figure 42. Observed to modeled mean skin temperatures; CoWEDA and Hickey et al., [81] for 100 minute exposure to extreme cold conditions -40°C



When combining all of the three datasets above [80-82] and assessing the CoWEDA predictions to all of the observed skin temperatures, and given the variability in cold responses, we find relatively acceptable accuracy. The total aggregated data found a bias, MAE, and RMSE, of: bias, $-0.77 \pm 3.69^{\circ}\text{C}$; MAE, $2.22 \pm 3.05^{\circ}\text{C}$; and RMSE, $1.49 \pm 3.05^{\circ}\text{C}$. Table 15, shows grouped body segments and predictive accuracies, specific to fingers and mean skin temperatures. Figures 43-45 shows the plotted observed to CoWEDA modeled for all data [80-82] (Figure 43), only fingers (Figure 44), and only reported mean skin (Figure 45) temperatures.

Table 15. Cold exposure skin temperature predictions to observations grouped regions

Region	Observed mean (°C)	Predicted mean (°C)	Bias	MAE	RMSE	Ref#
All N = 38	23.14 ± 9.35	22.37 ± 9.43	-0.77 ± 3.69	2.22 ± 3.05	1.49 ± 3.05	[80-82]
Fingers N = 17	16.24 ± 8.99	15.83 ± 6.30	-0.41 ± 3.37	2.68 ± 2.09	1.64 ± 2.09	[80-82]
Mean T_{sk} N = 16	30.27 ± 1.56	30.24 ± 2.51	-0.03 ± 1.25	1.06 ± 0.65	1.03 ± 0.65	[80 & 82]

Figure 43. Observed to modeled temperatures; CoWEDA and published data [80-82]

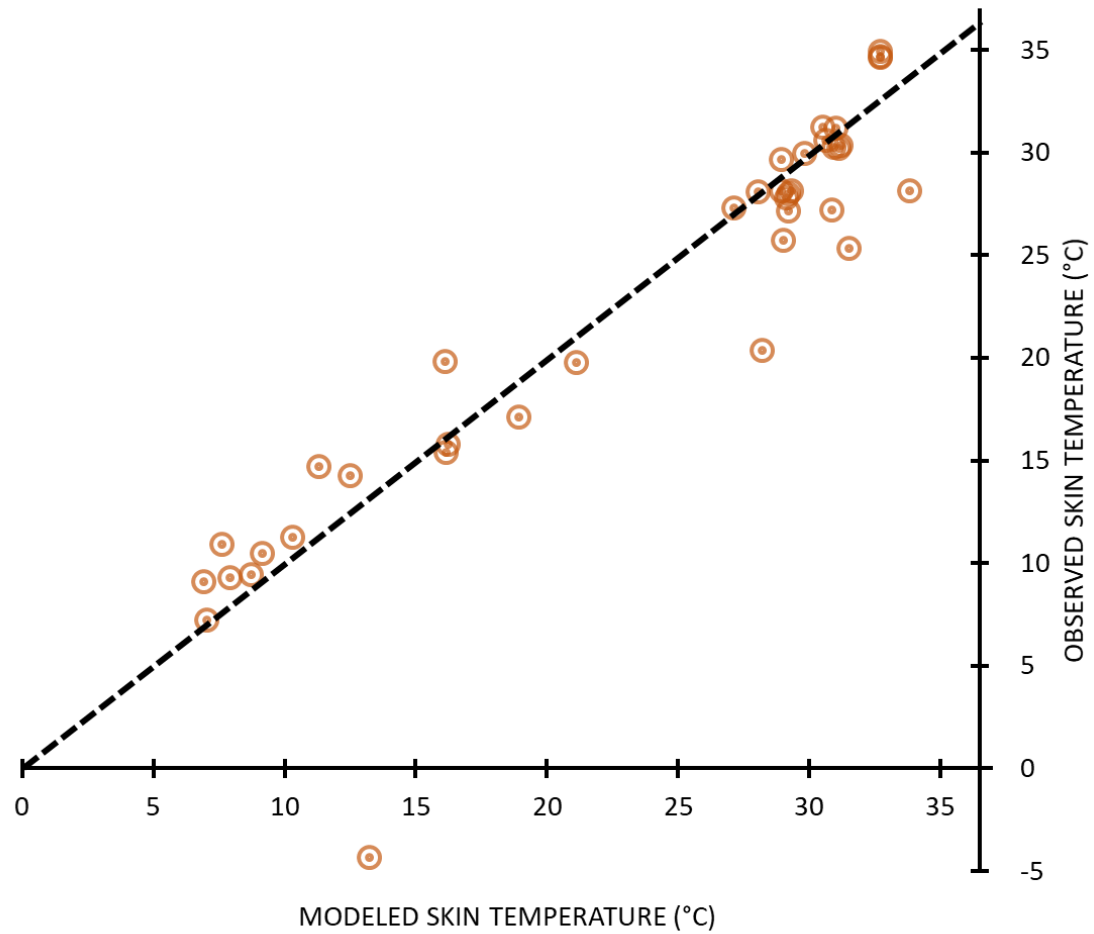


Figure 44. Observed to modeled finger temperatures; CoWEDA and published data [80-82]

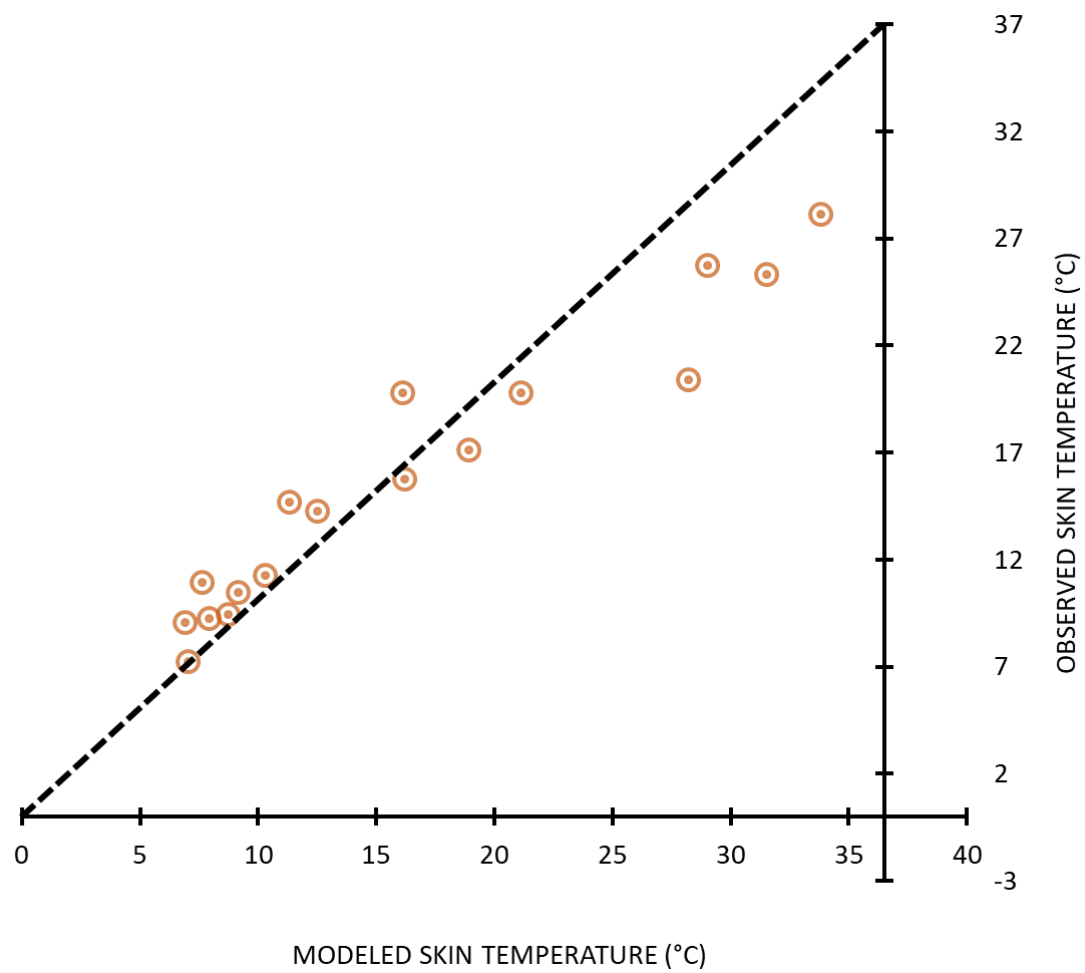
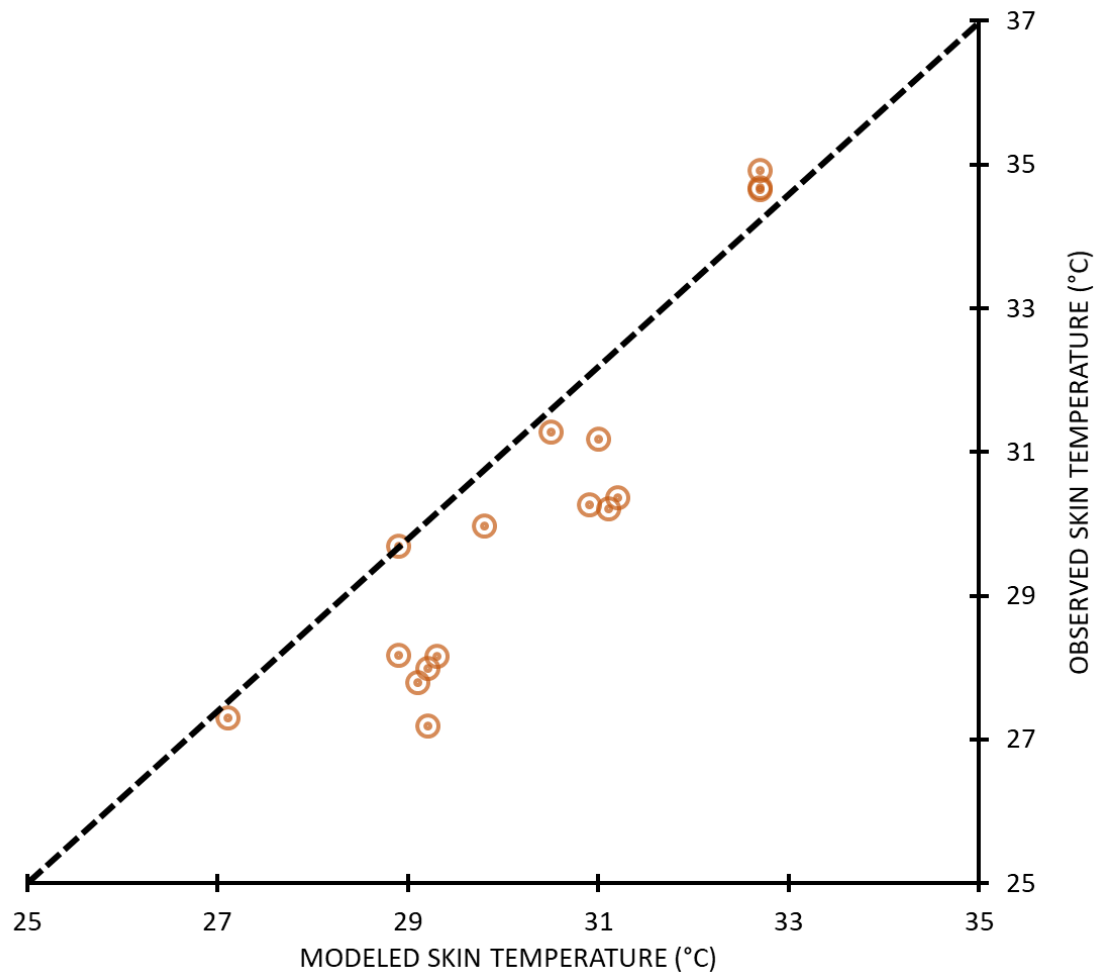


Figure 45. Observed to modeled mean skin temperatures; CoWEDA and published data [80, 82]



As the clothing insulation (clo) values were reported specific to the data, comparisons of Gonzalez et al., [80] data was made using *IREQ* predictions [98]. These predictions are shown in Table 16. As shown in Table 16, from these predictions using the *IREQ* method, there is less risk of cold injury due to exposure during the activity phases than resting, as each predicts a safe exposure time of greater than eight hours. However, during the resting conditions, it becomes significantly less safe as total insulation (clo) and temperature is reduced; where none of these clothing configurations provide safe protection for up to an hour in -30°C conditions. Comparisons of endurance

time reported are made to the resting predictions in Table 17. The calculated total insulation values were done based on individual glove values, exchanged with the total insulation reported (3.6 clo). While there is relatively little change to the overall total ensemble insulation value due to the weighted impact of the small surface area of the hands (~6% for both), the accuracy of the predictions is fairly close for the -20 and -30°C conditions.

Table 16. Cold exposure IREQ and DLE predictions to Gonzalez et al., [80] data

Ensemble	Total Insulation (clo)	Rest (71Wm ²)			Exercise (171Wm ²)		
		0°C IREQmin /DLE	-20°C IREQmin /DLE	-30°C IREQmin /DLE	0°C IREQmin /DLE	-20°C IREQmin /DLE	-30°C IREQmin /DLE
ECWC with Glove A	3.59	3 clo > 8 hours	5.2 clo ~1.1 hours	6.3 clo < 1 hour	0.9 clo > 8 hours	1.8 clo >8 hours	2.3 clo >8 hours
ECWC with Glove C	3.60	3 clo > 8 hours	5.2 clo ~1.2 hours	6.3 clo < 1 hour	0.9 clo > 8 hours	1.8 clo >8 hours	2.3 clo >8 hours
ECWC with Glove C	3.62	3 clo > 8 hours	5.2 clo ~1.2 hours	6.3 clo < 1 hour	0.9 clo > 8 hours	1.8 clo >8 hours	2.3 clo >8 hours

Note: ECWC, US Army Extreme Cold Weather Clothing

Table 17. Cold exposure reported resting endurance time (minutes) to DLE predictions to Gonzalez et al., [80] data

Ensemble	Glove Insulation (clo)	Reported Mean Endurance Time (minutes)			IREQ – DLEminimum (minutes)		
		0°C (minutes)	-20°C (minutes)	-30°C (minutes)	0°C (minutes)	-20°C (minutes)	-30°C (minutes)
Glove A	0.86	116 ± 9.7	62 ± 37	25.5 ± 3	>480 min	66 min	42 min
Glove B	1.05	108 ± 16.7	62 ± 31	46 ± 43	>480 min	72 min	42 min
Glove C	1.46	120 ± 0	81 ± 25	N/A	>480 min	72 min	48 min

V. Discussion

These assessments and can help improve the current military and public health-state awareness, specifically information from this study can enable improved understanding of the rates of injuries service members as well as predictive methods that can prove useful for defining mitigation strategies. This study also seeks to outline the knowledge products in the form of algorithms and models that provide insight and potential for mitigation of risks where individuals are more susceptible to hot or cold related injuries. While the majority of this information was collected on a military populations, the outcomes can likely be generalized to directly translate into meaningful insights for public society [112]; as information on susceptibility to hot or cold injuries has global relevance. This global influence also has larger future implications specific to climate changes and the increased likelihood of hot or cold related injuries [4, 113-115] or specific to semi-isolated incidences such as heat waves [116].

5.1 Limitations

A limitation to each of these models, specifically from the data reported, are the models' inability to maintain accuracy during activity transition periods. This is specifically shown in the HSDA analysis seen in Figure 31, where the majority of the data up to 38.5°C is fairly symmetrical around the zero line, but were the observed data is higher than the modeled predictions when T_c exceeded 38.5°C. An easy explanation for this issue is that HSDA was initially designed using data from steady-state continued exercise conditions and therefore there is a current accuracy drift that occurs when exercise is interrupted with rest periods. Future improvements to account for dynamic activities is needed to improve the modeling robustness.

There are a number of limitations to each of the models described in this work that currently reduce the applicability to the broader general public. Some of these important limitations are the lack of resolution to account age-, gender-, and fitness-related differences in heat loss responses. However, recent work has been conducted specifically outlining the heat loss profile differences related to age [117-118], gender [119-120], as well as a combination of both [121-122]. Additionally research has shown a path for developing modeling improvements related to body composition [123] and fitness differences [124-126] specifically with respect changes blood flow and sweating responses.

There are also inherent limitations to both the use of complex models as well as simple models and indices. However, a great deal of these limitations can be overcome by the use of computer implemented methods that enable mixed or multi-model approaches, allowing for computation of multiple methods on single scenario data entries. Implementation of a computer- or application- based approach like those included in this work can lead to improved health-state awareness as well as provide guidance to help injury prevention. Broad use of models and decision aids also enables a feedback loop of quantitative data to be used for improved methods and understanding of individualized factors that increase susceptibility of hot and/or cold related injuries (e.g., fitness, body composition).

Given the complexity of obtaining clinical or real-world data from active duty service members, and the time and resources required for regulatory compliance, data management, and data analysis, studies to this scale are not likely to occur outside this work. However, an example model to emulate is the Probability of Survival Decision

Aid (PSDA), a computer model used to predict hypothermia and dehydration impact on functional time (i.e., duration of ability for useful work), and survival time while exposed to marine environments [127]. The PSDA model is underpinned by the rational SCTM model [90] with a customized graphical user interface for use by Search and Rescue (SaR) personnel. The SCTM continues to be refined and verified based on real-world feedback and data collected [128].

5.2 Other Modeling Methods to Consider

While often difficult to implement in time series and complex physiological modeling; a variety of predictive modeling methods could also provide unique benefits to outlining risk and potential outcomes of heat- and cold-related injuries. Some of these methods include: k-nearest neighbor (KNN) [129-130], random decision forests (RDF) [131], and generalized linear models (GLM) [132-133] and generalized additive models (GAM) [134-135].

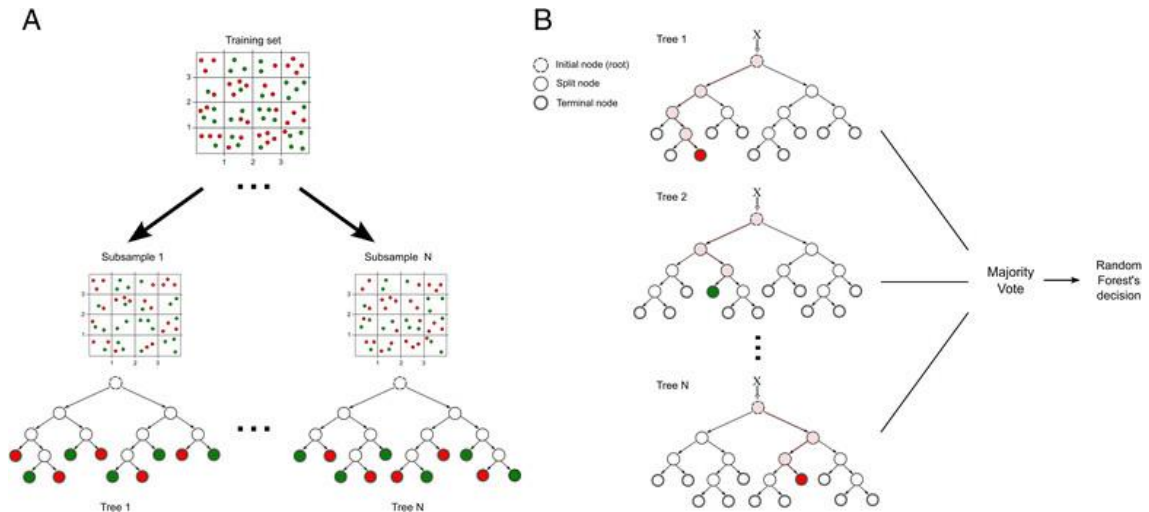
K-nearest neighbor (KNN) uses the principle that by using data points (neighbors) you can determine mathematically a prediction and with the idea that the more the data points (neighbors) the better the predictive outcome. In this KNN method we would first classify the samples and determine distances of the ‘neighbors’; we do this using Euclidean Distance (d) [130], seen as:

$$d(x_i + x_j) = \sqrt{\sum_{r=1}^n (a_r(x_i) - a_r(x_j))^2} \quad (\text{Eq 58})$$

Following this determination of distances we would arrange the ‘neighbors’ in non-decreasing order and assume k is a positive integer and accept a sorted list based on distance (e.g., $k = 1$).

Random decision forests (RDF) [131] can be useful by providing predictive outcomes that are outside that of the normal expected (contrary to regression methods). This means we would take our original dataset and select random data within it to extract features. These features with the data would then be paired together with split points continuously to form a prediction tree of potential chain of events ([136]; example Figure 46).

Figure 46. Graphical example of random decision forests method [136]



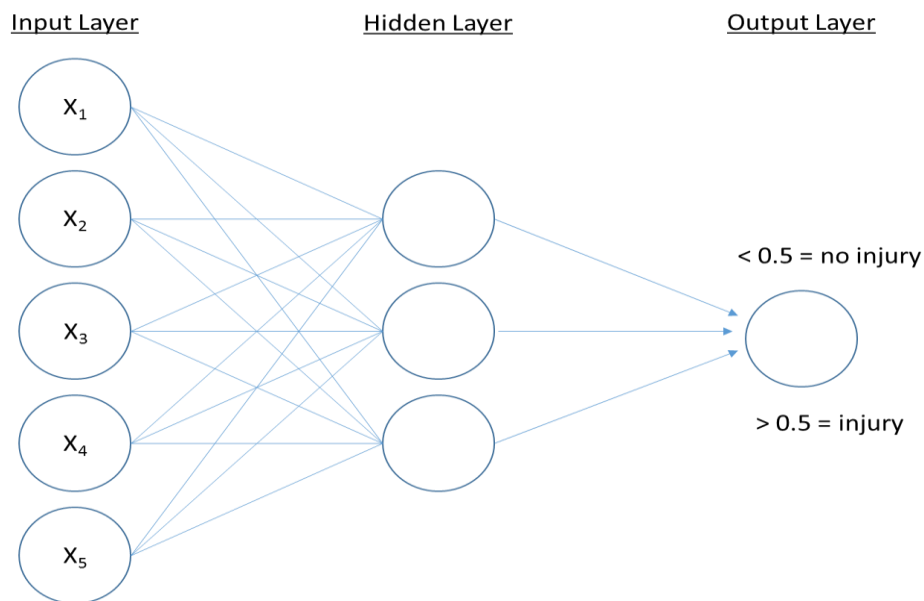
Generalized linear models (GLM) [132-133] (not to be confused with term general linear model; considered standard regression and statistical models) refers to a broader class of models (including these standard models) that seek to make predictions. The class of GLM include a set of models including regression models (linear, logistic, and Poisson regression) as well as mixed models (ANCOVA, Multinomial response), and

categorical models (ANOVA, Loglinear) [137]. In GLM there is a focus on three key elements, a random component (probability distribution; i.e., normal, binomial, Poisson, multinomial), a systematic component (explanatory variables of the model; i.e., continuous, categorical, mixed), and a link function between the two, random and systematic components (i.e., identity, logit, log, generalized logit).

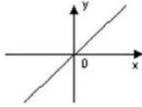
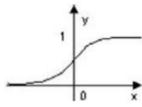
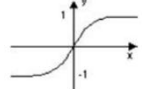
Generalized additive models (GAM) [134-135] take the methods of linear models and combines them with an ‘additive’ component; where GAM consist of a random component, an additive component, and a function that links the two together. These GAM methods are useful for analyzing nonparametric, semiparametric additive modeling methods, and is helpful for using multidimensional data. This method is helpful as an easy way of extending linear models and is easy to use in combination with data smoothing methods.

Other modeling method that should be considered are machine learning methods such as artificial neural network (ANN or NN) methods [138]. The ANN concept is founded on mathematical constructs that meant to be of similar design to that of biological brain functioning [139]. Neural network modeling has been shown useful in a number of medical predictive use cases [140-142] or even in financial outcome predictions [143]. These modeling methods generally include a three piece structure that includes an input layer (i.e., data inputs), a hidden layer (mathematical methods; ‘learning’), and an output layer (i.e., the prediction) (Figure 47).

Figure 47. Notional example of neural network method for injury prediction



Within the hidden layer the model typically uses forward and back propagation to calibrate the weight of each input and modeling method. Forward propagation calculates an output based on randomly selected weights; while back propagation measures error margin and makes adjustments to the selected weights to reduce the level of error in the output prediction. Typically within the hidden layer a number of activation functions are used (linear, sigmoid (logistic), or hyperbolic tangent); where these functions would be:

Linear	$y = x$	
Sigmoid – logistic	$y = \frac{1}{1 + e^{-x}}$	
Hyperbolic tangent	$y = \frac{1 - e^{-2x}}{1 + e^{2x}}$	

5.2 Future Directions

Future improvements and advancements to these predictive methods are currently being broached by a number of researchers in the field. However, some key areas that require specific attention include: 1) improvement of model confidence during transition points, 2) improved resolution to account for individual variabilities, 3) implementation into usable and accessible platforms (e.g., mobile apps, smart devices, web-based), and 4) inclusion of improving methods in machine learning. To address these issues directly, the below set of initial hypothesis can be used for establishing the basis for future work:

- ***Future work Hypothesis 1:*** Accuracy in the predictions during transition states (e.g., rest-activity) can be improved by adding individualized factors for temperature rates of change.
- ***Future work Hypothesis 2:*** Improvements to the modeling resolution can be done by weighting factors based on individual features or by using a scaled approach.
- ***Future work Hypothesis 3:*** Targeted adjustments to sweating response calculations (specifically E_{req} and E_{max} (Eqs. 28 and 30 respectively)) can significantly improve model predictions.
- ***Future work Hypothesis 4:*** Simple to use software (web- or app-based) can significantly improve transferability of these methods into public use.

- ***Future work Hypothesis 5:*** Significant improvements to predictive accuracy can be obtained using a multi-model approach with machine learning techniques to help shape data upper and lower limits and provide probabilistic estimates.
- ***Future work Hypothesis 6:*** A multi-model platform could increase confidence and accuracy of model predictions.

While each of the above hypotheses are fairly broad, they allow for a narrowing of the scope for future model improvements. These improvements will surely add to the resolution, accessibility, and quality of these predictive methods. However, an era of improved computational power and technology miniaturization, each of these or similar models are likely headed for use in near- or actual real-time [144-145]. There have been several attempts to make real-time predictions [146-148] or forecasts [149-150] of human responses based on human measures alone with some success. These include key human elements of heat production based on movement and energy expenditure [151-153].

To ensure accuracy within varied environments, individuals, and activities, there is a requirement for more inclusive sets of inputs (e.g., weather, individualized inputs). For example, body temperatures alone provide a single element that is often very useful but without the proper context can lose some influence (e.g., an elevated core temperature during exercise is expected; while an elevated temperature at rest could indicate other serious issues). Similarly, if an individual has an elevated core body temperature while exercising in a dry environment (low humidity) they may be relatively safe; while if this same individual was in a humid environment they would be at significant risk due to the restricted ability to dissipate evaporative heat. Additionally, individualized elements

such as health status, hydration status, or confounding comorbidities can be used to put reasonable bounds on individual limits.

These are just a few examples that outline the significant need for inclusion of more context into the modeling predictions, both initially and periodically. A helpful approach to emulate can be found in weather forecasting, where multiple predictions are made from various models and given updates they are re-run to improve and narrow predictions. This method is often displayed graphically using spaghetti plots for a given forecast [154-155]. While meteorology forecasts are typically very complex and larger scaled, similar approaches could be used for the predictions of less complex elements such as an individual's physiological response given the real-time information of their state, clothing, environment, and activity. Using multi-model approaches as well as the inclusion of bounds based on probability and uncertainty analyses, similar to those used in other fields of study [156-158], provide a key methods for expansions and improved model robustness.

V. Conclusions

The analyses from this work prove the initial hypotheses and provide an initial justification in the case for the accuracy of predictive methods for use in mitigation of hot and cold related injuries. Each of the initial hypotheses are restated and justified below:

- H₁: Thermoregulatory responses (e.g., skin and core temperature rise/fall) can be mathematically described and accurately predicted (TRUE). Based on the work outlined for both empirical and rational modeling methods, the physiological responses to hot and cold exposures, at rest and during exercise can accurately describe and predict skin and core temperature rise and fall.
- H₂: Existing population-based models can acceptably predict group mean responses and can accurately predict individualized rise in core body temperature to within $\pm 0.27^{\circ}\text{C}$ of observed data with the inclusion of individual characteristics (TRUE). An assessment using group mean data showed relatively accurate predictions can be made in hot laboratory conditions (within $2 \times \text{SD}$ of observed). Additionally, by correcting for individual characteristics and more accurate predictions of metabolic cost, this empirical approach has shown initially successful at predicting core body temperature rise to within an acceptable bias of $\pm 0.27^{\circ}\text{C}$ for individual responses (0.16°C).
- H₃: Existing rational models can be modified to accurately predict skin temperature to within observed SD of collected data. (TRUE). From the assessments related to cold exposure, this analysis showed that rational modeling can predict skin temperature fall in cold environments during both rest and exercise with MAE and RMSE rates within the SD of the observed values.

References

1. Carter III R, Cheuvront SN, Williams JO, Kolka MA, Stephenson LA, Sawka MN, & Amoroso PJ. Epidemiology of Hospitalizations and Deaths from Heat Illness in Soldiers. *Medicine & Science in Sports & Exercise*, 37(8)1338–1344, 2005.
2. DeGroot DW, Castellani JW, Williams JO, & Amoroso PJ. Epidemiology of US Army cold weather injuries, 1980–1999. *Aviation, Space, and Environmental Medicine*, 74(5), 564-570, 2003.
3. Candler WH and Ivey H. Cold injuries among U.S. soldiers in Alaska: a five-year review. *Military Medicine*, 162(12):788-791, 1997.
4. Voiland A. Going hot and cold in February. NASA's Earth Observatory, 2015. <https://climate.nasa.gov/news/2250/going-hot-and-cold-in-february/>
5. Heat-related deaths -- United States, 1999–2003. *Morbidity and Mortality Weekly Report (MMWR)*, Jul 2006;55(29): 796-798.
6. Jurkovich GJ. Environmental cold-induced injury. *Surgical Clinics*, 87(1), 247-267, 2007.
7. Berko J, Ingram DD, Saha S, and Parker JD. Deaths attributed to heat, cold, and other weather events in the United States, 2006-2010. *National Health Statistics Reports*. Number 76. National Center for Health Statistics, 2014. <https://www.cdc.gov/nchs/data/nhsr/nhsr076.pdf>
8. Bouchama A, and Knochel JP. Heat stroke. *New England Journal of Medicine*, 346(25), 1978-1988, 2002.
9. Glazer JL. Management of heatstroke and heat exhaustion. *American Family Physician*. 1;71(11):2133-40, 2005.

10. Epstein Y, Druyan A, Heled Y. Heat injury prevention—a military perspective. *The Journal of Strength & Conditioning Research*. 1;26:S82-6, 2012
11. Medical Surveillance Monthly Report (MSMR). Armed Forces Health Surveillance Center; *Update: Heat illness, active component, U.S. Armed Forces, 2016*. 24(3), pp 9-13, March 2017.
12. Medical Surveillance Monthly Report (MSMR). Armed Forces Health Surveillance Center; *Heat-related injuries, U.S. Armed Forces, 2006*. 14(2), pp 14-15, May 2007.
13. Medical Surveillance Monthly Report (MSMR). Armed Forces Health Surveillance Center; *Update: Heat injuries among U.S. military members, 2007*. 15(2), pp 2-3, February-March 2008.
14. Medical Surveillance Monthly Report (MSMR). Armed Forces Health Surveillance Center; *Update: Heat injuries, active component, U.S. armed forces, 2009*. 17(3), pp 6-8, March 2010.
15. Medical Surveillance Monthly Report (MSMR). Armed Forces Health Surveillance Center; *Update: Heat injuries, active component, U.S. armed forces, 2010*. 18(3), pp 6-8, March 2011.
16. Medical Surveillance Monthly Report (MSMR). Armed Forces Health Surveillance Center; *Heat injuries, active component, U.S. armed forces, 2011*. 19(3), pp 13-16, March 2012.
17. Medical Surveillance Monthly Report (MSMR). Armed Forces Health Surveillance Center; *Update: Heat injuries, active component, U.S. armed forces, 2012*. 20(3), pp 17-20, March 2013.

18. Medical Surveillance Monthly Report (MSMR). Armed Forces Health Surveillance Center; *Update: Heat injuries, active component, U.S. armed forces, 2013*. 21(3), pp 10-13, March 2014.
19. Medical Surveillance Monthly Report (MSMR). Armed Forces Health Surveillance Center; *Update: Heat injuries, active component, U.S. armed forces, 2014*. 22(3), pp 17-20, March 2015.
20. Castellani JW, Young AJ, Ducharme MB, Giesbrecht GG, Glickman E and Sallis RE. Prevention of Cold Injuries during Exercise. *Medicine & Science in Sports & Exercise* 38: 2006.
21. Keatinge WR, and Cannon P. Freezing-point of human skin. *Lancet* I: 11-14, 1960
22. Hamlet MP. Nonfreezing cold injuries. In: Textbook of Wilderness Medicine, P.S. Auebach (Ed.). St. Louis, MO: Mosby, pp 129-134-2001.
23. Evans TM, Rundell KW, Beck KC, Levine AM, Baumann JM. Cold air inhalation does not affect the severity of EIB after exercise or eucapnic voluntary hyperventilation. *Medicine and Science in Sports and Exercise*; 37(4):544-549, 2005.
24. Wilber RL, Rundell KW, Szmedra L, Jenkinson DM, Im J, Drake SD. Incidence of exercise-induced bronchospasm in Olympic winter sport athletes. *Medicine & Science in Sports & Exercise*; 32(4):732-7, 2000.

25. Pozos RS & Danzl DF. Human physiological responses to cold stress and hypothermia. In: Textbooks of Military Medicine: Medical Aspects of Harsh Environments, Volume 1, K. B. Pandolf and R. E. Burr (Eds.). Falls Church, VA: Office of the Surgeon General, U. S. Army, pp. 351- 382, 2002.
26. Prevention and management of cold-weather injuries. Washington, DC: Department of the Army; 2005. Report No.: TB MED 508.
27. O'Donnell FL, Stahlman S, and Oetting AA. Medical Surveillance Monthly Report (MSMR). Armed Forces Health Surveillance Center; *Update: Cold Weather Injuries, Active and Reserve Components, U.S. Armed Forces, July 2012–June 2017*. 24(10), pp 12-21, October 2017.
28. O'Donnell FL, and Taubman SB. Medical Surveillance Monthly Report (MSMR). Armed Forces Health Surveillance Center; *Update: Cold Weather Injuries, Active and Reserve Components, U.S. Armed Forces, July 2011–June 2016*; 23(10), pp 12-20, October 2016.
29. Nagarajan S. Medical Surveillance Monthly Report (MSMR). Armed Forces Health Surveillance Center; *Update: Cold Weather Injuries, Active and Reserve Components, U.S. Armed Forces, July 2010–June 2015*; 22(10), pp 7-12, October 2015.
30. Connor RR. Medical Surveillance Monthly Report (MSMR). Armed Forces Health Surveillance Center; *Update: cold weather injuries, active and reserve components, U.S. Armed Forces, July 2009–June 2014*; 21(10), pp 14-19, October 2014.

31. Medical Surveillance Monthly Report (MSMR). Armed Forces Health Surveillance Center; *Update: cold weather injuries, active and reserve components, U.S. Armed Forces, July 2008-June 2013*; 20(10), pp 12-17, October 2013.
32. Medical Surveillance Monthly Report (MSMR). Armed Forces Health Surveillance Center; *Update: Cold weather injuries, active and reserve components, U.S. Armed Forces, July 2007-June 2012*; 19(10), pp 2-6, October 2012.
33. Medical Surveillance Monthly Report (MSMR). Armed Forces Health Surveillance Center; *Update: Cold Weather Injuries, U.S. Armed Forces, July 2006-June 2011*; 18(10), pp 14-18, October 2011.
34. Medical Surveillance Monthly Report (MSMR). Armed Forces Health Surveillance Center; *Cold weather injuries, U.S. Armed Forces, July 2005-June 2010*; 17(10), pp 7-11, October 2010.
35. Medical Surveillance Monthly Report (MSMR). Armed Forces Health Surveillance Center; *Cold weather-related injuries, U.S. Armed Forces, July 2004- June 2009*; 16(9), pp 2-6, September 2009.
36. Medical Surveillance Monthly Report (MSMR). Armed Forces Health Surveillance Center; *Cold weather-related injuries, U.S. Armed Forces, July 2003-June 2008*; 15(8), pp 2-6, October 2008.
37. Medical Surveillance Monthly Report (MSMR). Armed Forces Health Surveillance Center; *Cold weather injuries, U.S. Armed Forces, July 2002-June 2007*; 14(6), pp 12-16, September-October 2007.

38. Medical Surveillance Monthly Report (MSMR). Armed Forces Health Surveillance Center; *Cold weather injuries, U.S. Armed Forces, July 2001-June 2006*; 12(7), pp 14-17, October 2006.
39. Medical Surveillance Monthly Report (MSMR). Armed Forces Health Surveillance Center; *Cold injuries, active component members, US Armed Forces, July 2000-June 2005*; 11(5), pp 7-11, December 2005.
40. Medical Surveillance Monthly Report (MSMR). Armed Forces Health Surveillance Center; *Cold injuries, active duty, US Armed Forces, July 1999-June 2004*; 10(5), pp 7-11, September-October 2004.
41. Medical Surveillance Monthly Report (MSMR). Armed Forces Health Surveillance Center; *Cold weather injuries, active duty, US Armed Forces, 1998-2003*; 9(7), pp 7-11, November-December 2003.
42. Medical Surveillance Monthly Report (MSMR). Armed Forces Health Surveillance Center; *Cold weather injuries among active duty soldiers, US Army, January 1997-July 2002*; 8(7), pp 2-5, September-October 2002.
43. Medical Surveillance Monthly Report (MSMR). Armed Forces Health Surveillance Center; *Cold weather injuries among active duty soldiers, US Army, 1997-2001*; 7(9), pp 2-5, November-December 2001.
44. Medical Surveillance Monthly Report (MSMR). Armed Forces Health Surveillance Center; *Cold weather injuries, active duty soldiers*; 6(10), pp 2-3, December 2000.
45. Astrand A, and Rodahl I. Textbook of work physiology. New York, NY: McGraw Hill; 1986. p. 104–12.

46. Sawka, M. N., Latzka, W. A., Montain, S. J., Cadarette, B. S., Kolka, M. A., Kraning, K. K., & Gonzalez, R. R. Physiologic tolerance to uncompensable heat: intermittent exercise, field vs laboratory. *Medicine and Science in Sports and Exercise*, 33(3), 422-430, 2001.
47. Sawka MN, and Young AJ. Physiological systems and their responses to conditions of heat and cold. In: American College of Sports Medicine. ACSM's advanced exercise physiology. Lippincott Williams & Wilkins; pp 535-563; 2006.
48. Johnson JM, Niederberger MA, Rowell LB, Eisman MM, and Brengelmann GL. Competition between cutaneous vasodilator and vasoconstrictor reflexes in man. *Journal of Applied Physiology*, 35: p. 798-803, 1973.
49. Charkoudian N. Skin blood flow in adult human thermoregulation: how it works, when it does not, and why. In: Mayo Clinic Proceedings 2003 May 31 (Vol. 78, No. 5, pp. 603-612). Elsevier.
50. Potter AW, Gonzalez JA, and Xu X. Ebola response: Modeling the risk of heat stress from personal protective clothing. *PloS One*;10(11):e0143461, 2015.
51. Xu X, Gonzalez JA, Karis AJ, Rioux TP, and Potter AW. Use of Thermal Mannequins for Evaluation of Heat Stress Imposed by Personal Protective Equipment, in: Performance of Protective Clothing and Equipment: 10th Volume, Risk Reduction Through Research and Testing, ASTM STP1593, B. Shiels and K. Lehtonen, Eds., ASTM International, West Conshohocken, PA, 2016, pp. 286–296,

52. Potter AW, Gonzalez JA, Karis AJ, Santee WR, Rioux TP, and Blanchard LA. Biophysical characteristics and measured wind effects of chemical protective ensembles with and without body armor. US Army Research Institute of Environmental Medicine, Natick, MA, 01760, USA, Technical Report, T15-8, 2015. ADA#621169, accessible at: www.dtic.mil/dtic/tr/fulltext/u2/a621169.pdf
53. American Society of Testing and Materials International (ASTM): Standard Test Method for Measuring the Thermal Insulation of Clothing Using a Heated Manikin (ASTM F1291-16). [Standard] Philadelphia, Pa.: ASTM, 2016.
54. American Society of Testing and Materials International (ASTM): Standard Test Method for Measuring the Evaporative Resistance of Clothing Using a Sweating Manikin (ASTM F2370-16). [Standard] Philadelphia, Pa.: ASTM, 2016.
55. Gagge AP, Burton AC, and Bazett HC. A practical system of units for the description of the heat exchange of man with his environment. *Science*, 94: 428-430, 1941.
56. Woodcock AH. Moisture transfer in textile systems, Part I. *Textile Research Journal*, 32(8), 628-633, 1962.
57. Woodcock AH. Moisture permeability index - A new index for describing evaporative heat transfer through fabric systems. Quartermaster Research and Engineering Command, Natick, MA 01702 USA, Technical Report (TR-EP-149), 1961.

58. Potter AW, Gonzalez JA, Karis AJ, Rioux TP, Blanchard LA, and Xu X. Impact of estimating thermal manikin derived wind velocity coefficients on physiological modeling. US Army Research Institute of Environmental Medicine, Natick, MA, 01760, USA, Technical Report, 2014, ADA#607972, accessible at: www.dtic.mil/dtic/tr/fulltext/u2/a607972.pdf
59. Potter AW. Method for estimating evaporative potential (im/clo) from ASTM standard single wind velocity measures. US Army Research Institute of Environmental Medicine, Natick, MA, 01760, USA, Technical Report, T16-14, 2016, ADA#637325.
60. Potter AW, Blanchard LA, Friedl KE, Cadarette BS, and Hoyt RW. Mathematical prediction of core body temperature from environment, activity, and clothing: The heat strain decision aid (HSDA). *Journal of Thermal Biology*; 64:78-85, 2017.
61. Givoni B, and Goldman RF. Predicting rectal temperature responses to work, environment, and clothing. *Journal of Applied Physiology*, 32: 812-822, 1972.
62. Gonzalez RR, McLellan TM, Withey WR, Chang SK, and Pandolf KB. Heat strain models applicable for protective clothing systems: comparison of core temperature response. *Journal of Applied Physiology*, 83(3), 1017-1032, 1997.
63. Kraning II KK and Gonzalez RR. A mechanistic computer simulation of human work in heat that accounts for physical and physiological effects of clothing, aerobic fitness, and progressive dehydration. *Journal of Thermal Biology*, 22(4), 331-342, 1997.

64. Welles AP, Tharion WJ, Potter AW, and Buller MJ. Novel method of estimating metabolic rates of soldiers engaged in chemical biological defense training. US Army Research Institute of Environmental Medicine, Natick, MA, 01760, USA, Technical Report, T17-02, 2017, ADA#1022691
65. McCullough EA, Jones BW, and Huck J. A comprehensive data base for estimating clothing insulation. *ASHRAE Trans* 91: 29-47, 1985.
66. McCullough EA, Jones BW, and Tamura P. A database for determining the evaporative resistance of clothing. *ASHRAE Trans* 95: 316-328, 1989.
67. Al-ajmi FF, Loveday DL, Bedwell KH, Havenith G. Thermal insulation and clothing area factors of typical Arabian Gulf clothing ensembles for males and females: Measurements using thermal manikins. *Applied Ergonomics* 39, 407-414, 2008.
68. ISO 9920. 2007. Ergonomics of the thermal environment - Estimation of the thermal insulation and evaporative resistance of a clothing ensemble. International Standard Organization. Geneva.
69. Osczevski R, Bluestein M. The new wind chill equivalent temperature chart. *Bulletin of the American Meteorological Society*; 86(10):1453-8, 2005.
70. National Weather Service. Windchill Temperature Index. Office of Climate, Water, and Weather Services, Washington, D.C., National Oceanic and Atmospheric Administration 2001.

71. Potter AW, Blanchard LA, Gonzalez JA, Berglund LG, Karis AJ, and Santee WR. Black versus gray t-shirts: Comparison of spectrophotometric and other biophysical properties of physical fitness uniforms and modeled heat strain and thermal comfort. US Army Research Institute of Environmental Medicine, Natick, MA, 01760, USA, Technical Report, T16-15, 2016, ADA#1016232.A
72. Xu X, Rioux TP, and Potter AW. Fabric thermal resistance and ensemble thermal resistances are two different concepts. *Journal of Occupational and Environmental Hygiene*, 11(11), D187-188, 2014.
73. Potter AW, Gonzalez JA, Xu X, Looney DP, Montain SJ. Thermal Manikin and Mathematical Modeling Evaluation of Military Head worn Covers. US Army Research Institute of Environmental Medicine, Natick, MA, 01760, USA, Technical Report, T19-02, 2018. AD1061686
74. Mansager B. Model test model. Naval Postgraduate School, Monterey, CA, Department of Mathematics (No. NPS-MA-94-007), 1994, ADA#290429; accessible at: www.dtic.mil/dtic/tr/fulltext/u2/a290429.pdf
75. van den Heuvel, A., Caldwell, J., Patterson, M. & Taylor, N. A.S. Physiological impact of first-responder chemical, biological and radiological protective ensembles.. Thirteenth International conference on environmental ergonomics; Boston, USA: 2009. 39-43.
76. Taylor N. A. S. and M. J. Patterson. Military Clothing and Protective Material: Protection at the Limits of Physiological Regulation. In: The Mechanobiology and Mechanophysiology of Military-Related Injuries, edited by A. Gefen and Y. Epstein. Switzerland: Springer, 2016, pp. 304-332.

77. Santee WR. A Simplified Modeling Approach for Estimating Heat Loss During Cold Exposure. US Army Research Institute of Environmental Medicine, Natick, MA, 01760, USA, Technical Report, T96-7, 1996. ADA#311468.
78. Santee WR, Endrusick TL, Pensotti LS. Comparison of light duty gloves with natural and synthetic materials under wet and dry conditions. *Advances in Industrial Ergonomics and Safety II*, 347-354, 1990.
79. Santee WR, Mcgrath M, Endrusick T, Wells LP. EVALUATION OF TWO COLD WEATHER GLOVES DURING ACTIVE NON- CONTACT AND PASSIVE CONTACT ACTIVITIES.
80. Gonzalez RR, Endrusick TL, Santee WR, editors. Thermoregulatory responses in the cold: Effect of an extended cold weather clothing system (ECWCS)1989. Ottawa, Canada.
81. Hickey Jr CA, Woodward Jr AA, Hanlon WE. A pilot study to determine the thermal protective capability of electrically heated clothing and boot inserts. ARMY RESEARCH LAB ABERDEEN PROVING GROUND MD; 1993.
82. Castellani JW, Yurkevicius BR, Jones ML, Driscoll TJ, Cowell CM, Smith L, et al. The effect of localized microclimate heating on peripheral skin temperatures and manual dexterity during cold exposure. *Journal of Applied Physiology*, 2018.
83. Potter AW, Karis AJ, and Gonzalez JA. *Biophysical characterization and predicted human thermal responses to U.S. Army body armor protection levels (BAPL)*. U.S. Army Research Institute of Environmental Medicine, Natick, MA 01760 USA, Technical Report, T13-5, 2013, ADA#585406, accessible at: www.dtic.mil/dtic/tr/fulltext/u2/a585406.pdf

84. Potter AW, Gonzalez JA, Carter AJ, Looney DP, Rioux TP, Srinivasan S, Sullivan-Kwantes W, and Xu X. Comparison of Cold Weather Clothing Biophysical Properties: US Army, Canadian Department of National Defence, and Norwegian Military. US Army Research Institute of Environmental Medicine, Natick, MA, 01760, USA, Technical Report, T18-02, 2018. ADA#1051229
85. Potter AW, Walsh M, and Gonzalez JA. *Explosive ordnance disposal (EOD) ensembles: Biophysical characteristics and predicted work times with and without chemical protection and active cooling systems*. US Army Research Institute of Environmental Medicine, Natick, MA, 01760, USA, Technical Report, T15-5, 2015, ADA#618081, accessible at: www.dtic.mil/dtic/tr/fulltext/u2/a618081.pdf
86. Potter AW, Karis AJ, and Gonzalez JA. *Comparison of biophysical characteristics and predicted thermophysiological responses of three prototype body armor systems versus baseline U.S. Army body armor systems*. US Army Research Institute of Environmental Medicine, Natick, MA, 01760, USA, Technical Report, T15-6, 2015, ADA#619765, accessible at: www.dtic.mil/dtic/tr/fulltext/u2/a619765.pdf
87. Potter AW, Hunt AP, Rioux TP, Looney DP, and Fogarty AL. Interlaboratory Manikin Testing, Mathematical Modeling, and Human Research Data. US Army Research Institute of Environmental Medicine, Natick, MA, 01760, USA, Technical Report, T18-03, 2018. AD1052856
88. Xu X, and Tikuisis, P. Thermoregulatory modeling for cold stress. *Comprehensive Physiology* 4: 1-25, 2014.

89. Gagge, A. P., Stolwijk, J. A. J., & Nish, Y. An effective temperature scale based on a simple model of human physiological regulatory response, *ASHRAE Trans* 77: 247-262, 1971.
90. Xu X, and Werner J. A dynamic model of the human/clothing/environment-system. *Applied Human Science: Journal of Physiological Anthropology*, 16(2), 61-75, 1997.
91. Department of the Army and Air Force. In: Heat stress control and heat casualty management. TB-MED 507, Washington, D.C., Government Printing Office, 2003.
92. Institute of Medicine. In: Dietary reference intakes for water, potassium, sodium, chloride, and sulfate. Washington, D.C., The National Academies Press, 2005.
93. Malchaire J, Piette A, Kampmann B, Mehnert P, Gebhardt HJ, Havenith G, Den Hartog E, Holmer I, Parsons K, Alfano G, Griefahn B. Development and validation of the predicted heat strain model. *The Annals of Occupational Hygiene*, 45(2):123-35, 2001.
94. Malchaire JB. Occupational heat stress assessment by the Predicted Heat Strain model. *Industrial Health*, 44(3):380-7, 2006.
95. ISO 2004 Ergonomics of the thermal environment—analytical determination and interpretation of heat stress using calculation of the predicted heat strain *ISO7933* (Geneva: International Organization for Standardization)
96. Holmer I. Required clothing insulation (IREQ) as an analytical index of cold stress. *ASHRAE Trans* 90: 1116-1128, 1984.

97. Holmer I. Assessment of cold stress in terms of required clothing insulation IREQ. *International Journal of Industrial Ergonomics*. 1988;3(2):159-66.
98. ISO 11079. 2007. Ergonomics of the thermal environment – analytical determination and interpretation of cold stress using calculation of the required clothing insulation (IREQ) and the assessment of local cooling effects. International Organization for Standardization. Geneva.
99. Besnard Y, Launay JC, Guinet-Lebreton A, Savourey G. PREDICTOL®: a computer program to determine the thermophysiological duration limited exposures in various climatic conditions. *Computer methods and programs in biomedicine*. 2004 Dec 1;76(3):221-8.
100. *JAVA applet for ISO 11079, version 4.2; 2008. Calculation of Required Clothing Insulation (IREQ), Duration Limit Exposure (Dlim), Required Recovery Time (RT), and Wind Chill Temperature (twc)* [Hosted online by: Lund University Ergonomics and Aerosols Technology Division].
http://www.eat.lth.se/fileadmin/eat/Termisk_miljoe/IREQ2009ver4_2.html
101. Xu X, Rioux TP, Gonzalez JA, Hansen EO, Castellani JW, Santee WR, Karis AJ and Potter AW. Development of a cold injury prevention tool: The Cold Weather Ensemble Decision Aid (CoWEDA). US Army Research Institute of Environmental Medicine, Natick, MA, 01760, USA, Technical Report, T19-06, 2019.
102. Bland JM and Altman DG. Statistical methods for assessing agreement between two methods of clinical measurement. *Lancet*; 307-310, 1986.

103. Bland JM and Altman DG. Measuring agreement in method comparison studies. *Statistical Methods in Medical Research*; 8: 135-160, 1999.
104. Krouwer JS. Setting performance goals and evaluating total analytical error for diagnostic assays. *Clinical Chemistry*, 48(6), 919-927, 2002.
105. Giavarina D. Understanding Bland Altman analysis. *Biochemia Medica*. 25(2):141-151, 2015.
106. Potter AW, Hunt AP, Rioux TP, Looney DP, and Fogarty AL. Interlaboratory Manikin Testing, Mathematical Modeling, and Human Research Data. US Army Research Institute of Environmental Medicine, Natick, MA, 01760, USA, Technical Report, T18-03, 2018. AD1052856
107. Potter AW, Hunt AP, Cadarette BS, Fogarty A, Srinivasan S, Santee WR, Blanchard LA, and Looney DP. Heat Strain Decision Aid (HSDA) accurately predicts individual-based core body temperature rise while wearing chemical protective clothing. *Computers in Biology and Medicine*, 107: 131-139, 2019.
108. Looney DP, Potter AW, Pryor JL, Bremner PE, Chalmers CR, McClung HM, Welles AP, Santee WR. Metabolic Costs of Standing and Walking in Healthy Military-Age Adults: A Meta-regression.
109. Looney DP, Santee WR, Hansen EO, Bonventre PJ, Chalmers CR, Potter AW. Estimating Energy Expenditure during Level, Uphill, and Downhill Walking. *Medicine and science in sports and exercise*. 2019 Apr.
110. Cadarette BS, Montain SJ, Kolka MA, Stroschein L, Matthew W, and Sawka MN. Cross validation of USARIEM heat strain prediction models. *Aviation, Space, and Environmental Medicine* 70:996-1006, 1999.

111. Casa DJ, Becker SM, Ganio MS, Brown CM, Yeargin SW, Roti MW, Siegler J, Blowers JA, Glaviano NR, Armstrong LE. Validity of devices that assess body temperature during outdoor exercise in the heat. *Journal of Athletic Training*. 2007 Jul;42(3):333.
112. Cooper JK. Preventing heat injury: military versus civilian perspective. *Military Medicine*, 162(1), 55-58, 1997.
113. Vyrostek SB, Annest JL, and Ryan GW. Surveillance for fatal and nonfatal injuries—United States, 2001. *Morbidity and Mortality Weekly Report (MMWR) Surveillance Summaries*, 53(7), 1-57, 2004.
114. Basu R, and Samet JM. Relation between elevated ambient temperature and mortality: a review of the epidemiologic evidence. *Epidemiologic Reviews*, 24(2), 190-202, 2002.
115. Anderson BG, and Bell ML. Weather-related mortality: how heat, cold, and heat waves affect mortality in the United States. *Epidemiology* (Cambridge, Mass.), 20(2), 205, 2009.
116. Ebi KL, and Meehl GA. The heat is on: climate change and heatwaves in the Midwest. *Regional Impacts of Climate Change: four case studies in the United States*, 8-21, 2007.
117. Larose J, Boulay P, Wright-Beatty HE, Sigal RJ, Hardcastle S, Kenny GP. Age-related differences in heat loss capacity occur under both dry and humid heat stress conditions. *Journal of Applied Physiology* 117(1):69-79, 2014.

118. Larose J, Boulay P, Sigal RJ, Wright HE, Kenny GP. Age-related decrements in heat dissipation during physical activity occur as early as the age of 40. *PLoS One* 8(12):e83148, 2013.
119. Kenny GP, Jay O. Sex differences in postexercise esophageal and muscle tissue temperature response. *American Journal of Physiology-Regulatory, Integrative and Comparative Physiology* 292(4):R1632-40, 2007.
120. Gagnon D, Jay O, Lemire B, Kenny GP. Sex-related differences in evaporative heat loss: the importance of metabolic heat production. *European journal of applied physiology*. 2008 Nov 1;104(5):821-9.
121. Notley SR, Poirier MP, Hardcastle SG, Flouris AD, Boulay P, Sigal RJ, Kenny GP. Aging impairs whole-body heat loss in women under both dry and humid heat stress. *Medicine & Science in Sports & Exercise* 49(11):2324-32, 2017.
122. Notley SR, Meade RD, D'Souza AW, Friesen BJ, Kenny GP. Heat Loss Is Impaired in Older Men on the Day after Prolonged Work in the Heat. *Medicine & Science in Sports & Exercise* 50(9):1859-67, 2018.
123. Notley SR, Park J, Tagami K, Ohnishi N, Taylor NA. Morphological dependency of cutaneous blood flow and sweating during compensable heat stress when heat-loss requirements are matched across participants. *Journal of Applied Physiology* 121(1):25-35, 2016.
124. Cramer MN, Jay O. Explained variance in the thermoregulatory responses to exercise: the independent roles of biophysical and fitness/fatness-related factors. *Journal of Applied Physiology* 119(9):982-9, 2015.

125. Lamarche DT, Notley SR, Louie JC, Poirier MP, Kenny GP. Fitness-related differences in the rate of whole-body evaporative heat loss in exercising men are heat-load dependent. *Experimental Physiology* 103(1):101-10, 2018.
126. Ravanelli N, Coombs GB, Imbeault P, Jay O. Maximum Skin Wettedness after Aerobic Training with and without Heat Acclimation. *Medicine & Science in Sports & Exercise* 50(2):299-307, 2018.
127. Xu X, Amin M, and Santee WR. Probability of survival decision aid (PSDA). U.S. Army Research Institute of Environmental Medicine, Natick, MA 01760 USA, Technical Report, T08-05, 2008, ADA#478415, accessible at: www.dtic.mil/dtic/tr/fulltext/u2/a478415.pdf
128. Xu X, Allen A, Rioux T, Patel T, Sinha P, Yokota M, and Santee W. Refinement of probability of survival decision aid (PSDA). U.S. Army Research Institute of Environmental Medicine, Natick, MA 01760 USA, Technical Note, TN14-02, 2014, ADA#599590, accessible at: www.dtic.mil/dtic/tr/fulltext/u2/a599590.pdf
129. Peterson LE. K-nearest neighbor. *Scholarpedia*; 4(2):1883, 2009.
130. Mitchell TM. Machine Learning: McGraw-Hill Science/Engineering/Math, 1997.
131. Ho TK. Random decision forests. In: Document Analysis and Recognition, 1995, Proceedings of the Third International Conference on 1995 Aug 14 (Vol. 1, pp. 278-282). IEEE.
132. Nelder JA, and Baker RJ. Generalized linear models. John Wiley & Sons, Inc.; 1972.
133. Faraway JJ. Extending the linear model with R: generalized linear, mixed effects and nonparametric regression models. *CRC press*; 2016.

134. Hastie T, and Tibshirani R. Generalized additive models. John Wiley & Sons, Inc.; 1990.
135. Wood SN, Goude Y, and Shaw S. Generalized additive models for large data sets. *Journal of the Royal Statistical Society: Series C (Applied Statistics)*; 64(1):139-55, 2015.
136. Machado G, Corbellini LG, and Mendoza MR. What variables are important in predicting bovine viral diarrhea virus? A random forest approach. *Veterinary Research*; 46(1):85, 2015.
137. Agresti A, and Kateri M. Categorical data analysis. In: International encyclopedia of statistical science 2011 (pp. 206-208). Springer Berlin Heidelberg.
138. Wasserman PD. Neural computing: theory and practice. *Vannortrand Reinhold Press*, 1989.
139. Greenwood D. An overview of neural networks. *Behavioural Sciences*, 36: 1-33, 1991.
140. Tu JV. Advantages and disadvantages of using artificial neural networks versus logistic regression for predicting medical outcomes. *Journal of Clinical Epidemiology*; 49(11):1225-31, 1996.
141. Abdolmaleki P, Yarmohammadi M, and Gity M. Comparison of logistic regression and neural network models in predicting the outcome of biopsy in breast cancer from MRI findings. *Iranian Journal of Radiation Research*; 1(4):217-28, 2004.

142. Eftekhari B, Mohammad K, Ardebili HE, Ghodsi M, and Ketabchi E. Comparison of artificial neural network and logistic regression models for prediction of mortality in head trauma based on initial clinical data. *BMC Medical Informatics and Decision Making*; 5(1):3, 2005.
143. Odom MD, and Sharda R. A neural network model for bankruptcy prediction. In: Neural Networks, 1990. *IJCNN International Joint Conference 1990 Jun 17* (pp. 163-168). IEEE.
144. Sawka MN, Friedl KE. Emerging wearable physiological monitoring technologies and decision aids for health and performance. *Journal of Applied Physiology*, 2017, 124(2): 430-431.
145. Tharion WJ, Potter AW, Duhamel CM, Karis AJ, Buller MJ, Hoyt RW. Real-time physiological monitoring while encapsulated in personal protective equipment. *Journal of Sport and Human Performance*, 2013;1(4):14-21.
146. Looney DP, Buller MJ, Gribok AV, Leger JL, Potter AW, Rumpler WV, Tharion WJ, Welles AP, Friedl KE, Hoyt RW. Estimating resting core temperature using heart rate. *Journal for the Measurement of Physical Behaviour*, 2018 1;1(2):79-86.
147. Welles AP, Xu X, Santee WR, Looney DP, Buller MJ, Potter AW, Hoyt RW. Estimation of core body temperature from skin temperature, heat flux, and heart rate using a Kalman filter. *Computers in Biology and Medicine*. 2018; 99:1-6.
148. Eggenberger P, MacRae BA, Kemp S, Bürgisser M, Rossi RM, Annaheim S. Prediction of core body temperature based on skin temperature, heat flux, and

- heart rate under different exercise and clothing conditions in the heat in young adult males. *Frontiers in physiology*. 2018; 9:1780.
149. Reifman J, Laxminarayan S, Rakesh V, Ramakrishnan S, Liu J, inventors; US Government Amy, Secretary of, assignee. Real-Time Estimation of Human Core Body Temperature Based on Non-Invasive Physiological Measurements. United States Patent Application US 16/327,846. 2019 Jun 27.
 150. Laxminarayan S, Rakesh V, Oyama T, Kazman JB, Yanovich R, Ketko I, Epstein Y, Morrison S, Reifman J. Individualized estimation of human core body temperature using noninvasive measurements. *Journal of Applied Physiology*, 2018; 124(6):1387-402.
 151. Clements CM, Moody D, Potter AW, Seay JF, Fellin RE, Buller MJ. Loaded and unloaded foot movement differentiation using chest mounted accelerometer signatures. *In 2013 IEEE International Conference on Body Sensor Networks* 2013 May 6 (pp. 1-5). IEEE.
 152. Welles AP, Buller MJ, Looney DP, Rumpler WV, Gribok AV, Hoyt RW. Estimation of metabolic energy expenditure from core temperature using a human thermoregulatory model. *Journal of Thermal Biology*. 2018; 72:44-52.
 153. Looney DP, Santee WR, Blanchard LA, Karis AJ, Carter AJ, Potter AW. Cardiorespiratory responses to heavy military load carriage over complex terrain. *Applied Ergonomics*, 2018; 73:194-8.
 154. Veiga GM, Ferreira DR. Understanding spaghetti models with sequence clustering for ProM. *In International Conference on Business Process Management* 2009 Sep 7 (pp. 92-103). Springer, Berlin, Heidelberg.

155. Ferstl F, Kanzler M, Rautenhaus M, Westermann R. Time-hierarchical clustering and visualization of weather forecast ensembles. *IEEE Transactions on Visualization and Computer Graphics*. 2016 Aug 10;23(1):831-40.
156. Tebaldi C, Smith RL, Nychka D, Mearns LO. Quantifying uncertainty in projections of regional climate change: A Bayesian approach to the analysis of multimodel ensembles. *Journal of Climate* 2005; 18(10):1524-40.
157. Palmer TN, Buizza R, Doblas-Reyes F, Jung T, Leutbecher M, Shutts GJ, Steinheimer M, Weisheimer A. Stochastic parametrization and model uncertainty. *ECMWF Technical Memoranda*. 2009 Oct 8;598:1-42.
158. Gillingham K, Nordhaus WD, Anthoff D, Blanford G, Bosetti V, Christensen P, McJeon H, Reilly J, Sztorc P. Modeling uncertainty in climate change: A multi-model comparison. *National Bureau of Economic Research*; 2015 Oct 15.

Appendix Table A1. Tested clothing biophysical values

Type 1: Physical fitness clothing (PT#) (shorts, t-shirt, sneakers)

Type 2: Regular clothing (RC#) (Long-sleeve shirt, undershirt, underwear, pants, boots/sneakers)

Type 3: Combat clothing with body armor (CC#) (Type 2 plus equipment and body armor)

Type 4: Chemical protective clothing (CB#; with body armor (BA) (e.g., hazmat suits, face masks, respirators)

Type 5: Explosive ordnance disposal suits (EOD#) (full armor protection suits with equipment)

Type 6: Cold weather clothing (CWC#) (full body clothing coverage)

Ensemble	0.4 ms ⁻¹ Standard test values			1ms ⁻¹ (values used in HSDA)				Type
	clo	i _m	i _m /clo	clo	cloV ^g	i _m /clo	i _m /cloV ^g	
PT-1	0.877	0.467	0.536	0.646	-0.334	0.742	0.354	1
PT-2	0.910	0.462	0.507	0.652	-0.364	0.730	0.397	1
PT-3	0.909	0.473	0.528	0.652	-0.363	0.738	0.366	1
PT-4	0.919	0.464	0.522	0.655	-0.370	0.727	0.362	1
PT-5	0.891	0.461	0.518	0.653	-0.340	0.728	0.371	1
RC-1	1.368	0.410	0.276	1.092	-0.246	0.377	0.340	2
RC-2	1.405	0.422	0.300	1.118	-0.249	0.439	0.438	2
RC-3	1.354	0.451	0.333	1.085	-0.242	0.470	0.348	2
RC-4	1.323	0.475	0.359	1.052	-0.250	0.513	0.345	2
RC-5	1.302	0.468	0.360	1.040	-0.245	0.510	0.344	2
RC-6	1.373	0.483	0.352	1.086	-0.255	0.481	0.316	2
RC-7	1.290	0.421	0.327	1.035	-0.240	0.468	0.245	2
CC-1	1.566	0.401	0.246	1.230	-0.264	0.327	0.307	3
CC-2	1.586	0.391	0.246	1.247	-0.263	0.316	0.274	3
CC-3	1.619	0.396	0.245	1.290	-0.248	0.308	0.251	3
CC-4	1.578	0.385	0.238	1.243	-0.260	0.311	0.292	3
CC-5	1.574	0.382	0.237	1.248	-0.253	0.306	0.280	3
CC-6	1.577	0.383	0.236	1.251	-0.253	0.306	0.282	3
CC-7	1.583	0.363	0.217	1.261	-0.248	0.283	0.288	3
CC-8	1.603	0.358	0.223	1.290	-0.237	0.278	0.244	3
CC-9	1.632	0.350	0.217	1.283	-0.263	0.270	0.238	3
CC-10	1.529	0.374	0.223	1.202	-0.263	0.311	0.362	3
CC-11	1.466	0.437	0.298	1.184	-0.234	0.413	0.327	3
CC-12	1.675	0.440	0.262	1.344	-0.240	0.356	0.308	3
CC-13	1.423	0.537	0.377	1.116	-0.265	0.457	0.296	3
CC-14	0.882	0.350	0.396	1.652	-0.177	0.238	0.185	3
CC-15	1.524	0.400	0.263	1.240	-0.225	0.364	0.262	3
CC-16	1.648	0.422	0.256	1.338	-0.228	0.330	0.251	3
CC-17	1.603	0.433	0.270	1.286	-0.241	0.360	0.279	3
CC-18	1.641	0.453	0.276	1.307	-0.249	0.365	0.281	3
CC-19	1.614	0.416	0.258	1.298	-0.238	0.332	0.255	3
CC-20	1.510	0.373	0.250	1.251	-0.206	0.304	0.227	3
CC-21	1.510	0.418	0.280	1.258	-0.198	0.340	0.221	3
CC-22	1.900	0.448	0.240	1.533	-0.232	0.337	0.385	3

CB-BA-1	1.832	0.280	0.152	1.504	-0.215	0.196	0.276	4
CB-BA-2	1.976	0.310	0.157	1.657	-0.192	0.205	0.292	4
CB-BA-3	2.002	0.304	0.152	1.697	-0.180	0.188	0.233	4
CB-BA-4	1.894	0.148	0.079	1.577	-0.200	0.105	0.314	4
CB-BA-5	2.016	0.301	0.149	1.722	-0.172	0.185	0.240	4
CB-BA-6	2.033	0.294	0.145	1.733	-0.174	0.182	0.252	4
CB-BA-7	1.740	0.264	0.151	1.436	-0.210	0.192	0.263	4
CB-BA-8	2.231	0.284	0.128	1.925	-0.161	0.154	0.207	4
CB-1	1.729	0.293	0.172	1.416	-0.218	0.223	0.281	4
CB-2	1.864	0.330	0.178	1.577	-0.182	0.226	0.261	4
CB-3	1.868	0.320	0.171	1.616	-0.158	0.210	0.225	4
CB-4	1.773	0.157	0.088	1.467	-0.207	0.119	0.324	4
CB-5	1.934	0.301	0.156	1.609	-0.201	0.204	0.294	4
CB-6	1.945	0.301	0.155	1.632	-0.192	0.199	0.270	4
CB-7	1.716	0.261	0.152	1.447	-0.186	0.190	0.242	4
CB-8	1.685	0.250	0.149	1.449	-0.165	0.176	0.178	4
CB-9	1.777	0.262	0.148	1.507	-0.180	0.188	0.259	4
CB-10	1.782	0.251	0.140	1.531	-0.166	0.166	0.186	4
CB-11	1.849	0.266	0.149	1.558	-0.187	0.188	0.258	4
CB-12	1.796	0.255	0.142	1.545	-0.164	0.168	0.184	4
CB-13	1.393	0.430	0.309	1.097	-0.260	0.440	0.286	4
CB-14	1.651	0.429	0.260	1.351	-0.219	0.326	0.279	4
CB-15	1.926	0.411	0.213	1.517	-0.261	0.298	0.332	4
CB-16	2.079	0.402	0.193	1.712	-0.212	0.253	0.282	4
CB-17	2.530	0.394	0.156	2.203	-0.151	0.183	0.240	4
CB-18	2.392	0.360	0.151	1.939	-0.229	0.218	0.289	4
CB-19	2.582	0.349	0.135	2.248	-0.151	0.172	0.265	4
EOD-1	3.031	0	0	2.360	N/A	2.118	N/A	5
EOD-2	3.209	0	0	2.766	N/A	1.808	N/A	5
EOD-3	3.039	0	0	2.502	N/A	1.998	N/A	5
EOD-4	3.501	0	0	3.063	N/A	1.633	N/A	5
CWC-1	1.296	0.518	0.400	0.918	-0.347	0.552	0.370	6
CWC-2	1.548	0.548	0.354	1.090	-0.343	0.485	0.366	6
CWC-3	1.729	0.361	0.209	1.386	-0.232	0.269	0.267	6
CWC-4	2.806	0.390	0.139	2.205	-0.161	0.165	0.207	6
CWC-5	1.490	0.325	0.218	1.230	-0.232	0.282	0.266	6
CWC-6	1.825	0.367	0.201	1.457	-0.227	0.258	0.263	6
CWC-7	1.342	0.313	0.233	1.124	-0.237	0.305	0.270	6
CWC-8	1.316	0.368	0.280	1.058	-0.268	0.374	0.298	6
CWC-9	1.554	0.382	0.246	1.233	-0.256	0.324	0.288	6
CWC-10	1.812	0.399	0.220	1.420	-0.245	0.286	0.279	6
CWC-11	2.103	0.449	0.214	1.606	-0.248	0.276	0.282	6
CWC-12	2.445	0.415	0.170	1.901	-0.203	0.211	0.243	6
CWC-13	2.328	0.458	0.197	1.775	-0.234	0.251	0.271	6
CWC-14	2.657	0.434	0.163	2.052	-0.196	0.202	0.238	6

CWC-15	3.109	0.460	0.148	2.384	-0.174	0.179	0.220	6
CWC-16	2.638	0.494	0.187	1.988	-0.228	0.237	0.267	6
CWC-17	2.509	0.438	0.175	1.933	-0.210	0.218	0.250	6
CWC-18	1.812	0.361	0.199	1.452	-0.225	0.255	0.261	6
CWC-19	1.638	0.358	0.218	1.318	-0.237	0.283	0.271	6
CWC-20	1.671	0.408	0.244	1.302	-0.260	0.321	0.292	6
CWC-21	2.199	0.360	0.163	1.756	-0.194	0.202	0.234	6
CWC-22	2.406	0.354	0.147	1.922	-0.175	0.178	0.217	6
CWC-23	1.484	0.361	0.244	1.195	-0.251	0.321	0.283	6
CWC-24	1.742	0.386	0.222	1.376	-0.244	0.289	0.277	6
CWC-25	1.806	0.394	0.218	1.420	-0.243	0.283	0.277	6
CWC-26	2.516	0.416	0.165	1.957	-0.198	0.204	0.239	6
CWC-27	2.516	0.454	0.180	1.925	-0.218	0.226	0.257	6
CWC-28	2.000	0.419	0.209	1.551	-0.240	0.269	0.275	6